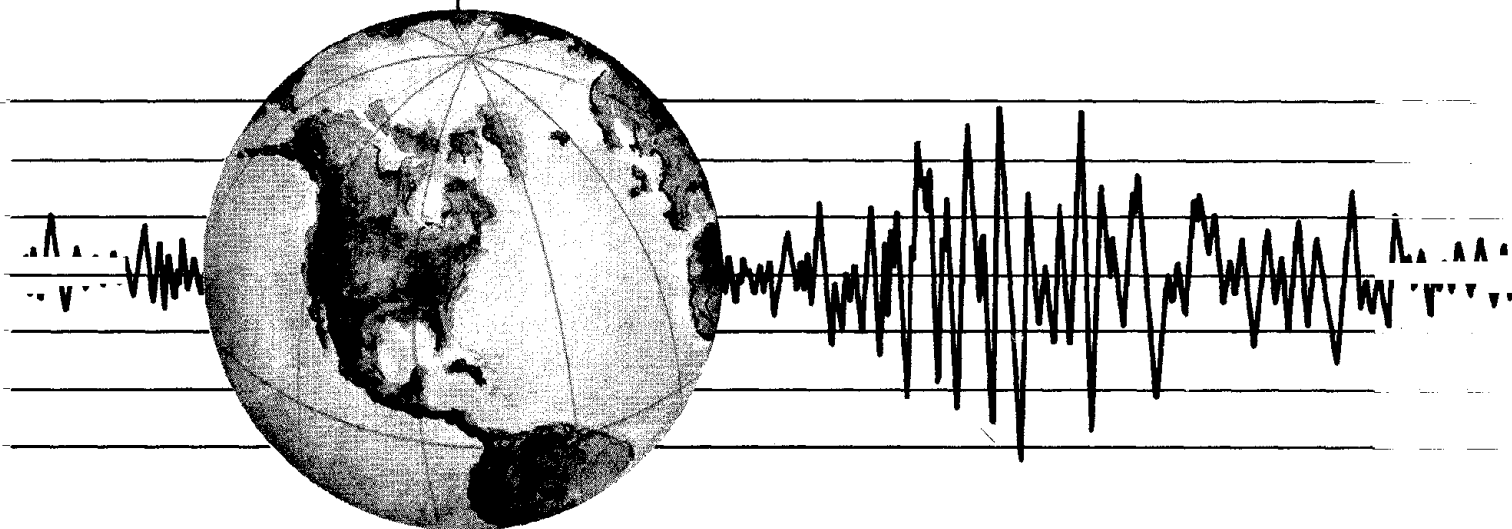EARTHQUAKE ENGINEERING RESEARCH CENTER

EXPERIMENTAL AND ANALYTICAL PREDICTIONS OF THE MECHANICAL CHARACTERISTICS OF A 1/5-SCALE MODEL OF A 7-STORY R/C FRAME-WALL BUILDING STRUCTURE

by

A. E. AKTAN
V. V. BERTERO
A. A. CHOWDHURY
T. NAGASHIMA

COLLEGE OF ENGINEERING

UNIVERSITY OF CALIFORNIA · Berkeley, California

For sale by the National Technical Information Service, U.S. Department of Commerce, Springfield, Virginia 22161.

See back of report for up to date listing of EERC reports.

DOCUMENTATION PAGE	1. REPORT NO. NSF/CEE-83017	2.	3. Recipient's Accession No. PB₄ 119213

Title and Subtitle	5. Report Date
Experimental and Analytical Predictions of the Mechanical Characteristics of a 1/5-scale Model of a 7-story R/C Frame-Wall Building Structure	June 1983
	6.

Author(s) A. E. Aktan, V. V. Bertero, A. A. Chowdhury, T. Nagashima	8. Performing Organization Rept. No. UCB/EERC-83/13

Performing Organization Name and Address	10. Project/Task/Work Unit No.
Earthquake Engineering Research Center University of California, Berkeley 47th Street and Hoffman Blvd. Richmond, Calif. 94804	11. Contract(C) or Grant(G) No. (C) (G) CEE-8009478

Sponsoring Organization Name and Address	13. Type of Report & Period Covered
National Science Foundation 1800 G. Street, N. W. Washington, D.C. 20550	14.

Supplementary Notes

Abstract (Limit: 200 words)

This report documents the preliminary series of static and dynamic tests in Japan to measure the flexibility, frequency, and damping characteristics of a frame-wall structure and the associated analytical work conducted at U.C. Berkeley, as part of the U.S.-Japan Cooperative Research Program. The global flexibility, fundamental frequency and damping characteristics of the full-scale structure were simulated successfully.

The bare model, prior to applying the auxiliary mass, which could be considered as a distorted model, had flexibility characteristics more than 100 percent different from those of the full-scale structure.

The analytically generated static and dynamic characteristics of the structure agreed reasonably well with those of the undistorted model. The flexibility characteristics of the bare model, however, could not be simulated by the linearly elastic analytical model.

Although the global static and dynamic characteristics of the full-scale structure were represented successfully by the undistorted model, simulation was not as successful at the member level.

If similitude between model and prototype is desired at the initial serviceability limit state so that there is no distortion in the flexibility characteristics or in the distribution and redistribution of internal forces of the model, the model microconcrete should be selected so that its volumetric change characteristics are similar to those of the prototype material.

17. Document Analysis   a. Descriptors

b. Identifiers/Open-Ended Terms

c. COSATI Field/Group

Availability Statement	19. Security Class (This Report)	21. No. of Pages 140
Release Unlimited	20. Security Class (This Page)	22. Price

(See Z39.18)   See Instructions on Reverse   OPTIONAL FORM 272 (4-77) (Formerly NTIS-35) Department of Commerce

EXPERIMENTAL AND ANALYTICAL PREDICTIONS OF THE MECHANICAL CHARACTERISTICS OF A 1/5-SCALE MODEL OF A 7-STORY R/C FRAME-WALL BUILDING STRUCTURE

by

A. E. Aktan
Associate Research Engineer
Department of Civil Engineering
University of California, Berkeley

V. V. Bertero
Professor of Civil Engineering
University of California, Berkeley

A. A. Chowdhury
Research Assistant
University of California, Berkeley

T. Nagashima
Visiting Scholar
Takenaka Komuten Co., Ltd.
Japan

i

ii

ABSTRACT

This report documents the preliminary series of static and dynamic tests and the associated analytical work conducted at the University of California, Berkeley, on the 1/5-scale model of a 7-story full-scale frame-wall structure tested in Japan as part of the "Reinforced Concrete Building Structures" phase of the U.S.-Japan Cooperative Research Program.

The main objective of this investigation was to assess the state of the art in predicting the static and dynamic response characteristics of R/C frame-wall structures at the serviceability limit state, incorporating both analytical and physical models. The 1/5-scale model of the 7-story full-scale structure was subjected to static and dynamic tests in order to measure its flexibility, frequency, and damping characteristics. These tests were conducted before and after the mass of the model was augmented by lead ballast in order to satisfy the similitude requirements for the gravity forces and mass (acceleration) characteristics of the 1/5-scale model structure.

Evaluating the results of: (1) Static and dynamic tests conducted on the 1/5-scale model before and after installation of the auxiliary mass, (2) Similar tests which were carried out on the full-scale structure in Japan, and (3) Results obtained from analytical modeling schemes and computer codes commonly used for linear analysis; led to a number of conclusions regarding the reliability of predicting the initial serviceability level responses of R/C frame-wall structures through analytical and physical models.

The main conclusions of research may be formulated as follows:

(1) The global flexibility, fundamental frequency and damping

iii

characteristics of the full-scale structure were simulated successfully, within 10 percent, by the undistorted 1/5-scale model with auxiliary mass.

(2) The bare 1/5-scale model, prior to applying the auxiliary mass, which could be considered as a distorted model, had flexibility characteristics more than 100 percent different from those of the full-scale structure. The proper simulation of the gravity force levels of wall elements was observed to be a prerequisite in the experimental analysis of walls or subassemblages of structures incorporating walls.

(3) The analytically generated static and dynamic characteristics of the structure agreed reasonably well with those of the undistorted model. The flexibility characteristics of the bare (distorted) model, however, could not be simulated by the linearly elastic analytical model. This was recognized as being due to the inadequacy of the analytical model to incorporate the significant dependence of the shear modulus of rigidity of concrete on axial stress.

(4) Although the global static and dynamic characteristics of the full-scale structure were represented successfully by the undistorted 1/5-scale model, the simulation was not as successful at the member level. Due to the difference in the shrinkage characteristics of the walls and the thicker columns, the walls at the base of the bare model were measured to be under tension, rather than the expected level of compression. The distortion in the gravity force levels of the walls continued after loading the model with the auxiliary mass and this was assessed to have affected the responses of the structure.

It becomes apparent that if similitude between the model and prototype is desired at the initial serviceability limit state so that there is no distortion in the flexibility characteristics or in the distribution and redistribution of internal forces of the model, the model microconcrete

should be selected so that its volumetric change characteristics, in addition to other characteristics associated with material response, are similar to those of the prototype material. Improvements in the state of the art and particularly in the state of the practice of R/C reduced scale model construction, were assessed to be necessary to achieve better similitude with the prototype.

ACKNOWLEDGMENTS

Preceding page blank

TABLE OF CONTENTS

— —

LIST OF TABLES

LIST OF FIGURES

xiv

1. INTRODUCTION

1.1 General Information

The research reported herein was carried out within the R/C Building
Structures phase of the U.S.-Japan Cooperative Research Program. In
accordance with recommendations made by the U.S.-Japan Cooperative Planning
Group (Ref. 8), a 7-story R/C frame-wall building (Fig. 1.1) was designed,
constructed, and tested in full-scale at the Large-Size Structures Labora-
tory, Building Research Institute, Tsukuba, Japan (Refs. 5,6). Following
the master program envisioned by this Planning Group (Ref. 8), numerous
associated experimental and analytical research programs were initiated in
Japan and the U.S., coordinated by the Joint Technical Coordinating Committee.
Among these were: (1) Earthquake simulator tests of medium- and small-scale
models of the full-scale structure; (2) Static tests of components and sub-
assemblages from this structure of different scales and complexity; (3)
Analytical studies; and (4) Studies aimed at the correlation of results from
these analytical and experimental investigations carried out at major research
institutions in Japan and the U.S.

In addition to the Reinforced Concrete Building Structures phase of
the cooperative research program, Steel Building Structures and Pseudo-
Dynamic Test Method were phases recommended by the planning Group which
were subsequently initiated in the U.S. and Japanese institutions.

1.2 Objectives and Scope

1.2.1 General Objectives and Scope

The design, construction, and testing of a 1/5-scale true-replica
model of the 7-story, full-scale R/C structure (Fig. 1.1) within an exten-
sive static, dynamic, and earthquake simulator testing program, and the

1

associated analytical and correlation studies constituted the primary research effort during the initial phases of the research program in U.C. Berkeley, conducted within the R/C Building Structures phase of the U.S.-Japan Cooperative Research Program. The general objectives of the U.C. Berkeley program were formulated as (Ref. 1): (1) Review and improve (if necessary) the design of the R/C full-scale test building; (2) Determine the reliability of predicting the seismic performance of buildings through the use of available linear and nonlinear structural analysis programs; (3) Determine the reliability of experimental analysis based on tests conducted on the earthquake simulator facility available at Berkeley; (4) Determine the reliability of formulating mathematical models based on experiments conducted on reduced-scale models of the basic subassemblages of a building, using controlled loading facilities available at Berkeley, and predict seismic response based on such mathematical models; (5) Evaluate the implications of the results obtained regarding the seismic resistant design and construction of R/C frame-wall buildings.

The general objectives of the Berkeley research were motivated by the unique opportunities provided by the Cooperative Research Program, in which destructive testing of a full-scale building structure could be accompanied by earthquake simulator tests of true-replica as well as distorted models of medium- and small-scales, by static tests of different subassemblages of the building of various scales, and by extensive integrated analytical investigations carried out in the major institutions conducting earthquake engineering research in Japan and the U.S. Such a coordinated major research effort was a way to generate answers to basic questions which the state of the art in R/C earthquake engineering had not yet provided. These questions were:

2

(1) How does a current, well-designed, multistory R/C frame-wall structural system, with a precisely controlled and documented design and construction, and with a precisely documented history of forces and deformations, respond to earthquakes of different intensity and damage potential, ranging from minor to major? What would be the actual stiffness, strength, energy dissipation, frequency, and damping characteristics of this structure and the changes in these characteristics during the responses to successive earthquakes? What would be its failure and collapse characteristics? What would be the effect of different types of non-structural elements on the responses of such a structure?

(2) Are destructive tests of full-scale structures necessary to answer the questions in (1)? What is the extent of the applicability of dynamic true-replica or distorted models of medium- or small-scale in simulating the different limit-state responses of R/C structures to earthquakes?

(3) What are the actual levels of force, deformation, and energy dissipation demands from different subassemblages of a current, well-designed R/C frame-wall structure during different limit states of response to earthquakes? What is the reliability in predicting the seismic responses of the complete structure based on information derived from static tests of its components? Are the loading histories commonly applied during component and subassemblage testing realistic, or are these being over-tested?

(4) What is the state of the art in analytically predicting seismic responses of R/C frame-wall structures at all the limit states? What is the correct procedure to advance the state of the art of such analyses? Is it possible to generate and improve analytical models and analysis procedures based on static tests of reduced-scale components or subassemblages of structures, or dynamic tests of small- or medium-scale distorted or true-replica models of structural systems?

3

(5) What would be the agreement on basic conclusions of the different studies coordinated by the Joint Technical Coordinating Committee and conducted in different institutions? What would be their assessments of, and conclusions to, the questions in (1)-(4)? Is it possible to establish international standards in the conduct of experimental and analytical research on the earthquake engineering aspects of reinforced concrete?

The cooperative research program was not expected to provide thorough assessments and conclusions to all the questions formulated above, partly because of the shortcomings of investigating just one selected prototype structure of the many possible variations when multistory R/C frame-wall structural systems are used, and partly because of limitations of the pseudo-dynamic test scheme (Ref. 4) with which the full-scale structure was tested. The information obtained from the testing of the full-scale structure should not be considered fully adequate to answer question (1). Especially since the structure was tested along only one horizontal response direction, idealized as a single degree of freedom system in establishing its displacement program (Ref. 6), and as completely fixed at the foundation level to the test floor, the relation of the attained responses to the actual responses of a structure, with a deformable soil-foundation system and excited by three-dimensional base motion, should be evaluated.

1.2.2 Objectives and Scope of this Report

This report will document the preliminary series of experimental and analytical studies carried out to determine the serviceability level flexibility, frequency, and damping characteristics of the 1/5-scale model structure. The design and construction of the 1/5-scale model has been documented (Ref. 7). Specially designed and manufactured internal force transducers were placed in all the columns at mid-height of the first

4

story to investigate the actual distribution of forces at the base of this highly redundant structure. Information about the model structure and force transducers is provided in subsequent sections.

The model structure was subjected to: (1) Lateral loading applied at each floor level; (2) Ambient vibration tests; (3) Dynamic analyzer tests; (4) Forced vibration tests; and (5) Free vibration tests. The above were all conducted at a stress level computed to be below cracking, characterizing the "uncracked" serviceability limit state of the structure. Of course the structure might have experienced some cracking during construction, curing, installation of force transducers, or testing. In fact, cracking, which was suspected to be especially due to volumetric changes caused by temperature fluctuations and shrinkage, was observed within the structure at the completion of the preliminary experiments. The flexibility, frequency, and damping characteristics of the structure were obtained from these tests, conducted before and after the mass of the model was augmented by lead ballast, as required by the dynamic similitude theory in order to attain a true replica, undistorted model.

The results from the experimental program were complemented by the results of analytical studies, aimed at the analytical generation of the experimentally obtained response characteristics of the model. Evaluations were made of: (1) The internal force distributions at the base, flexibility characteristics, and dynamic response characteristics of the model obtained through different experimental techniques, before and after maintaining the gravity stress level and mass similitude characteristics by auxiliary lead weights prestressed to the floor slabs; (2) These same static and dynamic response characteristics but generated analytically; and (3) The corresponding characteristics measured on the full-scale structure.

These evaluations constituted the means of attaining the following

5

objectives: (1) To assess the extent of applicability of reduced-scale model analysis in predicting the service level responses of R/C frame-wall structures. (2) To assess the reliability of predicting the initial "uncracked" static and dynamic response characteristics of frame-wall structures through the use of commonly applied analytical modeling schemes and available linear structural analysis programs.

It is of particular importance that both assessments constituting the objectives of this phase of research were carried out for the "uncracked" serviceability limit state of response, during which the "linearly elastic, homogeneous and isotropic material" assumption is most likely to be applicable. Both the theory of elastic models and theory of elastic structural analysis are based on this assumption.

It should be emphasized that testing the accuracy of the theory of elastic models and elastic structural analysis was not within the objectives of this study. These theories would be correct within the validity of their basic assumptions and postulates. The research objectives were directed instead, towards investigating whether there exists a limit state in the responses of an actual R/C frame-wall structure, for which the theories of elastic models and elastic structural analysis might be applied to yield reasonable accurate predictions of the mechanical characteristics, as well as the forces and deformations within the structure.

1.3 The Model Structure

A number of publications have documented the design, preparation of the materials, and construction of the 1/5-scale model structure (Ref. 7). The scale of the model was established in order to test the largest possible true-replica model of the full-scale structure on the earthquake simulator at EERC, U.C., Berkeley. The maximum weight capacity of the

6

earthquake simulator, 120,000 pounds, in conjuction with the gravity load and mass similitude requirements for an undistorted, true-replica model of the full-scale structure, led to the established scale of the model. The weight of the model with its foundation, and with the required auxiliary ballast in the form of lead bricks prestressed through the floor slabs, was evaluated as approximately 120,000 pounds.

The earthquake simulator, with this load, was rated to be capable of introducing base accelerations in the order of 0.6 g, velocities in the order of 20 in. per sec., and displacements of 5 in.. These limits, provided that the frequency characteristics of a base motion with high damage potential may be generated by the earthquake simulator, are considered to be adequate to induce extensive damage to the model so that its collapse limit state characteristics may be observed.

The model was designed geometrically similar to the full-scale structure tested in Tsukuba, Japan, except for the foundation. The foundation was designed in accordance with the tie-down locations of the earthquake simulator, and in order to provide fixed-base conditions with the minimum possible weight, see Fig. 1.2. The plan and elevations of the model are shown in Figs. 1.3-1.5, where all dimensions are given in dual units.

In the design of the model, it was decided to use structural materials with similar physical properties and mechanical characteristics of those materials used in the full-scale structure in Japan. The results obtained in the analytical predictions of the structure's seismic responses were evaluated with regard to the difficulties in developing model materials with similar physical and mechanical characteristics of the full-scale structure. This evaluation indicated that the behavior of the structure was controlled by the flexural behavior of its members, particularly that

7

of the shear wall. Furthermore, the inelastic behavior was controlled by the reinforcement characteristics, rather than by those of the concrete. Thus, it was decided to fabricate reinforcing bars that would be geometrically similar to those of the prototype and that would exhibit similar primary mechanical characteristics.

Three types of main reinforcement were used in the columns, beams, walls, and slabs of the full-scale structure. These were modeled on a one-to-one basis by specially fabricated deformed bars for the column and beam reinforcement, and by wire knurled in the laboratory for the slab and wall reinforcement. This wire was also used for all ties and crossties. All three types of reinforcement were subjected to heat treatment cycles until the main characteristics of their uniaxial stress-strain responses were adequately close to those of their counterparts used in the full-scale structure. The modulus of elasticity, yield strength, length of the yield plateau, initial strain hardening slope, maximum strength and the rupture strain were the parameters which were incorporated in the effort to produce similar steel response. The comparison of the model and prototype material responses are shown in Figs. 1.6-1.8, for these three reinforcement types.

Fabrication of the model reinforcement, with the stress-strain similitude shown in Figs. 1.6-1.8, was an expensive and time-consuming undertaking. These efforts and expenses were justified because a major research objective was to assess whether the state of the art in R/C model analysis would be adequate in successfully simulating all the limit-state responses of the full-scale structure, as explained in Sec. 1.2. Consequently, no conceivable measure was spared in order to satisfy the similitude requirements between the stress-strain relations of the model and prototype reinforcement.

The concrete mix designed for the construction of the model was evaluated for its maximum compressive strength, strain at maximum stress, and

8

the secant modulus of elasticity (Fig. 1.9). The unusual gain of strength after 28 days, as observed from Fig. 1.9, was not expected of the microconcrete.

The shear modulus of rigidity, Poisson's ratio, tensile strength and strain capacities, bond, interlocking, decay in interlocking under stress reversals, and the volumetric changes due to temperature, shrinkage and creep, are some characteristics of concrete which could not be directly incorporated into the efforts to maintain similitude. These characteristics of concrete are known to be consequential in all the response limit states of frame-wall structures, particularly when the shear behavior of the wall(s) governs the response. The state of the art in R/C model construction, however, was evaluated to be incapable of producing a microconcrete which would have responses similar to those of a prototype concrete, considering all the characteristics discussed above. This was assessed to be a significant limitation in R/C model analysis, as will be discussed in subsequent sections.

The reinforcement detailing of the 1/5-scale model was directly adapted from construction drawings and specifications prepared for the full-scale structure. Typical detailing of the exterior and interior frames of the model in the main response direction, as well as the detailing of the slabs, is shown in Figs. 1.10-1.12. The force transducers indicated at mid-height of the first-story columns constituted the only significant design difference between prototype and model. These transducers are discussed briefly in the next section.

1.4 Internal Force Measurements

1.4.1 General Comments and Statics

One of the main objectives in testing the 1/5-scale model was to

9

evaluate the state of the art in analytical response prediction, as discussed in Sec. 1.2. Since the distribution of internal force was considered as a response characteristic at least as important as the displacements and distortions of the structure, it was decided to measure the internal forces of all the first-story columns directly, by using specially designed force transducers located at the mid-height of the columns.

Transducers were, therefore, installed at mid-height of all the 10 peripheral columns of the first story, see Figs. 1.4 and 1.5. It may be observed from the plan of the structure shown in Fig. 1.3, that if the total shear force along the B-axis of the structure is known, then the shear force attracted by the main shear wall and the four peripheral walls (along their weak direction) may be obtained from equilibrium. As the flexural stiffness of the four peripheral walls along their weak direction may be assumed negligible, an evaluation of the shear forces resisted by the columns and the main wall at the base of the structure would be possible from the shear forces monitored by the transducers.

Determination of the total lateral force requires careful consideration. During static tests, the applied lateral forces were easily measured by load cells. During dynamic tests, however, the accelerations at all floor levels need to be measured, and the total seismic base shear then evaluated from these accelerations and the effective reactive mass of each floor level of the structure. In this procedure it is implicitly assumed that the translational mass may be considered lumped at each floor level. Since the auxiliary mass required to have similar accelerations in the 1/5-scale model and the full-scale structure was

10

approximately five times the mass of the bare 1/5-scale model, and since
this auxiliary mass was applied by laying a compact layer of lead bricks on
the floor slabs of the model structure, most of the effective translational
mass was indeed lumped at the floor levels. This will be discussed
further in Sec. 3.1.

Another consideration in evaluating the distribution of the shear
force at the base of the structure during dynamic response, is the resist-
ing force component arising from the damping of the structure. The total
damping force at a certain time instant should be estimated and incorpor-
ated in the equilibrium relations of the structure in order to evaluate
the shear forces resisted by the columns and the wall at that time.

Although the column transducers may be assumed to render the structure
statically determinate for the evaluation of shear forces at the base, this
is not the case when the distribution of axial force and flexure is con-
cerned. The four peripheral walls have substantial axial stiffness, and
the contribution of the axial forces in these members to the vertical force
and overturning moment resistance at the base remain redundant. These walls,
however, were instrumented extensively by concrete strain gages, which were
useful in estimating the axial forces in these members at the serviceability
limit state.

A further consideration in evaluating the contributions of different
components to the base overturning moment resistance during dynamic response
regards the estimation of the effective rotational mass characteristics of
the structure. The contribution of mass moments to the base overturning
moment requires the determination of the effective rotational mass and
angular accelerations in addition to the translational mass and accelera-
tions. The effective rotational mass characteristics along the structure

11

may be estimated only with uncertainty, while a direct measurement of angular acceleration is not possible. Angular accelerations are derived from measured translational accelerations, and the associated numerical process is particularly error prone. Consequently, an evaluation of the contributions of different mechanisms to the overturning resistance of the structure during dynamic response may be carried out with considerable uncertainty, even after utilizing the force transducers. The information yielded by the force transducers, however, was considered to be adequately significant and necessary for understanding structural behavior, to justify the time, expense, and effort required to incorporate these in the research.

1.4.2 Design of the Force Transducers

Detailed information regarding the design, fabrication (machining, welding, heat treating, and tempering), electronic instrumentation, calibration, and installation of the force transducers are provided elsewhere (Ref. 9). Brief information provided in this section is in order to discuss the basic problems confronted in the design and installation of the transducers as this pertains to the responses of the model structure.

The main criteria considered in the design of the transducers were: (1) The transducer was required to be sensitive enough and remain linearly elastic while monitoring the strains induced by the possible lower and upper bounds of axial force, flexure, and shear force in the columns and to enable the simultaneous recording of these internal forces independently; (2) The discontinuity in the stiffness and mass introduced at the mid-height of the first-story columns was required to be sufficiently small so as not to alter the responses of these elements at any of the response limit states. Since the stiffnesses of a column would change during different response limit states while the transducer should remain linearly elastic,

12

the axial and flexural stiffnesses of the transducer were designed to correspond to estimated average values of the corresponding column stiffnesses.

The resulting design is shown in Figs. 1.13(a), (b), and (c). Aluminum, 6061, with a minimum yield of 35 ksi and a modulus of elasticity of 10500 ksi, was selected. A hollow tube was welded to two plates, and the two sides of the tube were machined, as indicated in Fig. 1.13(a), in order to increase the sensitivity of the transducer in shear. Three strain gage bridges were used to pick up the strains corresponding to shear, axial force, and flexure independently (Ref. 9).

1.4.3 Installation of the Force Transducers

The scheme devised to install the force transducers is illustrated in Fig. 1.14. During construction of the model, the column stubs were first cast up to the level of the transducers. The reinforcement of these stubs was welded to steel plates, see Fig. 1.14. The reinforcement of the upper sides of the columns was similarly welded to steel plates, and the upper steel plates were positioned over the lower plates by means of four threaded rods, one at each corner of the plates. Dummy steel tubes were used to substitute for the transducers during the construction process (Ref. 9).

After construction was completed, the dummy tubes were removed by raising the top plate approximately 0.01 in., using the four threaded rods. The transducer subsequently was moved into place, shimmed, and the top plate lowered back to its original configuration. Hydrostone was applied

13

between the column and the transducer plates for even bearing. After the hydrostone hardened, the four corner rods were completely loosened, transferring all the force to the transducer whose end plates were bolted to the column plates by means of eight bolts.

2. EXPERIMENTAL DETERMINATION OF THE STATIC AND DYNAMIC CHARACTERISTICS OF THE BARE MODEL

2.1 Axial Force Distribution at the Base

The axial force distribution of the structure, as measured after the installation of the force transducers, is shown in Fig. 2.1. The transducers were installed 28 days after the casting of the top story, and 5 months after casting the first floor.

The average unit weight of the model material was evaluated as 144 lb/cu ft , after weighing samples of microconcrete and steel reinforcement used in the construction of the model. A computation of the member axial forces at the first floor level, based on the tributory areas of the members as shown in Fig. 2.2(a), indicated the forces shown in Fig. 2.2(b).

The sum of the axial forces at the base of the structure are computed to add up to 18.34 kips, the weight of the structure above the footing. The sum of the axial forces measured in only the columns, as shown in Fig. 2.1, is 33.02 kips, indicating that the center shear wall and the four peripheral walls should be under a tensile axial force of 14.68 kips, instead of the computed levels of compression.

Assuming that the 14.68 kips is shared by the walls proportional to their cross sectional area, the peripheral walls and the shear wall would have a tensile stress of approximately 10 psi. Such a stress was considered to be possibly caused by the different shrinkage characteristics of the columns and the relatively thinner walls. The distribution of the measured axial forces in columns adjacent to the peripheral walls are larger than those in the other columns, which would be the case due to larger shrinkage of the peripheral walls than the adjacent columns. The shrinkage coefficient of the microconcrete was estimated as approximately 750×10^{-6} in./in., from

15

shrinkage deformation measurements of 3 in. x 3 in. x 11 in. sample prisms taken during casting. Since shrinkage is inversely proportional to the square of the thickness of the member, the walls should be expected to shrink approximately ten times more than the columns. The measured stress of 10 psi was, therefore, considered to be easily caused by the differential shrinkage.

2.2 Measured Dynamic Characteristics

The foundation of the model was prestressed to the floor slab at four locations and then was subjected to ambient, free and forced vibration tests before the auxiliary mass in the form of lead "pigs" was added.

2.2.1 Ambient Vibration Tests

The ambient vibration test was carried out by placing two sensitive seismometers along the two exterior frames at the top of the structure. These seismometers were calibrated to measure velocity, and were conditioned by amplifiers capable of amplifying or attenuating and filtering the outputs of the seismometers. The outputs of the seismometers could be averaged or subtracted, giving the translational or rotational velocity at the top floor. The resulting velocity time-history was fed into a fast fourier transform spectrum analyzer, which generated the fourier spectrum of the input time-history. The frequencies for which significant power (or energy) was indicated on the fourier spectrum were picked up as the predominant response frequencies of the structure.

An example of the fourier spectrum obtained from the spectrum analyzer (FFT 512/S Real Time Spectrum Analyzer, Rockland Systems Co., California) for the main response direction of the structure is given in Fig. 2.3. It was concluded that the fundamental frequency of the model, when excited by ambient sources, was 9.75 Hz. The second and third frequencies of the model may be interpreted as 29.5 Hz. and 43.13 Hz. from this figure. These

16

frequencies are observed to contain significantly less power than the fundamental frequency.

The fundamental frequency in the transverse direction was measured in a similar manner as 13 Hz., and the fundamental torsional frequency was measured as 18 Hz.

The ambient vibration tests were repeated 12 days later, after the force transducers were installed in the structure. The fundamental frequencies of the structure in the lateral response directions were measured as 9.75 Hz. again, while the torsional frequency was 17.63 Hz., as opposed to 18 Hz. which was obtained in the previous test. The slight change in the torsional frequency may be due to a change in the stiffness characteristics of the peripheral walls, which contribute the major part of the torsional rigidity of the structure.

2.2.2 Dynamic Analyzer Tests

The dynamic characteristics of the model were then evaluated by another technique, based on the low level random excitation responses of the structure*. The structure was excited by a small vibration generator which applied random pulses of small amplitude. The accelerations at each floor level were measured at a number of locations and these were input to a Hewlett Packard Model 5423A Structural Dynamics Analyzer, which basically is a frequency response analyzer, evaluating the fast fourier transforms of the response. The frequencies corresponding to the main and transverse translational and the torsional responses were obtained in this manner as 9.75 Hz., 12.77 Hz. and 17.73 Hz., respectively. The damping coefficients corresponding to these modes were 2.36%, 4.33%, and 2.28%, respectively.

---

*Carried out by URS/John A. Blume and Associates, Engineers, Berkeley, California Office.   17

The second frequencies of the main and transverse translational responses were also evaluated as 42.54 Hz. and 56.84 Hz., with damping coefficients of 2.16% and 2.14%, respectively. Since a frequency of 29.5 Hz. was observed to contain power during the ambient vibration tests (Fig. 2.3), this was considered to possibly represent the second frequency. This is contradicted by the frequency response analyzer which gave the second frequency as 42.54 Hz. It appears that the energy indicated by the spectrum analyzer to correspond to 29.5 Hz. was misleading. This exemplifies the relative uncertainty of ambient vibration test results in evaluating higher frequencies.

2.2.3 Forced Vibration Tests

A vibration generator was installed at the roof level of the model as indicated in Fig. 2.4 in order to conduct forced vibration tests of the structure. The vibration generator consisted of two weights rotating in a synchronized manner with a certain phase difference at a determined frequency. Depending on the phase difference between the two weights, the structure may be excited by a harmonic force along either the main lateral response direction or the transverse response direction. The force in the main lateral response direction was along the axis of symmetry while the force generated in the transverse direction was with an eccentricity of approximately 20 in. with respect to the center of rigidity as shown in Fig. 2.4. The amplitude of the force was dependent on the weights, which were kept at the possible minimum, and the frequency of excitation. The maximum amplitude of the force did not exceed 5000 lbs at 10 Hz. and was smaller at lesser frequencies. The design of the vibration generator is documented by Hudson (Refs. 2, 3).

18

During the forced vibration tests, a number of accelerometers were placed on the roof and other locations of the structure. These, as well as a number of other force and displacement transducers, were monitored as the model was excited in a certain direction with a certain frequency of the harmonic force. The time-histories of the measured accelerations, displacements, and column shear forces (as obtained from the force transducers installed in the model), were plotted on visicorder paper for each frequency at which the harmonic forces were applied.

During the first vibration generator test, the model was excited along the main response direction as shown in Fig. 2.4. Harmonic force frequencies from 3.0 Hz. to 9.5 Hz. were applied. At the low (approx. 3.0 Hz. - 7.0 Hz.) and high (approx. 8.5 Hz. - 9.75 Hz.) frequencies, the measured responses were observed to indicate steady-state harmonic response patterns. Between the frequencies of 7.0 Hz. and 8.0 Hz., a phenomenon termed as "beating" was observed, as illustrated and compared against normal steady-state responses obtained for the lower frequencies in Fig. 2.5. This may be explained by a change in the response characteristics of the model structure during excitation. As the excitation frequency approaches the resonant frequency of the model, the amplitude of structural responses increases. This may result in changes in the boundary conditions (uplift or rocking of the foundation) as well as the damping characteristics of the structure (opening and closing of microcracks and/or hairline cracks in concrete). Consequently, the response amplitudes decrease as the structure "pulls itself away from resonance". Another possible explanation of this phenomenon is that there may be errors in the synchronization of the rotating masses and the structure may be excited in more than one direction, and in more

19

than one mode. This results in an interference in the responses measured along the main response direction, hence beating. One other possible reason for beating may be explained by the interaction of the structure and the shaker. Since the vibrations of the structure are input as base vibrations to the shaker which is mounted at the top of the building, the harmonic force applied by the shaker will be affected by the vibrations of the building.

When the structure was excited with frequencies between 8.0 Hz. and 8.5 Hz., the response amplitudes increased progressively until they reached a level at which steady state response was observed, without beating. The slight changes in the dynamic characteristics of the model were not adequate to result in a reduction in response amplitudes, as the forcing function frequency was too close to the resonant frequency of the structure. At a forcing function frequency of 8.25 Hz., the response amplitudes increased to a level that the vibration generator had to be turned off in order to avoid possible cracking of the structure. The shear forces in the interior columns of the side frames were measured to reach 500 lbs. during 8.25 Hz. frequency. The shear force amplitudes measured during the lower frequencies of 3.0 Hz. - 7.0 Hz. were between 5.0 lbs and 25.0 lbs.

The typical acceleration and displacement response amplitudes obtained at different excitation frequencies are presented in Figs. 2.6 - 2.8. The resonant frequency is evaluated to be 8.25 Hz. from these figures, and the average equivalent viscous damping, obtained from the bandwidth method is 2.57 percent.

2.2.4 Free Vibration Tests

A fourth type of test applied to the model structure to determine its dynamic characteristics, was the free vibration test. The structure was pulled from the roof level by a steel cable, using a turnbuckle, and the end of the turnbuckle was attached, through a shackle, to a wide flange which was anchored on the concrete slab of the laboratory. Within the line from the roof to the floor, a load cell and a #2 reinforceing bar were also included. After applying a force of approximately 4 kips, the #2 reinforcing bar was cut by using a bolt-cutter, and the tension in the cable was thus suddenly released. The outputs of accelerometers and displacement transducers were monitored as the model structure, released from an initial displacement, went through transient response.

By measuring the decay (logarithmic decrement) of acceleration and displacement responses, the approximate equivalent viscous damping was evaluated to be between 2.4% - 2.5% of critical. The dominant frequency of the transient response was obtained as 8.7 Hz., by feeding the acceleration response history to the FFT frequency analyzer as well as by counting directly the zero crossing during the free vibration response.

The main results obtained from all the previous tests are summarized in Table 2.1.

2.3 Measured Flexibility Characteristics of the Model

2.3.1 General Remarks

The flexibility characteristics of the model structure, for the lateral displacement degrees of freedom at each floor level, were obtained

in order to: (1) Compare with the flexibility characteristics after loading the model with lead ballast necessary for mass similitude and assess the significance of gravity load on the lateral flexibility; (2) Compare with the analytically generated flexibility characteristics and evaluate the analytical model used to represent the structure at the serviceability response stage; (3) Use it to generate the frequencies and the mode shapes of the structure. Since the mass distribution could be computed, the use of this computed mass and of the measured flexibility characteristics allowed the frequencies and the mode shapes of the structure to be analytically generated, and then compared with the experimental results. This comparison could be used to evaluate the reliability of the simplified analytical modeling of structures for the purposes of generating dynamic characteristics; for example, lumped modeling of mass and considering only the lateral displacement degrees of freedom (among others). Further information on this procedure is provided in Appendix A.

2.3.2 Experimental Procedure

The structure was loaded at each floor slab level by a rigid steel beam, as illustrated in Fig. 2.9. Two cables were extended to the laboratory floor from the steel beam, and were connected to steel brackets anchored to the floor. A load cell and a turnbuckle was included in each line. The load was supplied by tightening the two turn-buckles simultaneously, while checking the two load cells in order to maintain equal tension in the two cables. The vertical component of the cable tension was resisted by two 4 by 4 in. posts, shown in Fig. 2.9.

During the tests, displacement transducers (LVDT's) were used to measure the lateral displacements at each floor level and any torsional rotations at the roof level. The foundation of the model was instrumented in order to measure any rotations and displacements at this level and the readings of these instruments were used to correct the measured lateral displacements of the upper floors.

An analysis was carried out to determine the permissible levels of force that could be applied before cracking of the structure. Loads ranging from 5 kips to 15 kips were applied at the different floor levels of the structure, from roof to the first floor level, resulting in a displacement of approximately 0.05 in. at the roof level during the loading of the floors.

2.3.3 Results of the Experiments

The results of the tests are presented in Table 2.2 in the form of the flexibility matrix of the structure, for the seven lateral displacement degrees of freedom measured:

Each column k of the matrix in Table 2.2 is generated during the loading of the floor at level k, i.e., the terms $f_{7,k}$ to $f_{1,k}$ of column k represent the lateral displacements at the successive floor levels (7-1) of the structure as shown in Fig. 2.10, when loaded with a unit load applied at level k.

It is observed that the experimental flexibility matrix is not symmetric as it should be theoretically. The measured displacement

23

profiles of the structure, corresponding to loading of each floor level, and normalized for 1 kip, are shown in Fig. 2.11. It is observed that loading the lower floors of the structure led to a "shear" mode of deformation while loading the upper floors resulted in a "flexural" mode of deformation. The main shear wall governs the response of the structure, and the deformation characteristics of this wall, which has a (story) height/depth aspect ratio of 0.68 at the first floor, and 0.55 at other floors, are strongly influenced by the moment-to-shear ratio, as reflected in Fig. 2.11.

The reasons which led to unsymmetry of the generated flexibility matrix were considered to be: (1) Nonlinear response of the structure - particularly the shear wall - and particularly the shear force-shear distortion characteristics of this member. To illustrate, consider $f_{1,7}$ and $f_{7,1}$ in Table 2.2. $f_{1,7}$ represents the first floor displacement when the top floor is loaded, and $f_{7,1}$ represents the top floor displacement when the first floor is loaded. The main deformation mechanism of the wall, when the first floor is loaded, is by shear, which is not the case when the top floor is loaded. Consequently, any nonlinearity (expected in especially the shear distortion mode), would result in a loss of the reciprocity. It should be noted that when the roof was loaded only a 5 kip load was applied; however, when the first floor was loaded, a force of 15 kips was applied. Thus, in the latter case, the shear acting on the wall was considerably higher in the story below where the

24

load is applied. However, the average axial-flexural stress level in the structure produced by the 5 kips applied at the top was higher, contributing to generally larger values for the coefficients in the lower triangle of the experimental flexibility matrix. (2) Displacements of the structure caused by foundation distortion and lifting and sliding at the foundation. Although these were measured and corrections were made for these effects, these corrections were based on rigid foundation assumption. The displacements and distortions of foundation were observed to be of a different order of magnitude when the top and the first floor levels were loaded by ≈5 kips and ≈15 kips, respectively. This should be expected to disturb the reciprocity. (3) Any axial distortion of the diaphragm. Since load was applied at one face of the building while the displacements were measured along the other face, any axial distortion of diaphragm would result in an erroneous flexibility matrix. (4) Errors arising from: the application of loads; in the measurement of the loads; and in the measurement of the displacements of the structure and of the foundation.

The force distribution at the base of the structure was measured by the force transducers and results are presented in Fig. 2.12. It is observed that the shear attracted by the shear wall increases as the structure is loaded between the roof to the second floor level and then decreases when the first floor level is loaded. This indicates a change in the lateral force resisting mechanism of the wall and frames when the first floor is loaded. Also observed from Fig. 2.12 is that the incremental axial force distribution in the first floor columns during the loading of the first floor indicates compression in columns at the loading face of the building.

25

In evaluating the axial force and bending moment distributions, the contribution of the peripheral walls should be considered. These members, although they are not expected to contribute to the shear force and flexural resistances of the columns significantly, are effective in resisting axial forces. The axial forces in the exterior columns, therefore, should be interpreted accordingly.

The distribution of the shear force between the columns are observed to be different within the plan of the structure for a particular loading, despite the anticipated symmetry of the structure and the loading. When the 7th floor was loaded, the shears carried by the two exterior frames were 129 lbs.and 145 lbs., for 1000 lbs. of external force. When the first floor was loaded, the same frames were resisting 83 lbs. and 92 lbs. of shear force, respectively. Hence, either the symmetry in structural stiffness was disturbed due to errors in construction and different volumetric changes, or due to errors in the loading system.

When the first floor is loaded, the columns in the loading side are observed to resist significantly higher shear forces, indicating possible axial distortion of the diaphragm.

3. EXPERIMENTAL DETERMINATION OF STATIC AND DYNAMIC CHARACTERISTICS OF THE MODEL AFTER ADDING AUXILIARY MASS

3.1 Changes in Axial Forces at the Base

3.1.1 General Remarks

The model structure was moved on rollers on to the earthquake simulator, and was leveled, hydrostoned and prestressed through the rigid R/C platform (table) of the earthquake simulator. This platform (a ribbed R/C slab) has a weight of approximately 95 kips and is supported by 4 vertical and 3 lateral actuators. During the moving and prestressing of the model, and all the subsequent experiments which will be explained in ensuing sections, the platform was mechanically horizontally restrained by screwjacks in addition to the restraint provided by the hydraulic actuators.

The model structure was then loaded by lead bricks ("pigs") of approximately 97 lbs each, distributed on the floor slabs, and pre-stressed through the slabs, as shown in Figs. 3.1 (a), (b), and (c).

Static and dynamic tests determined the installation and prestressing scheme for the lead ballast in order to verify that the ballast would: (1) Simulate as closely as possible the effects of the actual distribution of mass on the structure, particularly on the floor beams. (2) Be excited with the same acceleration as the floor slab during all expected response frequencies; and (3) Not increase the stiffnesses of the floor slab.

3.1.2 Distribution of Axial Force

The existing mass of each floor was increased approximately 5.9

27

times to satisfy the similitude requirements for the translational
mass characteristics, as well as gravity (dead and live) loads which
were incorporated in the testing of the full-scale model in Japan. The
weights of individual floors and the added masses are given in Table 3.1.

The distribution of bending moments (along the model girders) and
the axial forces (of columns and shear wall) were investigated for the
added lead ballast. This was done to determine the layout for the bal-
last which would lead to a similar distribution of gravity forces in
the model and prototype. The computed levels of axial force at the base
of the columns and walls for the full-scale building (reduced by 1/25)
and the 1/5-scale model, are given in Fig. 3.2.

It is observed in Fig. 3.2 that the total weight at the base of
the model is 105.85 kips, while 97.24 kips is the value obtained from
the weight of the prototype. The reason for the discrepancy is that
the model ballast was calculated based on mass similitude and not the
gravity load (own weight) similitude with the full-scale building.
Since the full-scale structure was tested with the pseudo-dynamic scheme,
the masses used to evaluate the lateral forces were not based on the
actual weight of the structure but on computed dead and live load
values fed to the computer. In order to be able to correlate, the bal-
last weights added to the model (Table 3.1) were in accordance with the
hypothetical masses used by the Japanese researchers in evaluating the
loading program of the full-scale structure. Consequently, a discre-
pancy of 19 percent is observed between the axial stress levels of the
main shear wall in the model and prototype. This discrepancy was not
considered important, especially since the main shear wall of the
1/5-scale model was under 5.40 kips of tension due to the shrinkage
effects discussed earlier.

28

The distribution of axial forces in Fig. 3.2 were evaluated based on assumptions on the tributary areas for vertical members and assumptions on the distribution of the weights of individual lead bricks within the beam-slab system. The measured incremental axial forces in the column transducers are compared in Fig. 3.3 to the computed increments of axial forces due to loading the ballast.

Except for one column, the column axial forces did not increase as much as expected. The implication is that the main shear wall and peripheral walls attracted more axial force than predicted. This was considered fortunate since these components were observed to be under tensile forces due to shrinkage, as explained previously.

The measured incremental axial forces add up to 50.78 kips in Fig. 3.3. Since the total added ballast weight was 87.51 kips (Table 3.1), the main shear wall and the peripheral walls should have attracted 36.73 kips of axial force. The axial force increases in the peripheral walls were estimated from concrete strain gages to be 3.6 kips each. Consequently, the main wall would have attracted 22.33 kips of axial compression as a result of the ballast loading.

In Sec. 2.1, the center shear wall and the peripheral walls were assessed to be under a tensile axial force of 14.68 kips. The peripheral walls were estimated to be under 2.32 kips of tension each, and the main wall was estimated to be under a tension of 5.4 kips. Assuming that the distribution of axial force at the base was as measured after the installation of the transducers (Fig. 2.1), just prior to loading of the ballast and the tensile forces in the walls were as evaluated, the final axial force distribution after loading the ballast may be estimated and compared to the calculated distribution (Fig. 3.4). It is observed, from results given in

29

Fig. 3.4, that the final computed and estimated (based on transducer readings and strain gage readings) levels of axial forces in the main shear wall, peripheral walls, and the columns adjacent to the peripheral walls, are significantly different. This difference is mainly due to the different levels of initial shrinkage in the walls and columns, as explained in previous sections. Since approximately three months had elapsed since the axial force distribution (Fig. 2.1) was measured, it is likely that these forces would have changed by the time the ballast was loaded. A number of shrinkage cracks were observed in the walls prior to loading the ballast, indicating that a force redistribution would have occurred from the release of the tensile stresses in the wall concrete. Unfortunately, the history of column axial loads could not be followed accurately over long periods because of long term drift problems in the force transducers, caused by temperature cycles in the laboratory.

It may be assumed, therefore, that the differences between the calculated and measured-estimated levels of axial forces (Fig. 3.4) would represent an upper bound and that the actual forces could be expected to be closer to the calculated ones. Nevertheless, the striking differences between computed and measured distributions of axial force indicate that maintaining similitude between a model and a prototype R/C structure cannot be achieved unless all aspects of material behavior, including volumetric changes particularly due to shrinkage and creep characteristics, are similar in the model and prototype. The state of the art in microconcrete construction was not observed to be adequate to maintain such a similarity in all aspects of concrete behavior.

3.2 Measured Dynamic Characteristics of the Test Structure after Loading with Ballast

The model was subjected to (1) ambient vibration, (2) dynamic analyzer, (3) forced vibration, and (4) free vibration tests, similar to those tests carried out prior to loading the model with ballast. The results obtained are presented below.

3.2.1 Ambient Vibration Tests

These tests indicated a fundamental frequency of 4.75 Hz. in the main response direction of the model. Frequencies of 5.85 Hz. and 8.50 Hz. were obtained for the transverse translational and torsional responses.

3.2.2 Dynamic Analyzer Tests

These tests indicated first and second mode frequencies of 4.78 Hz. and 17.86 Hz. in the main response direction, and viscous damping coefficients of 2.20 and 2.52% corresponding to these two modes, respectively. The torsional mode response frequency was measured as 8.49 Hz. with a damping coefficient of 2.18 percent of critical.

The frequencies, mode shapes and damping coefficients of the transverse response direction could not be generated because of a significant response of the shaking table on which the structure was prestressed. Although the table was mechanically restrained in the main response direction, it was restrained only by hydraulic cylinders in the transverse response direction. This restraint was discovered to be inadequate to generate fixed-base responses of the model, and the table vibrated with a frequency and lateral displacement magnitude close to that of the model in the transverse response direction.

3.2.3. Forced Vibration Tests

The forced vibration tests were repeated after loading the model with lead
ballast (Fig. 3.5). Two accelerometers mounted on the roof of the structure
were used to monitor and record the responses of the structure to different
excitation force frequencies.

The responses of the structure along the main response direction were
obtained for frequencies between 4.00 Hz. and 4.80 Hz. It was observed
that the responses of the structure exhibited significant "beating", a
phenomenon discussed in earlier sections. The test results as obtained
from the roof level accelerometers are presented in Figs. 3.6 and 3.7.

It is observed from Figs. 3.6 and 3.7 that the response amplitudes
of the two roof accelerometers, oriented in the main response direction
along the two exterior frames, are different by approximately 20%. This
may be due to a misalignment in the vibration generator or a mis-
synchronization of the rotating weights, resulting in a torsional response
component.

The minimum and maximum response amplitudes measured during each
frequency of the forcing function are indicated in Figs. 3.6 and 3.7,
as a measure of the beating. Further investigations of this phenomenon
indicated that this may be due to a change in the frequency of the forcing
function caused by the response of the structure. As the structure
vibrated, the frequency of this vibration affected the effective frequency
of the rotating weights. In other words, as the frequency of the forcing
function depended on the circular frequency of the rotating masses
relative to the structure, and since the frequencies of the rotating

masses were being affected by the response of the structure, the effective forcing function frequency may continuously change during response, leading to the phenomenon of beating.

The main frequency of the structure was obtained to be 4.55 Hz. with an average damping coefficient of 2.03%. The average amplitude-frequency relations were used to evaluate the damping.

An attempt was made to obtain the fundamental frequencies of the transverse and torsional responses of the structure. The rotating masses were used to apply a harmonic force along the transverse response direction, with an eccentricity with respect to the center of rigidity, as shown in Fig. 2.4 and discussed in the previous sections. The two roof accelerometers were placed at each end of the building oriented in the transverse response direction. From the measurement of the responses of these two accelerometers, the average translational and rotational response amplitudes at each forcing frequency were obtained and are shown in Fig. 3.8.

The average amplitude-forcing function frequency relations in Fig. 3.8 are not similar to the curves obtained for the main response direction. A significant interaction between the two modes of response is observed. The possible contribution of the response at the base of the structure, due to inadequate restraining of the earthquake simulators' platform in the transverse direction, should also be acknowledged.

The fundamental frequencies in the transverse translational and torsional response modes may be evaluated as 5.9 Hz. and 7.8 Hz., respectively, from Fig. 3.8. The damping coefficients obtained for these responses were approximately 8 and 6 percents, which are not realistic values. Since the two amplitude-frequency relations in Fig. 3.8 correspond to mixed responses, i.e., responses which do not represent one mode only, and since there may be considerable dissipation of energy due to the vibration of the shaking table, the damping quantities evaluated from Fig. 3.8 are not correct viscous damping coefficients for the two response modes considered.

3.2.4 Free Vibration Tests

The free vibration tests carried out on the model structure loaded with ballast indicated an average damping coefficient of 1.94% and a fundamental frequency of 4.75 Hz. in the main response direction. The testing procedure was as discussed in Sec. 2.2.4. The maximum force applied to the structure was approximately 4 kips. The cable was cut and free vibrations were initiated. The damping coefficients computed from the decay of the roof accelerations varied between a low of 1.37% and a high of 2.18%, as evaluated from the acceleration time histories of the roof level, yielding an average value of 1.94%.

3.3 Measured Flexibility Characteristics of the Model after Loading It with Ballast

3.3.1 General Remarks

The test procedure to obtain the flexibility coefficients of the model was similar to that explained previously in Sec. 2.3.2. The photographs in Figs.3.9 and 3.10 show the loading system and the instrumentation frame. Rotations (rocking) and lateral displacements of the shaking table were measured at all load steps. The structural displacements were then corrected by eliminating the rigid body components induced due to the displacements and rotations of the shaking table.

3.3.2 Results of the Experiments

The test results are presented in Table 3.2 in the form of the flexibility matrix of the structure loaded with ballast. The lateral displacement degrees of freedom were as explained for Table 2.2, Sect. 2.3.3.

The measured displacement profiles of the structure, for loading of each floor level, are shown in Fig. 3.11. These displacement profiles are normalized for a unit value of the lateral load.

The flexibility matrix shown in Table 3.2 is not symmetric, as was the matrix obtained for the structure prior to loading it with ballast, and presented in Table 2.2. The reasons considered for the loss of reciprocity of the flexibility matrix in Table 2.2 are also valid for the matrix presented in Table 3.2.

A comparison of the flexibility matrices in Tables 2.2 and 3.2, and the displacement profiles in Figs. 2.11 and 3.11 led to a number of observations. The flexibility coefficients decreased and the floor rotations along the structure increased when the model was loaded with ballast required to satisfy similitude requirements for mass and gravity load characteristics of the model.

The decrease in the diagonal flexibility coefficients $f_{1,1}$ to $f_{7,7}$ range from 28% to 35%, indicating an average increase in the structural stiffness of approximately 30%. Comparing the displacement profiles in Figs. 2.11 and 3.11, the decrease in the flexibility coefficients, when the upper 7th, 6th, and 5th floor levels were loaded, is observed to be more for the lower floor levels than the upper floor levels. This is better exemplified by comparing the first columns (j=7) of the two flexibility matrices in Tables 2.2 and 3.2, representing the displacements of the structure, when loaded at the top floor with a unit load, prior to and after loading the ballast. The top floor displacement ($f_{7,7}$ terms), decreased from 15.59×10^{-3} in. to 11.26×10^{-3} in., by 28%. The reduction in the third floor displacement was 42%, and in the first floor the reduction was 46%.

When the first floor was loaded laterally, the last columns (j=1) of the two flexibility matrices were obtained. The reductions in the top, third and first floor displacements, after loading the ballast, were obtained as 48, 44, and 32 percents respectively. The displacements of the upper floors were reduced more than those of the lower floors, unlike when the top floor was loaded laterally.

The results of an intermediate test, carried out prior to loading the structure with ballast, may be useful in discussing the reasons for the different manners in which gravity loading affected lateral flexibilities of the structure. In this test the top of the structure was loaded with 14 kips of ballast, and from the transducer readings it was evaluated that the increase in the axial load at the base of the main shear wall was just sufficient to overcome the axial tension in this member due to shrinkage.

The flexibility coefficients obtained during the loading of the top floor and the first floor, for no ballast load, 14 kips of ballast load,

36

and the full 87.5 kips of ballast load, are compared in Table 3.3.

When the top floor was loaded laterally, the decrease in the top floor deflection was 6% when 14 kips of ballast was placed at the roof, and the decrease became 28% when the full 87.5 kips of ballast was distributed in the seven floors of the model. Meanwhile, the decrease in the first floor deflection was 12% when 14 kips of ballast was added, and became 46% when the model was loaded with the total 87.5 kips of ballast.

When the first floor was loaded laterally, the decreases in the top displacements were 12% and 48% for 14 kips and 87.5 kips of ballast load, respectively. The corresponding decreases in the first floor displacements were 4% and 32%, respectively.

The lateral displacements in Table 3.3 were sketched in Figs. 3.12 and 3.13 to further illustrate how axial forces due gravity loads affect the lateral displacement characteristics of the structure differently, depending on whether the structure is laterally loaded at the top floor or at the first floor levels, i.e., with different overturning moment to base shear ratios.

The behavior observed from Table 3.3 and Figs. 3.12 and 3.13 may be explained if the relative contributions of the walls and frames to the stiffness of the building are considered. Since the shear wall dominates the response of the structure, any increase in the stiffness of this element due to increases in its axial compression level reflects on the responses of the structure.

When the structure is loaded at the roof level and axial loads are increased, since the wall contributes more to the stiffness of the

37

lower floors, the stiffness of these floors increase more than the stiffness of the upper floors. When the structure is loaded at the first floor level, the displacements of the upper floors are affected significantly by the relative contributions of the rotation and lateral displacements of the wall at the first floor level. Increasing axial force results in an increase in the wall stiffnesses and, therefore, the wall rotation and displacement at the first floor level is reduced. The reduction in particularly the rotation of the wall at the first floor level contributes significantly to reducing the displacements of the upper levels of the structure. This is demonstrated in Fig. 3.13 by relating the displacements of upper floors to the displacement and rotation at the first floor, by assuming a bilinear displacement profile of the structure.

The internal force distributions of the structure measured by the column transducers during the static tests are presented in Fig. 3.14. The shear forces attracted by the wall and the columns remain approximately constant at 83% and 17% of the total applied force. The minimum contribution of the wall was when the fourth floor was loaded, as 80.45%, and the maximum was when the second floor was loaded, as 88.01%. When the structure was tested without ballast, the contribution of the wall to the total base shear changed between 66.72% for loading at the top and 80.68% for loading at the second floor level. The average contribution was 73.58% for loading at all floor levels.

It is observed from these figures that the ballast load resulted in a larger increase in the wall stiffness at each floor than the frame stiffnesses. The ballast load resulted in a change of the first story wall axial stress from $\approx (-)10$ psi (tension) to 195 psi (compression), i.e., a total change of 205 psi. The change in the interior columns of

38

the side frames was from ≈129 psi (compression) to ≈548 psi, i.e., –
a change of 319 psi >>205 psi. For the end columns of the center frame,
which attract the least gravity load, the axial stress level changed from
≈256 psi to ≈426 psi, (i.e., 168 psi < 205 psi) upon the application
of the ballast. It appears that in most cases the column stiffnesses
were not affected from this as much as the shear wall, although the
increase in column axial stress level was more.

The balanced axial force levels for the columns and the shear
wall were calculated to be approximately 25 kips (1563 psi) and
175 kips (2000 psi), respectively, indicating that the columns at the
base of the structure had axial force levels varying from approximately
25% to 40% of their balanced axial force level upon loading of the
ballast. The shear wall, however, was loaded to only 10% of
its balanced axial force level. However, even this small amount
of axial compression increased the stiffness characteristics of
the shear wall considerably, and the stiffness of the shear wall,
relative to the sum of all the frame components, was increased from
≈74% to 83%. It becomes apparent, then that the manner in which the axial
force affects lateral response is different for the wall members than
for the more slender frame members, and the mathematical idealization
of wall members in exactly the same manner as frame members may lead to
significant errors in displacements and lateral force distributions
obtained for linear response stages. This will be investigated further
in the subsequent sections.

39

4. ANALYTICAL PREDICTIONS OF THE STATIC AND DYNAMIC CHARACTERISTICS OF THE MODEL

4.1 Analytical Model

Analytical studies were carried out to evaluate whether the linear analysis procedures, commonly applied for the serviceability limit state response prediction of reinforced concrete structures, are successful in simulating the experimentally obtained response of the building.

The analytical model was constructed in conjunction with the computer code ETABS (Ref. 10). Analytical studies were confined to investigating the static and dynamic characteristics in the loading direction of the model. The transverse and torsional characteristics were not studied.

The topological idealization of the structure is shown in Fig. 4.1. The two exterior frames and one interior frame were discretized into 1-D elements connected through rigid zones, except for the shear wall elements, for which rigid end zones were not considered.

The column, shear wall and typical beam cross sections, considered in determining the cross sectional properties of the analytical elements are shown in Fig. 4.2. The columns and shear wall had constant cross sectional characteristics throughout the elevation of the structure. Uncracked transformed cross-sectional properties were used for these elements.

The contribution of the axial stiffnesses of the peripheral walls was incorporated in the model by modifying the axial stiffness of the adjoining columns to include the axial stiffness of these walls.

One set of beam cross sectional properties was used to represent all the beams of the exterior and interior frames. The contribution of the slab concrete and steel in the initial lateral stiffnesses of the model was estimated to be represented approximately by one-quarter of the

Preceding page blank

adjacent span, as indicated in Fig. 4.2.

The modulus of elasticity, E_c, of 3500 ksi assigned for concrete, was evaluated from the stress-strain relationships obtained from tests on 3 in. x 6 in. concrete cylinders, and tested under constant strain. This value is an estimated value between the initial tangent E_c and the secant modulus of elasticity measured at 45% of the maximum strength of the cylinders which was 3150 ksi. The secant modulus of elasticity at lower stress levels was naturally larger. The value of 3500 ksi was close to the value of the initial tangent modulus of elasticity and it agrees with the average dynamic modulus obtained by sonic tests. This value of 3500 ksi for E_c was considered to be a good estimation of the E_c for the "uncracked" serviceability limit state stress levels.

The shear modulus G was assumed to be related to E by the Hook's law and using for Poisson's ratio the value of 0.2.

The model was assumed to be fixed at the base and the contributions of the transverse beams to the stiffness in the main response direction were neglected.

The mass characteristics were derived from Table 3.1.

The basic assumptions and limitations described in the ETABS Manual were assumed to be valid.

4.2 Results of Analyses

The model of Fig. 4.1 was analyzed to obtain: (1) frequencies and mode shapes with and without the ballast load; (2) flexibility matrix; (3) displacement profiles; and (4) the internal force distribution at the base, in order to directly compare with the experimental results.

42

The frequencies and mode shapes of the structure, considered with and without ballast, are presented in Fig. 4.3. The flexibility matrix is presented in Table 4.1. The displacement profiles and internal force distributions are given in Figs. 4.4 and 4.5 respectively.

The analytical and experimental results obtained are evaluated in the next Chapter.

5. EVALUATION OF THE EXPERIMENTAL AND ANALYTICAL RESULTS

5.1 Dynamic Characteristics of the Building

The fundamental frequencies and damping coefficients of the model in the loading direction with and without the added ballast, and obtained analytically and by different experimental techniques, are tabulated in Table 5.1. The last row in Table 5.1 was obtained by using the measured flexibility and actual masses and solving the eigenvalue problem, i.e., a semi-analytical procedure. This procedure is discussed further in Appendix A. In the attempts to obtain a stiffness matrix for the bare model, by inverting the experimental flexibility matrix, it was discovered that the flexibility matrix was not positive-definite. The possible manner in which the experimental flexibility matrix may be "conditioned" to yield a positive-definite stiffness matrix and a solution to the eigenvalue problem, is discussed in Appendix A.

Considering first the case of model without ballast, i.e., the values in the first column of Table 5.1, significant differences between the frequencies obtained by different experimental techniques are observed. The difference between the frequencies obtained by forced and ambient vibration methods differ by more than 15%. Although it is already well recognized that forced vibration leads to a lower frequency value than ambient vibration, the difference in this case is higher than usually observed. This may be because of the larger stress levels and foundation displacements and distortions induced during the forced vibrations. However, more important is that the weight of the shakers

Preceding page blank

added some significant mass to the roof (0.73 kips). The most striking

observation, however, is the difference between the analytical and

experimental frequencies. The analytical model is observed to yield

a frequency 28% larger than the highest experimental frequency.

Considering the case of model loaded with lead ballast, i.e.,

the second column of Table 5.1, the difference between the frequencies

obtained by different experimental techniques are observed to be less.

The maximum discrepancy is less than 5%. As the base fixity of the

structure loaded with ballast and prestressed to the shaking table was

significantly improved as compared to the previous tests, i.e., without bal-

last, this difference is possibly related to mainly the gravity stress lev-

el. As the ballast resulted in considerable gravity stress level already,

the different dynamic tests may not have caused a significant difference

in the average stress level of the structure as was the case prior to

loading of the ballast, thus improving the correlation between the different

types of tests shown in column 2 of Table 5.1. It should also be noted

that in the forced vibration tests of the loaded model, the mass equal

to the weight of shaker was removed from the roof to have the same

total mass during all dynamic tests.

Comparing the analytical to the experimental frequencies, the

discrepancy is observed to be 7 percent in the case of the ambient

and free vibration results. This is considerably less than the 28 per-

cent difference observed for the first column in Table 5.1. The reason

for a better accordance between the experimental and analytical frequencies after loading of the ballast, was discovered to be due to considerable increase in structural stiffness caused by the increase in gravity load, i.e., particularly due to increase in axial stress level of the columns and main wall. This is exemplified in the following and will be discussed further in the next section.

If the complete structure may be idealized as a single degree of freedom system with a mass equal to the existing mass of the structure, (Table 3.1), the stiffness corresponding to the frequency of 9.75 Hz. would be:

$$k_1 = (2\pi f)^2 \, m = (2x\pi x \, 9.75)^2 \times (17.88/386.2) = 173.75 \text{ kip/in.}$$

after loading the structure with ballast, the equivalent stiffness corresponding to the frequency of 4.75 Hz. may be obtained in a similar manner using the total mass of the structure with ballast (Table 3.1):

$$k_2 = (2x\pi x \, 4.75)^2 \times (105.39/386.2) \cong 243.07 \text{ kip/in.}$$

It follows that the added gravity load has caused an increase in the lateral stiffness of 40 percent. This is a significant change and indicates that model testing without the correct simulation of the gravity load level as required by the similitude theory, may lead to considerable distortion in the lateral stiffness characteristics of the model. Similarly, two identical structures loaded differently with live load (gravity forces) may have quite different lateral stiffnesses. This has not been carefully considered in interpreting the measured vs. analytically obtained dynamic characteristics of real buildings.

47

An interesting comparison may be carried out by considering the fundamental frequency obtained for the full-scale structure through a free vibration test, 2.33 Hz., and the 4.75 Hz. obtained for the model using the same test procedure. The frequency of the full scale structure should be modified by multiplying with $\sqrt{5}$, to convert to the model time reference. In this manner, 5.20 Hz. is obtained. This is 9.5% higher than the model frequency. It should also be considered, however, that the mass of the model was not modeled after the existing weight of the full-scale structure, but after the hypothetical mass used in the pseudo-dynamic test procedure. The actual weight of the full-scale structure, computed based on a specific gravity of 150 lb/cu.ft., was obtained as 2431 kips. At the 1/5 scale, this would correspond to 97.24 kips. The total weight of the model, however, was evaluated as 105.85 kips. If the frequency of 5.20 Hz. is modified by square root of the ratio of existing weights of the model and prototype, 4.98 Hz. is obtained This is approximately what the full-scale structures' frequency at the model's scale would have been, if it actually were as heavy as the model.

Considering the second frequency in the main response direction, the value obtained for the full-scale structure was 9.09 Hz. After correcting for the model scale and mass, this becomes 18.60 Hz. The corresponding value obtained for the model from the dynamic analyzer tests was 17.86 Hz.

5.2 The Flexibility Characteristics of the Building

Comparison of the experimental results have indicated significant changes in the flexibility characteristics of the structure upon the application of the ballast load. An evaluation of the experimental

48

displacement profiles in the previous sections have indicated significant changes both in the magnitude and distribution of displacements (drifts) along the structure due to the ballast load. It was also evaluated that the ballast load contributed more to the stiffness of the shear wall than to the frame elements.

An evaluation of the measured and analytically generated dynamic characteristics of the structure in the previous section indicated that the addition of the ballast load resulted in an increase of average structural stiffness in the order of 40%. The linear-elastic analytical model used to define the stiffness characteristics of the structure did not recognize such a significant contribution of axial force on the member lateral stiffnesses.

In order to be able to explain the inadequacy of the analytical model to recognize the observed effect of axial force, the displacement profiles obtained from the tests of the model, test of the full-scale structure, and analysis are compared in Fig. 5.1, for the two lateral loading cases of the top and the first floors.

In both cases, the analytical results and the experimental results obtained on the full-scale structure (converted to the model scale) and the model structure loaded with ballast are in good agreement, i.e., within ≈10% of each other. The experimental results obtained on the model structure prior to its loading with the ballast, however, are as much as ≈100% apart, as observed in Fig. 5.1.

The significance of maintaining the proper level and distribution of the gravity forces during scaled model testing of R/C structures becomes apparent from Fig. 5.1. The effects of different amounts of

shrinkage in walls and columns in regard to proper distribution of the gravity loads at the base of the structure, were discussed earlier. Estimated and calculated distributions of axial force at the base are given in Fig. 3.4.

The difference in the shrinkage between walls and columns resulted in a decrease of wall axial force from 26.37 kips to 16.93 kips. Since the balanced axial force level of this member was evaluated as 175 kips, the difference between 16.93 kips and 26.37 kips might appear insignificant. After observing the contribution of the ballast in Fig. 5.1, however, the significance of the discrepancy caused by different shrinkage of walls and columns becomes apparent. The decrease in axial force of the shear wall due to shrinkage of approximately 10 kips, is more than a third of the expected level of compression in this element due to the full gravity load. This points out the need to consider all the mechanical characteristics of the materials in satisfying the similitude requirements and not just the uniaxial monotonic stress-strain characteristics obtained from compression tests of cylinders.

The mechanisms through which the increase in the gravity load could affect structural stiffness and the reasons for the inadequacy of the analytical model to incorporate these mechanisms were investigated further.

The displacement profiles in Fig. 5.1 indicated a larger contribution of axial force to stiffness when the first floor of the structure was loaded. Since the contribution of the shear deformation in the shear wall to the total displacement was more significant when the walls were loaded with low moment to shear ratios, as associated with the loading of the first floor, the mechanism of the shear deformation of the wall was investigated further.

50

Considering the main shear wall as an isolated cantilever element, the effect of different shear moduli, G, on the analytical flexibility was computed as shown in Fig. 5.2. The effects of increasing only the shear distortion terms in the flexibility by a factor of 4 (i.e., G/4) and 10 (i.e., G/10) are observed in this figure. The contribution of shear terms is observed to be very significant throughout the elevation of the shear wall. The differences in flexibilities obtained by (1) neglecting shear distortions,and (2) incorporating shear distortions corresponding to a shear modulus which was 25% of the nominal value used in the analysis, were :(1) 12.2 times for the first floor level, and (2) 1.34 times for the seventh floor level. These observations,therefore,indicated that errors in the shear modulus of concrete, and/or the manner in which the shear distortions were incorporated in the analytical model,may easily cause the discrepancy between the analytical and the experimental results obtained prior to loading of the ballast.

The analysis of the structure was repeated to observe the possible effects of different assumptions on the shear rigidity of only the shear wall on the displacements of the complete structure. The results for the loading cases of the top floor and first floor are presented in Figs. 5.3 and 5.4. Since the shear wall dominated the response of the total structure, any assumption on the shear rigidity of this element is observed to be extremely consequential in the responses of the total structure. It is observed from the structural responses in Figs. 5.3 and 5.4 that it may be possible to explain, by the changes in the shear rigidity of the shear wall, the discrepancy between analytical and experimental results as well as different experimental results obtained prior to and after loading of the structure with ballast.

It is important to note that the actual shear displacement mechanism of the shear wall may be considerably different than as idealized in the

51

analytical model, even at the uncracked stage. The force-displacement

relations of a typical element may be transformed into the flexibility

relation presented in Fig. 5.5. The axial and lateral degrees

of freedom are not related. Shear distortions and flexural distortions are

related as shown, and are evaluated from cross sectional shear and flexural

rigidities, GA_V and EI assumed to be constant throughout the element.

These rigidities relate the shear force and bending moment at any cross

section, to the average shearing strain and curvature at that cross section.

E and G are related through the Hooke's Law, assuming isotropic material, as:

$$E/G = 2(1+\nu)$$

where ν is the Poisson's ratio. In the linear structural analysis

computer code ETABS, the Poisson's ratio is assumed to be 0.20, and the

corresponding value of G is used to generate the element stiffness

matrices.

In reality, even if the force-displacement relations given in

Fig. 5.5 may be assumed to represent the response of an R/C wall element

at the uncracked serviceability level, both E and G would depend on the

level of axial stress in the member as well as the strain gradient

over the cross section.

The secant modulus of elasticity at 45% of f_c', obtained from

constant strain testing of representative concrete cylinders of the

model material, may be considered to represent a reasonable average

quantity for E, at a stress level representative of the service level.

The value of G, however, is considerably difficult to establish. The value

of the Poisson's ratio, measured from concrete cylinder tests, varied

from 0.15 to 0.40, depending on the level of the axial stress. At

0.45 f_c', the value of ν was observed to approach 0.20. Although the

validity of the relation between ν, E and G as given by the Hooke's Law

is questionable in the case of concrete, the dependence of ν on the axial stress level is evidence that G should also be dependent on the axial stress level.

As conclusion, a plausible explanation for the stiffening of the structure by the added ballast weight, and the inability of the analytical model to simulate the structure prior to loading of the ballast, may be mainly through the effect of axial force on the shear stiffness of the shear wall. Before the loading of the ballast, due to different shrinkage characteristics of the walls and columns, the shear wall was subjected to tension. This should have resulted in a significant reduction of the shear rigidity and flexural stiffness of the wall, and have led to the displacements shown in Figs. 5.3 and 5.4 for the bare model. The flexural stiffnesses should also be expected to be less than as depicted in the analytical model, because due to the shrinkage tensile stress already, some cracks were detected.

When the ballast load is applied, the increase in axial compression would contribute to increasing the flexural stiffnesses, and particularly the shear stiffness of the wall, so that the experimental and analytical responses would now be considerably closer, as observed from Figs. 5.3 and 5.4.

6. CONCLUSIONS

From the results obtained in the experimental and analytical studies conducted to determine the static and dynamic mechanical characteristics of the 1/5-scale model, the following main observations can be drawn:

(1) There was good agreement among the values obtained for the model dynamic characteristics using different methods when the model was loaded with the artificial mass (lead ballast) necessary to satisfy similitude laws. Forced and free vibrations led to somewhat larger values of periods of the model, which are considered to be more realistic than the other methods.

(2) The results obtained from the loaded model agree very well with those reported by Japanese researchers for the full-scale test building when the slight differences in the weight (mass) are included.

(3) The experimental results also are in good agreement with the analytical prediction.

(4) The results obtained for the static as well as the dynamic characteristics of the bare, unloaded model (i.e., without lead ballast) neither agree with those expected from theory nor with those expected from the values of the loaded model.

(5) Although every possible effort was undertaken to satisfy the similitude requirements for the model materials, some of the concrete characteristics could not be incorporated in the microconcrete chosen to construct the model. The uniaxial compressive stress-strain relations attained for the model microconcrete were quite similar to the relations obtained for the material of the full-scale structure. This was the basis of selection of the model microconcrete, and it was considered at the time that this

Preceding page blank

might be adequate for a reasonable representation of the prototype material. Volumetric changes, particularly shrinkage characteristics and tensile strength of the concrete, were not considered.

After construction of the model, it was observed that the shrinkage of concrete, particularly the difference in the shrinkage of members of different sizes, was significant. Consequently, if one is interested in predicting behavior at the service load range, attempting to achieve just similitude of the uniaxial compressive stress-strain relation of the concrete material is not enough for fabrication of a "true replica" small- or medium-scaled model of an R/C structure. In fact, it is very doubtful that an adequate level of similitude may be at all attainable between full-scale concrete and microconcrete used for models of medium and small scale. This leads to a need to reevaluate the objectives in model testing, and whether testing of large-scale models is the only way to achieve "true replica" models when it is of interest to predict the behavior under small load at or below service level.

(6) In model tests of R/C frame-wall structures or subassemblages of such structures, representation of the correct axial force levels, particularly on wall elements, was observed to be extremely significant in correlation of the results obtained from the tests on different scale models. Even slight changes in the axial force level of a wall element, which might be only a small fraction of its balanced load level, was observed to affect significantly the lateral stiffness characteristics of the element. The shear stiffness was affected significantly more than the flexural stiffness.

(7) In the service level linear elastic analysis of frame-wall structures, the relation of the moduli of elasticity and rigidity, E and G, with the axial stress level, should be considered. In the one-dimensional

56

line element modeling of walls which can undergo considerable changes in their level of axial forces, the shear rigidity corresponding to the expected axial force level of the wall should be incorporated, rather than a constant value as is usually considered.

(8) In view of the above results, serious doubts are raised regarding the soundness of predicted responses of frame-wall structures based on analytical models that do not consider the variation, with change in level of axial forces, of stiffness (flexural and shear) of the structure's members.

Experimental research, to investigate the representative values of shear stiffness, in function of the axial load levels and moment to shear ratios of wall elements, is urgently needed.

REFERENCES

1. Bertero, V. V., and Clough, R. W., Research Proposal to National Science Foundation on "The Shaking Table Tests of a 7-Story Medium Scale R/C Frame-Wall Structural System," as part of the U.S.-Japan Cooperative Research Program.

2. Hudson, D. E., "A New Vibration Exciter for Dynamic Test of Full-Scale Structures," Earthquake Engineering Research Laboratory, California Institute of Technology, Pasadena, CA, Sept. 1961.

3. Hudson, D. E., "Synchronized Vibration Generators for Dynamic Tests of Full-Scale Structures," Earthquake Engineering Research Laboratory, California Institute of Technology, Pasadena, CA, Nov. 1962.

4. Mahin, S. A., and Williams, M. E., "Computer Controlled Seismic Performance Testing." Paper presented at the Second ASCE-EMD Specialty Conference on Dynamic Response of Structures, Atlanta, GA, Jan. 1981.

5. Proceedings of the First U.S.-Japan Joint Technical Coordination Committee Meeting, Building Research Institute, Tsukuba, Japan, Jan. 1981.

6. Proceedings of the Second U.S.-Japan Joint Technical Coordination Committee Meeting, Building Research Institute, Tsukuba, Japan, July 1981.

7. Proceedings of the Third U.S.-Japan Joint Technical Coordination Committee Meeting, Building Research Institute, Tsukuba, Japan, July 1982.

8. "Recommendations for a U.S.-Japan Cooperative Research Program Utilizing Large-Scale Testing Facilities," U.S.-Japan Planning

Preceding page blank

Group, Report No. UCB/EERC-79/26, Earthquake Engineering Research
Center, University of California, Berkeley, CA., Sept. 1979.

9. Sause, R., and Bertero, V. V., "A Transducer for Measuring
    the Internal Forces in the Columns of a Frame-Wall Reinforced
    Concrete Structure," Report No. UCB/EERC-83/05, Earthquake Engin-
    eering Research Center, University of California, Berkeley, CA.,
    May 1983.

10. Wilson, E. L., Hollings, J. P., and Dovey, H. H., "Three Dimensional
    Analysis of Building Systems-Extended Version," Report No. EERC
    75-13, Revised March 1979, Distributed by NISEE Computer Applications,
    University of California, Berkeley, CA.

TABLES

TABLE 2.1

RESULTS OF EXPERIMENTS CONDUCTED ON BARE
MODEL TO DETERMINE THE DYNAMIC CHARACTERISTICS

TECHNIQUE DYNAMIC CHARACTERISTICS	AMBIENT VIBRATION	DYNAMIC ANALYZER	FORCED VIBRATION	FREE VIBRATION
Fundamental Frequency and Damping Ratio Longitudinal Direction	9.75 Hz. ---	9.75 Hz. 2.4%	8.25 Hz. 2.6%	8.70 Hz. 2.5%
Fundamental Frequency, Torsional Vibrations	18 Hz.	17.73 Hz.	---	---
Fundamental Frequency, Transverse Direction	13 Hz.	12.77 Hz.	---	---

Preceding page blank

TABLE 2.2

LATERAL FLEXIBILITY MATRIX FOR THE BARE UNLOADED MODEL
Units (10^{-3} in./kip)

Columns j i Rows	7	6	5	4	3	2	1
7	15.59	13.49	10.81	7.96	5.64	3.54	1.92
6	13.14	11.87	9.77	7.06	5.15	3.28	1.71
5	10.47	9.68	8.08	6.17	4.51	2.86	1.58
4	8.04	7.66	6.49	5.20	3.94	2.56	1.38
3	5.73	5.56	4.77	3.89	3.21	2.16	1.19
2	3.80	3.73	3.25	2.66	2.27	1.77	0.99
1	1.98	1.93	1.71	1.41	1.22	1.00	0.74

Column and row numbers correspond directly to the floor levels
of the structure.

1 in./kip = 5.59 mm/kN

64

TABLE 3.1

WEIGHT OF INDIVIDUAL FLOORS OF THE MODEL

FLOORS: (CONCEIVED FOR MASS MODELING)		MODEL WEIGHT* KIPS	ADDED BALLAST WEIGHT** KIPS	TOTAL WEIGHT KIPS	TOTAL WEIGHT REQUIRED FOR SIMILITUDE KIPS
7 m_7		2.24	11.80	14.04	13.83
6 m_6		2.59	12.58	15.17	14.99
5 m_5		2.59	12.57	15.16	14.99
4 m_4		2.59	12.62	15.21	14.99
3 m_3		2.59	12.55	15.14	14.99
2 m_2		2.59	12.57	15.16	14.99
1 m_1		2.69	12.82	15.51	15.24
G	TOTALS	17.88	87.51	105.39	104.02

* Total weight of model, including full length of first floor vertical members, is calculated as 18.34 kips.

** Including all fixtures.

1 kip = 453 kg

65

TABLE 3.2

THE 7x7 FLEXIBILITY MATRIX FOR THE MODEL
LOADED WITH THE AUXILIARY WEIGHT
Units (10^{-3} in./kip)

Columns j i Rows	7	6	5	4	3	2	1
7	11.26	8.99	7.26	5.31	3.78	2.22	0.99
6	9.24	7.84	6.49	4.78	3.42	2.06	0.92
5	7.07	6.23	5.51	4.15	2.97	1.85	0.24
4	5.08	4.68	4.27	3.49	2.53	1.63	0.74
3	3.35	3.20	3.07	2.55	2.08	1.40	0.66
2	2.05	1.94	1.88	1.62	1.39	1.15	0.58
1	1.06	0.88	0.87	0.79	0.71	0.64	0.50

Column and row numbers correspond directly to the floor
levels of the structure.

1 in./kip = 5.59 mm/kN

TABLE 3.3

LATERAL EFFECT OF GRAVITY LOAD ON ROOF AND FIRST FLOOR FLEXIBILITY COEFFICIENTS

FLOOR LEVEL	DISPLACEMENTS AT EACH FLOOR LEVEL, 10^{-3} in., NORMALIZED FOR UNIT LATERAL FORCE					
	LOADING OF TOP FLOOR			LOADING OF FIRST FLOOR		
	NO BALLAST	14 KIPS OF BALLAST	87.5 KIPS OF BALLAST	NO BALLAST	14 KIPS OF BALLAST	87.5 KIPS OF BALLAST
7	15.59	14.60	11.26	1.92	1.69	0.99
6	13.14	12.14	9.24	1.71	1.56	0.92
5	10.47	9.59	7.07	1.58	1.37	0.84
4	8.04	7.26	5.08	1.38	1.23	0.74
3	5.73	5.15	3.35	1.19	1.07	0.66
2	3.80	3.38	2.05	0.99	0.91	0.58
1	1.98	1.78	1.06	0.74	0.71	0.50

1 kip = 453 kg

1 in. = 25.4 mm

TABLE 4.1

ANALYTICALLY GENERATED FLEXIBILITY MATRIX
OF THE MODEL
Units (10^{-3} in./kip)

Columns i Rows j	7	6	5	4	3	2	1
7	9.51						
6	7.94	6.99		SYMMETRIC			
5	6.21	5.58	4.87				
4	4.64	4.24	3.77	3.30			
3	3.14	2.91	2.67	2.36	2.04		
2	1.81	1.73	1.57	1.49	1.34	1.10	
1	0.78	0.75	0.71	0.68	0.62	0.56	0.40

Column and row numbers correspond directly to the floor
levels of the structure.

1 in./kip = 5.59 mm/kN

TABLE 5.1

FUNDAMENTAL FREQUENCY AND DAMPING COEFFICIENTS
OF THE MODEL IN THE LOADING DIRECTION

TECHNIQUE OF EVALUATION		Column 1 FREQ. AND DAMPING BEFORE BALLAST	Column 2 FREQ. AND DAMPING AFTER BALLAST
Ambient Vibration		9.75 Hz.	4.75 Hz.
Dynamic Analyzer		9.75 Hz./ 2.36%	4.78 Hz./ 2.20%
Forced Vibration		8.25 Hz./ 2.57%	4.55 Hz./ 2.03%
Free Vibration		8.70 Hz./ 2.45%	4.75 Hz./ 1.94%
Analytical	Pure*	12.45 Hz..	5.09 Hz.
	Semi-Analytical	9.55 Hz.	4.79 Hz.

Note: The frequency of the full-scale structure, after modifying it by the time scale factor of $\sqrt{5}$, was determined from free vibration test as 5.2 Hz. with a damping coefficient of 2.1%.

* Pure analytical result is based on the analytical work explained in Chapter 4.

FIGURES

Preceding page blank

SHEAR WALL 7.87"   SLAB 4.72"

6.56'

19.69'   FRAME A

19.69'   FRAME B
          GIRDER
          11.79" x 19.65"

6.56'   FRAME C
          COLUMN
          19.65" x 19.65"

19.69'   16.40'   19.69'

(a) PLAN OF FULL-SCALE STRUCTURE

GIRDER
11.79" x 19.6

SLAB
4.72"

6 @ 9.84'
= 59'

COLUMN
19.69" x 19.69"

SHEAR WALL
7.87"

12.30'

19.69'   16.40'   19.69'

1 in. = 25.4 mm
1 ft = 0.305 m
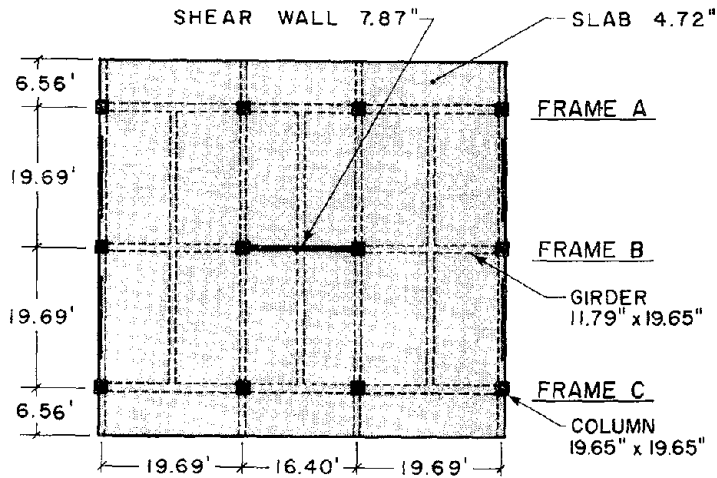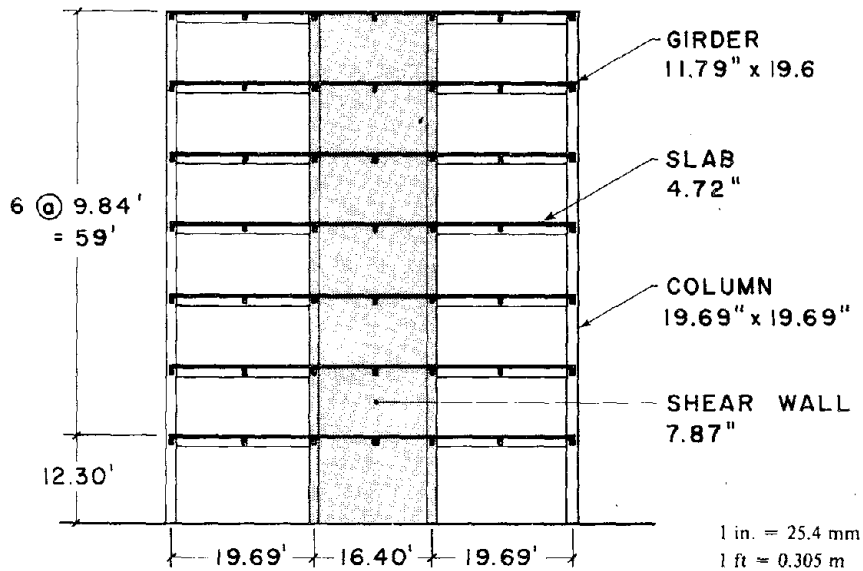
(b) ELEVATION OF FULL-SCALE STRUCTURE

FIG. 1-1 FULL-SCALE REINFORCED CONCRETE FRAME-WALL BUILDING,
THE MAIN SUBJECT OF THE R/C BUILDING STRUCTURES PHASE
OF THE U.S.-JAPAN COOPERATIVE RESEARCH PROGRAM.

73   Preceding page blank
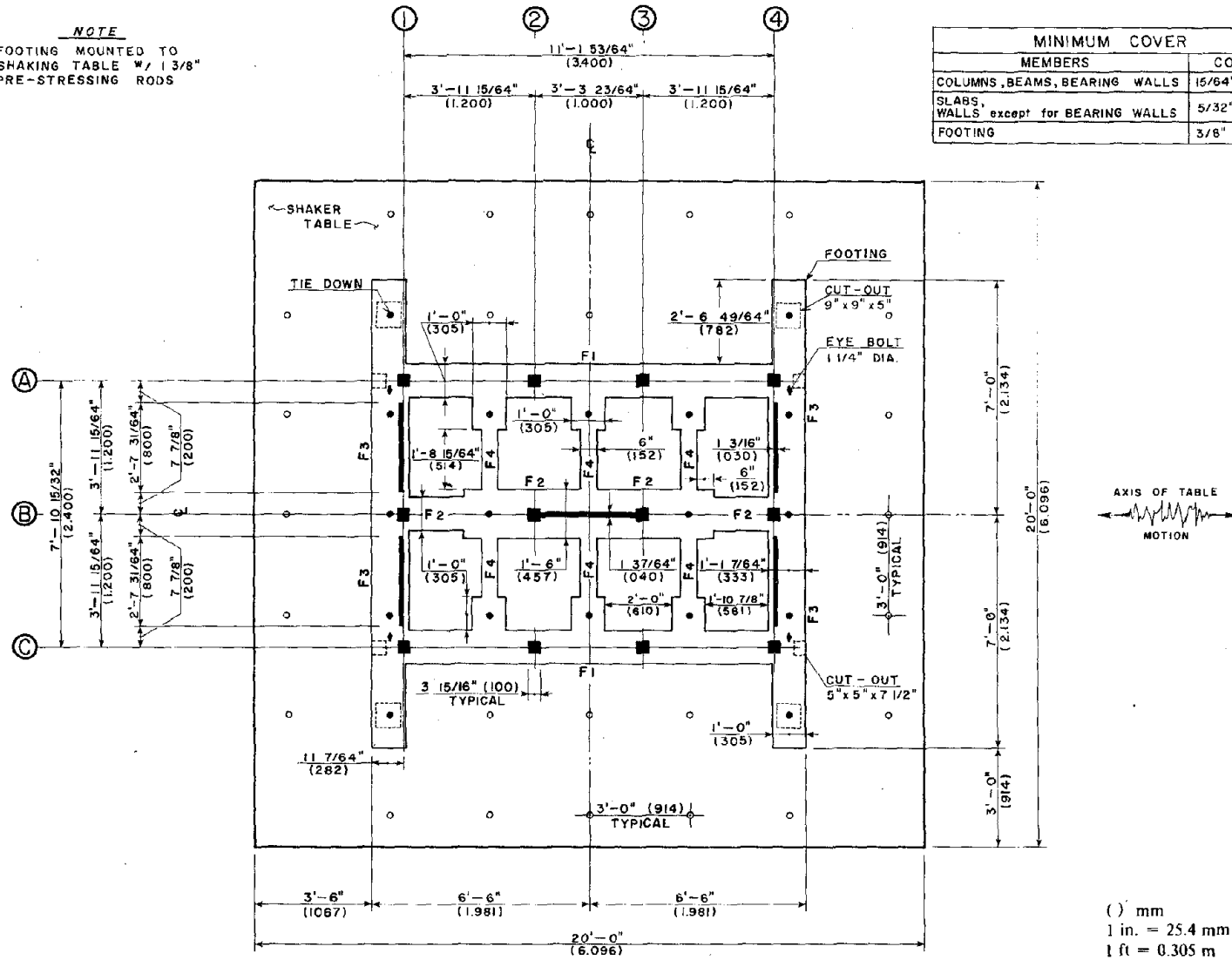
FIG. 1-2   THE FOUNDATION OF THE 1/5-SCALE MODEL.

SCHEDULE			
GIRDERS	1-3	2 23/64" x 3 15/16" (060) x (100)	
GIRDERS	4-7	2 23/64" x 3 35/64" (060) x (090)	
BEAMS	1-2	1 31/32" x 3 35/64" (050) x (090)	
COLUMNS	1-4	3 15/16" x 3 15/16" (100) x (100)	
SLABS	1-4	15/16" (024) THICK	

11'-1 53/64" (3.400)

3'-11 15/64" (1.200)   3'-3 23/64" (1.000)   3'-11 15/64" (1.200)

1'-11 39/64" (600)   1'-7 11/16" (500)   1'-11 39/64" (600)

10'-5 61/64" (3.200)

3'-11 15/64" (1.200)   1'-3 3/4" (400)

2'-7 31/64" (800)   7 7/8" (200)

1 3/16" (030)

1 37/64" (040)

AXIS OF TABLE
MOTION

( ) mm
1 in. = 25.4 mm
1 ft = 0.305 m
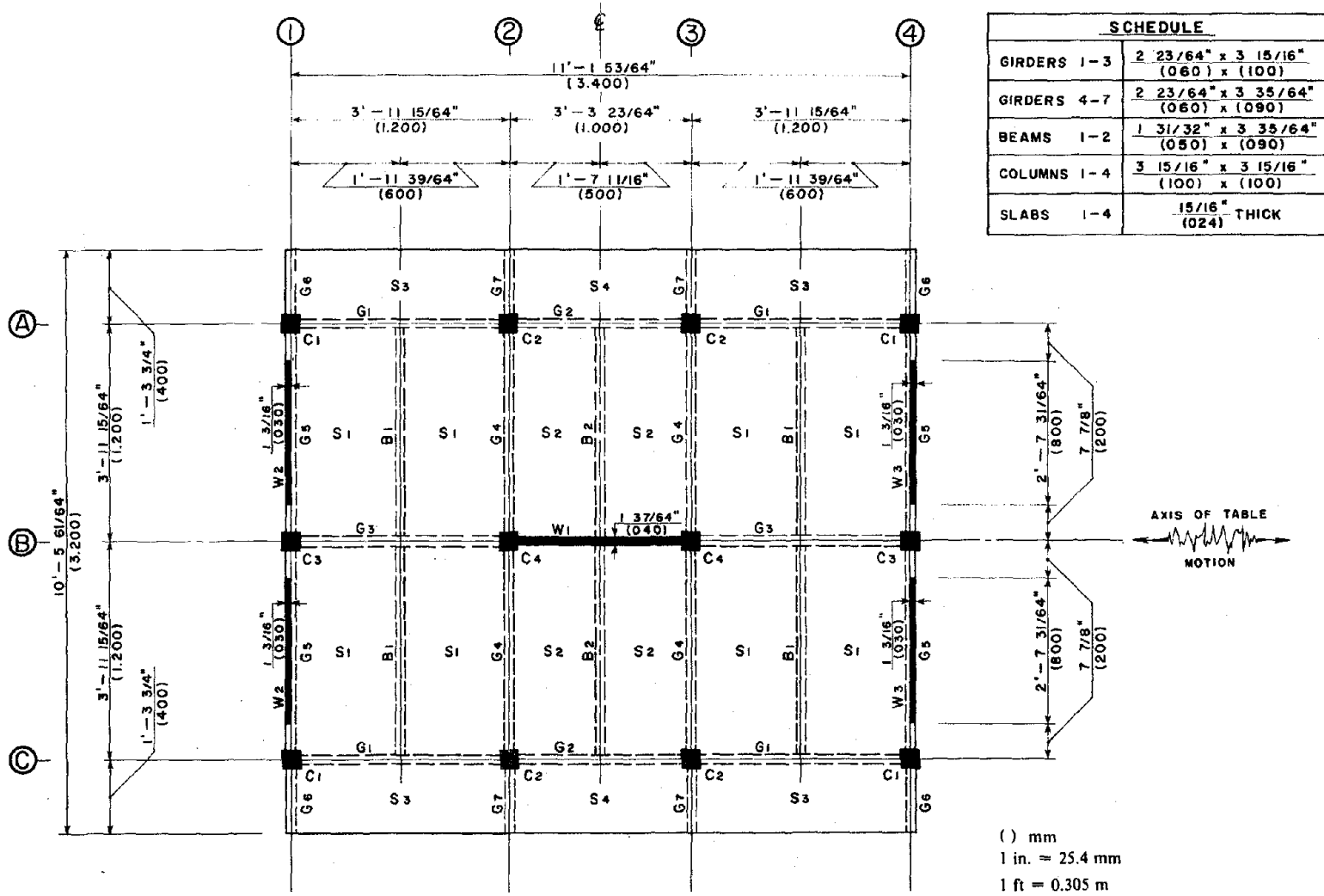
FIG. 1-3   TYPICAL FLOOR PLAN OF THE 1/5-SCALE MODEL.
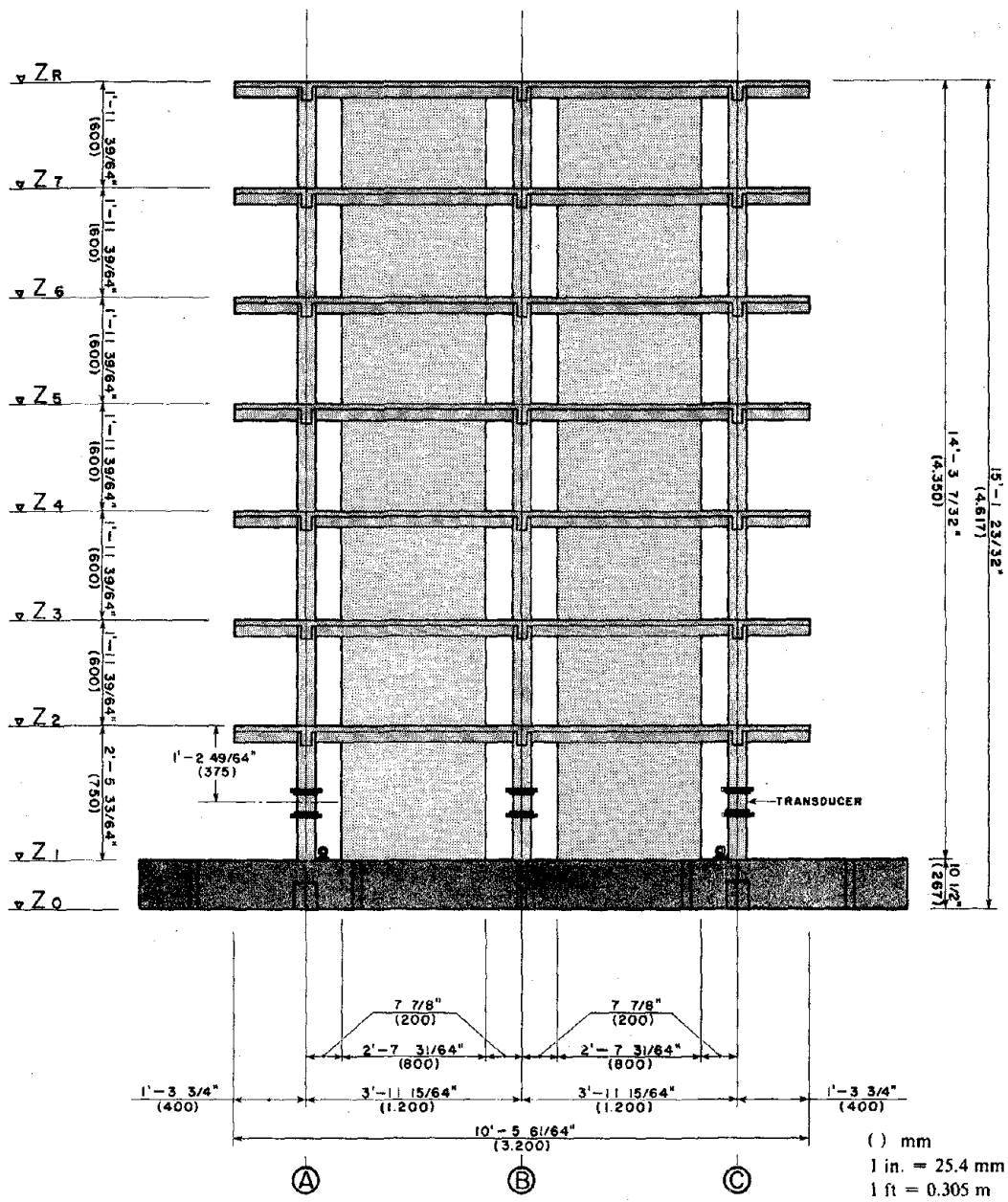
FIG. 1-4   FRONT ELEVATION OF THE 1/5-SCALE MODEL.

76
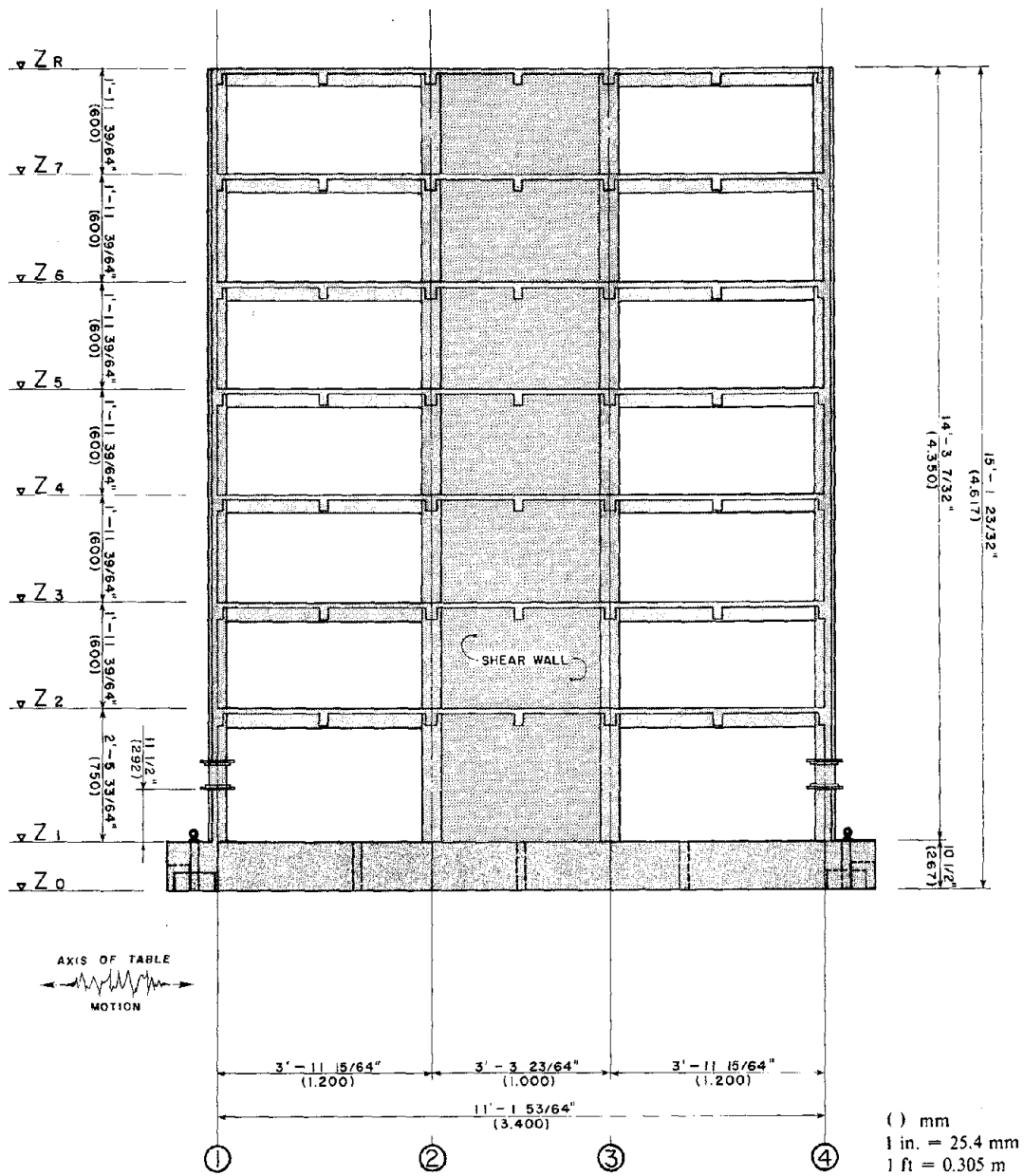
FIG. 1-5 ELEVATION OF THE INTERIOR WALL-FRAME OF 1/5-SCALE MODEL (FRAME B).

77
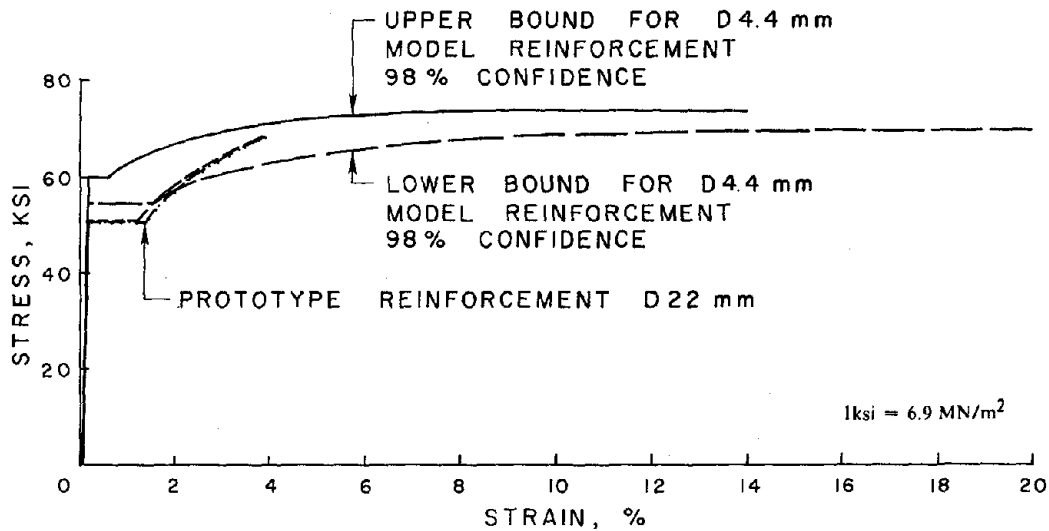
FIG.1-6   STRESS STRAIN DIAGRAM OF THE PROTOTYPE AND 1/5-SCALE MODEL
REINFORCING BARS USED IN THE COLUMNS.
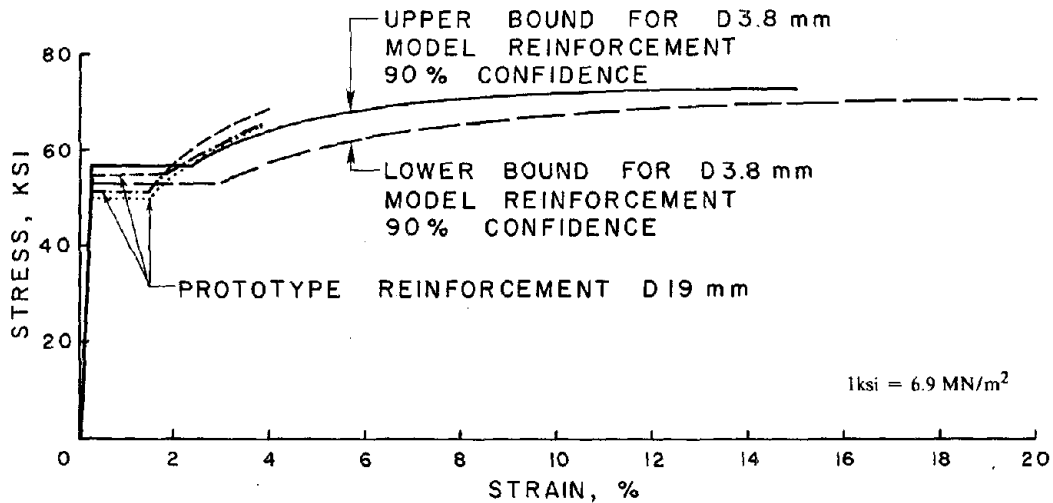
FIG. 1-7   STRESS-STRAIN DIAGRAM OF THE PROTOTYPE AND 1/5-SCALE MODEL
REINFORCING BARS USED IN THE BEAMS.
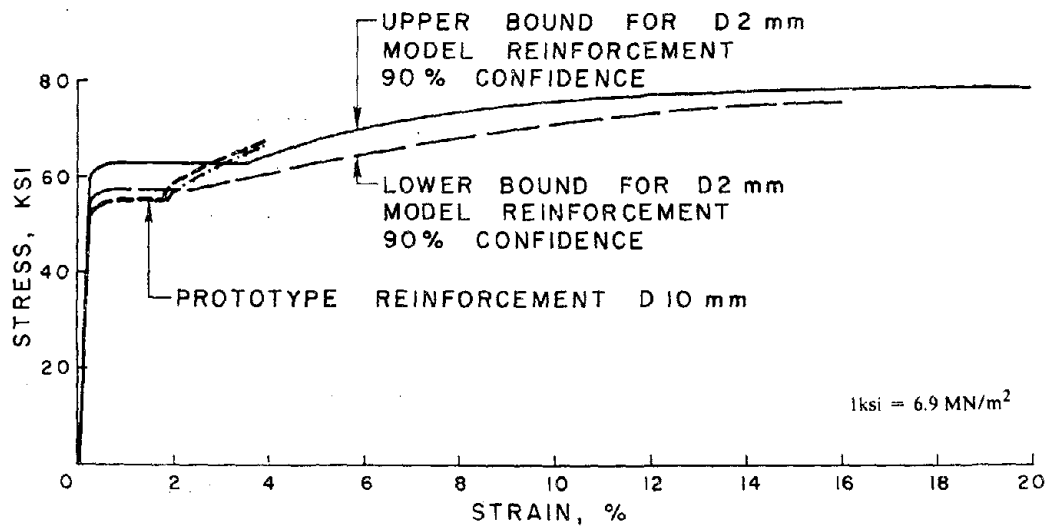
FIG. 1-8 STRESS STRAIN DIAGRAM OF THE PROTOTYPE AND 1/5-SCALE MODEL
REINFORCING BARS USED IN THE WALLS AND SLAB.
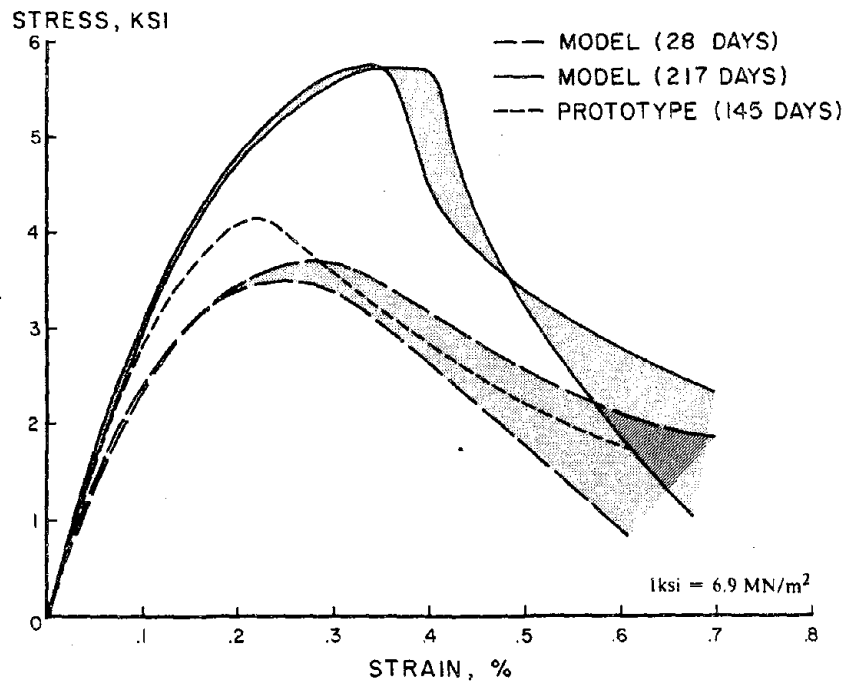
FIG. 1-9 STRESS STRAIN DIAGRAM OF THE PROTOTYPE CONCRETE AND
1/5-SCALE MODEL MICRO-CONCRETE FROM FIRST FLOOR.

FIG. 1-10 TYPICAL DETAILING OF THE EXTERIOR FRAMES OF
THE 1/5-SCALE MODEL.

( ) mm
1 in. = 25.4 mm
1 ft = 0.305 m
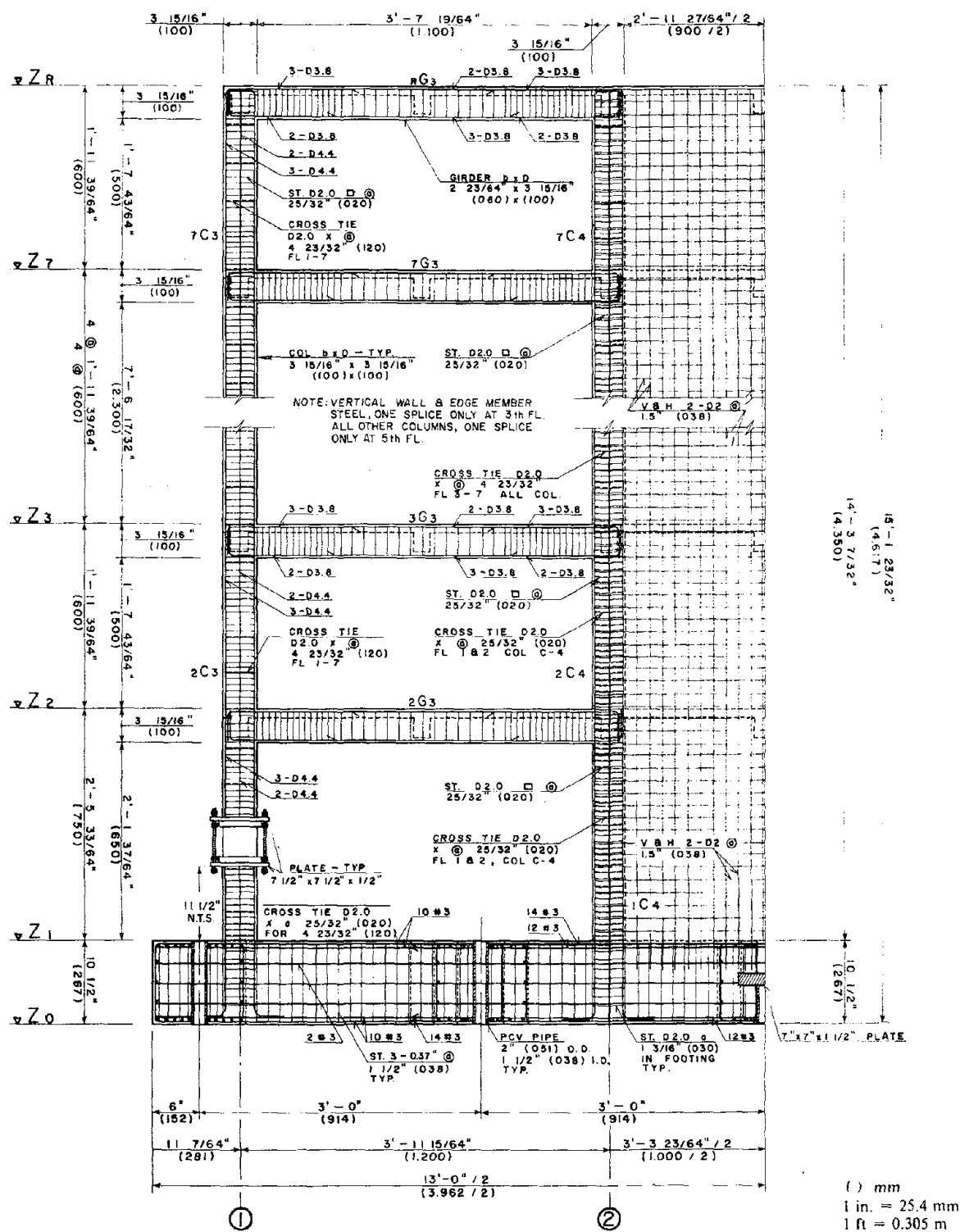
FIG. 1-11 TYPICAL DETAILING OF THE INTERIOR WALL-FRAME
OF THE 1/5-SCALE MODEL.

81
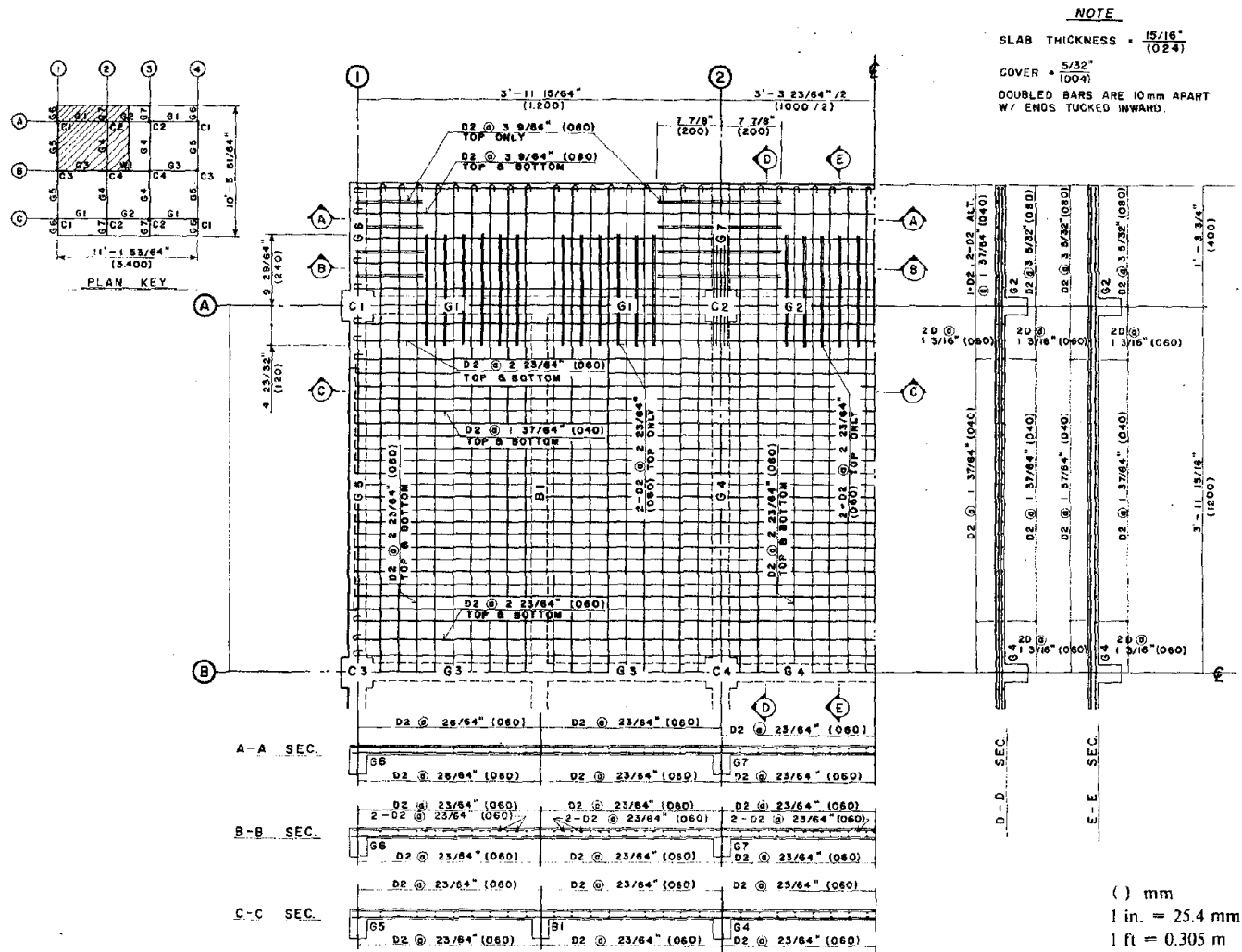
FIG. 1-12 TYPICAL DETAILING OF THE SLABS OF THE 1/5-SCALE MODEL.

82

RESPONSE
DIRECTION

1 in. = 25.4 mm

1/16"

1/16"

1 3/8" R.

COLUMN
AXIS

2" R.

1/8"
min.
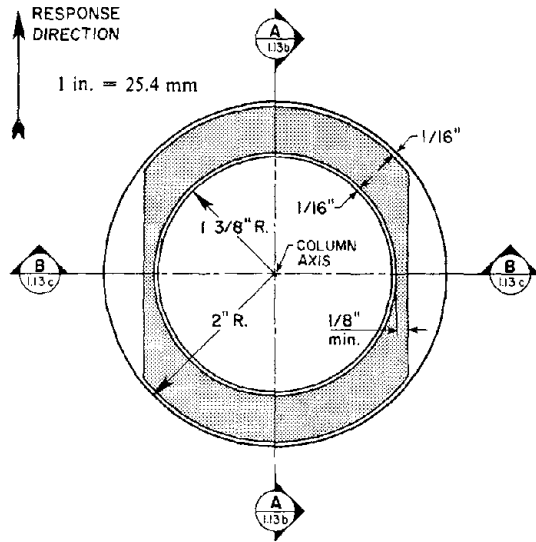
(a) SECTION PERPENDICULAR TO
COLUMN AXIS

1 in. = 25.4 mm

COLUMN
AXIS

5/8"

1/8"

1/2"

R = 2 3/16"

3/4"

1"

4"

5 1/4"

1/16"

1 7/16"

2 3/4"

G 3/8"

3/4"

5 1/2"

(b) SECTION A-A

1 in. = 25.4 mm

COLUMN
AXIS

5/8"

1/8"

R = 3/4"

R = 2 3/16"

3/4"

3/4"

1"

2 5/16"

1/8"

4"

5 1/4"

7/16"

1/16"

1 7/16"

2 3/4"

G 3/8"

3/8"

5 1/2"
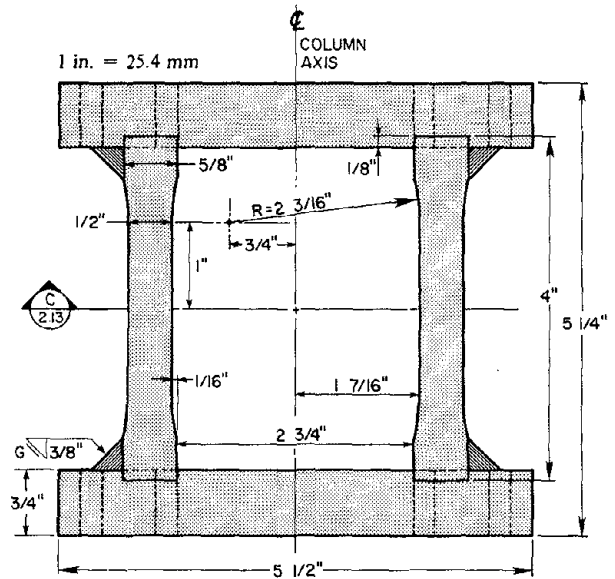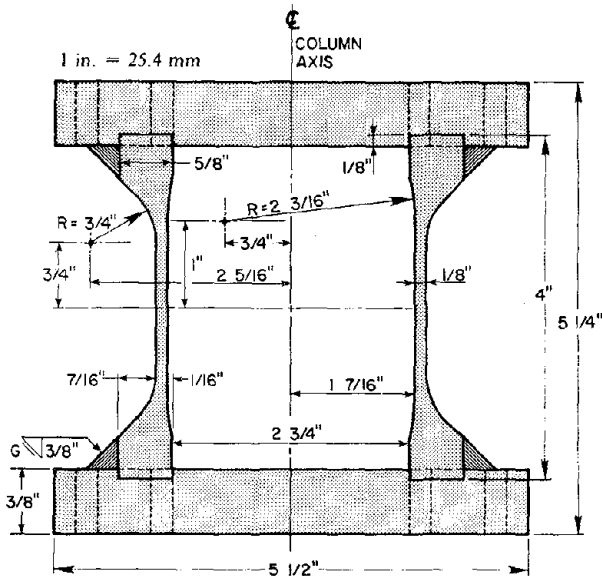
(c) SECTION B-B

FIG. 1-13 THE FORCE TRANSDUCER
DESIGNED FOR THE
1/5-SCALE MODEL.

STEEL PLATE
7 1/2" x 7 1/2" x 1/2"

1/4" HOLE W/ 45°
COUNTERSINK 1/4"
DEEP.

3/8" HOLE

1/8" HYDROSTONE

3/8" THREADED ROD
A325

IFT END PLATE
5 1/2" x 5 1/2" x 3/4"
6061 ALUMINUM

PRESTRESSING NUTS -
TO BE LOOSEND FOR
INSTALLATION, REMOVAL
OF TRANSDUCER &
TESTING

1/2" HOLE

D4.4 RE-BAR TO BE
WELDED BY DON CLYDE
AFTER POUR.

TRANSDUCER - TO BE
REPLACED BY TUBE
DURING CONSTRUCTION.

COLUMN

5 1/2"

11 1/2" TO
TOP OF
FOOTING.

4"

CHECK 1/4" HOLE LOCATION
DURING MACHINING W/
TYPICAL HOOP.

1 in. = 25.4 mm

BOTTOM PLATE TO BE REPLACED BY
TEMPLATE DURING INITAL POUR. WELD
STEEL PLATE AFTER POUR.

TOP PLATE TO BE WELDED BEFORE
PLACEMENT.

5 1/2"

1 1/2"

2 3/8"

3 1/4"

7 1/2"

FIG. 1-14   MOUNTING DETAILS FOR THE FORCE TRANSDUCER.
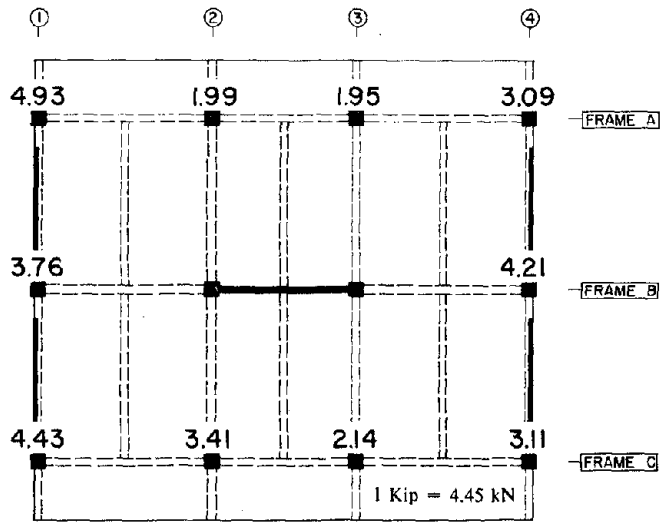
FIG. 2-1   AXIAL FORCES MEASURED IN THE FIRST STORY
COLUMNS OF THE 1/5-SCALE MODEL. (Kips)
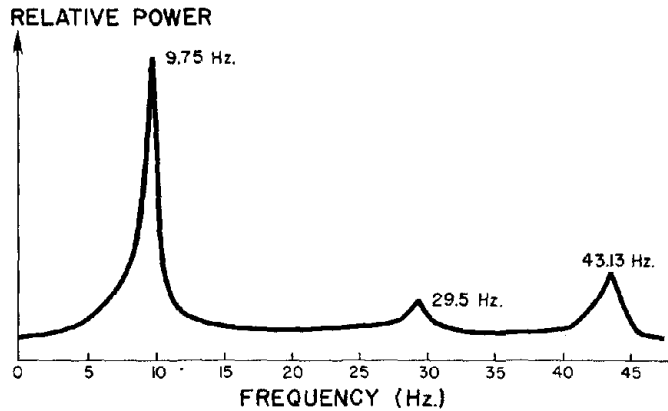
FIG. 2-3   OUTPUT FROM F.F.T. SPECTRUM ANALYSIS
DURING AMBIENT VIBRATION TEST OF THE
MODEL, MAIN RESPONSE DIRECTION.
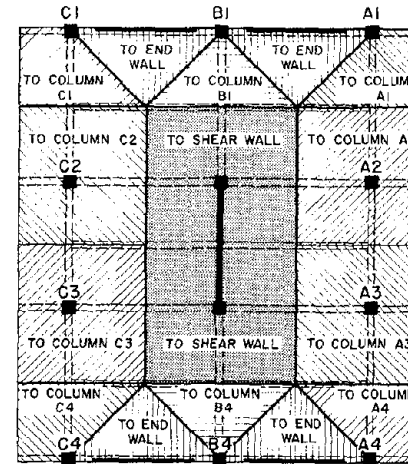
(a) TRIBUTARY AREAS ASSUMED
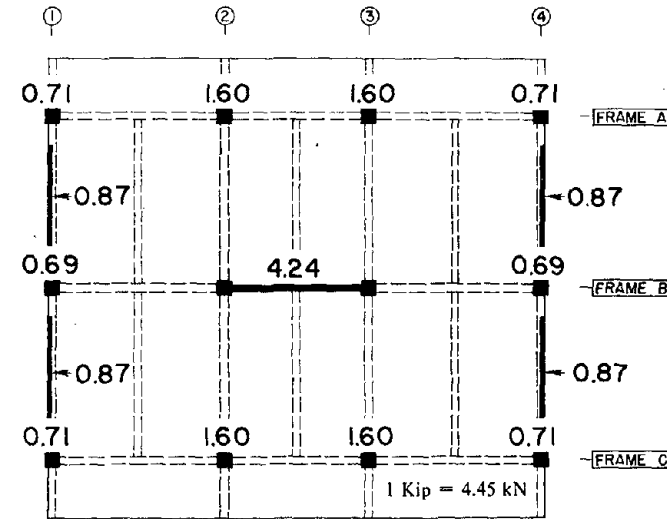
(b) RESULTING COMPUTED AXIAL FORCES. (Kips)

FIG. 2-2   TRIBUTARY AREAS ASSUMED FOR THE VERTICAL
MEMBERS AND THE CORRESPONDING COMPUTED
AXIAL FORCES AT THE BASE.
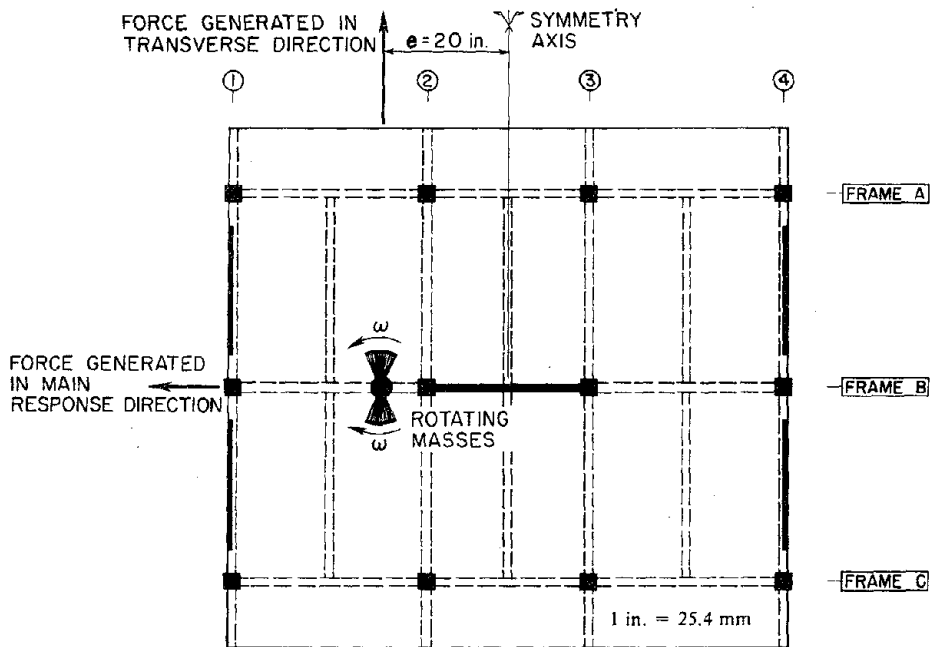
FIG. 2-4   THE ROTATING WEIGHT VIBRATION GENERATOR
          INSTALLED ON THE ROOF OF THE MODEL.
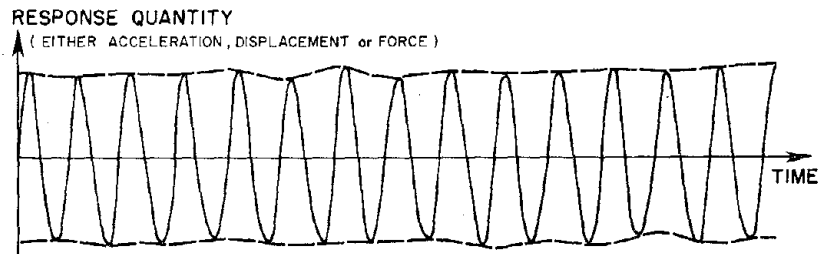
(a) RESPONSE REFLECTING "BEATING" CHARACTERISTICS.
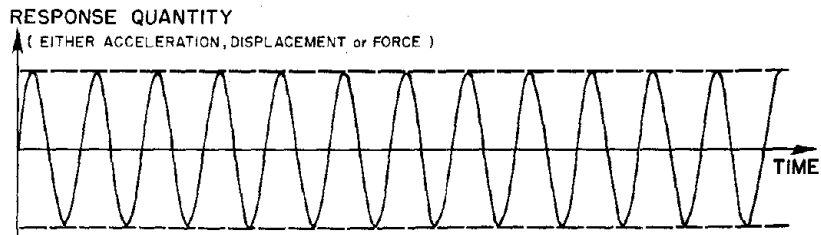
(b) NORMAL STEADY-STATE RESPONSE.

FIG. 2-5   EXAMPLES OF THE NORMAL STEADY-STATE AND
          BEATING RESPONSE.

86

AMPLITUDE (10^{-1} g)

ρ_{MAX} = 0.568 g

$\dfrac{\rho_{MAX}}{\sqrt{2}}$ = 0.40 g

f_1 = 7.96 , f_2 = 8.43

$\dfrac{f_1 + f_2}{2}$ = 8.20

$\xi = \dfrac{f_2 - f_1}{f_2 + f_1}$ = 2.86 %

FREQUENCY (Hz)

FIG. 2-6   TOP FLOOR ACCELERATION-FORCING
FREQUENCY RELATIONS.

AMPLITUDE (10^{-1} g)

ρ_{MAX} = 0.489 g

$\dfrac{\rho_{MAX}}{\sqrt{2}}$ = 0.346 g

f_1 = 8.01 , f_2 = 8.40

$\dfrac{f_1 + f_2}{2}$ = 8.21

$\xi = \dfrac{f_2 - f_1}{f_2 + f_1}$ = 2.38 %
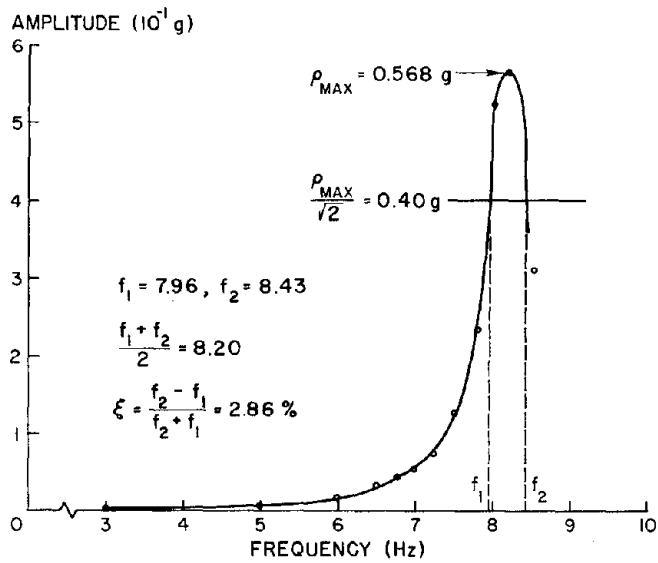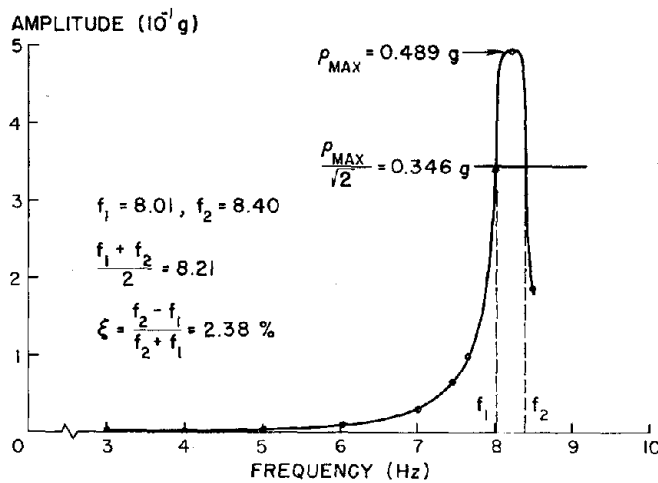
FREQUENCY (Hz)

FIG. 2-8   FOURTH FLOOR ACCELERATION-FORCING
FREQUENCY RELATIONS.

AMPLITUDE (10^{-1} g)

ρ_{MAX} = 0.1638 g

$\dfrac{\rho_{MAX}}{\sqrt{2}}$ = 0.1158 g

f_1 = 8.11 , f_2 = 8.52

$\dfrac{f_1 + f_2}{2}$ = 8.32

$\xi = \dfrac{f_2 - f_1}{f_2 + f_1}$ = 2.47 %
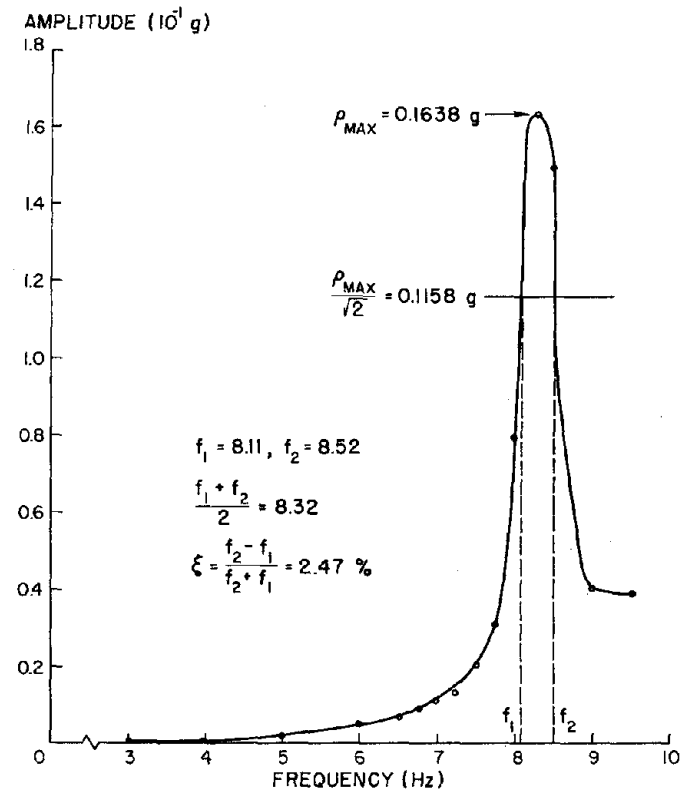
FREQUENCY (Hz)

FIG. 2-7   TOP FLOOR DISPLACEMENT-FORCING
FREQUENCY RELATIONS.

87
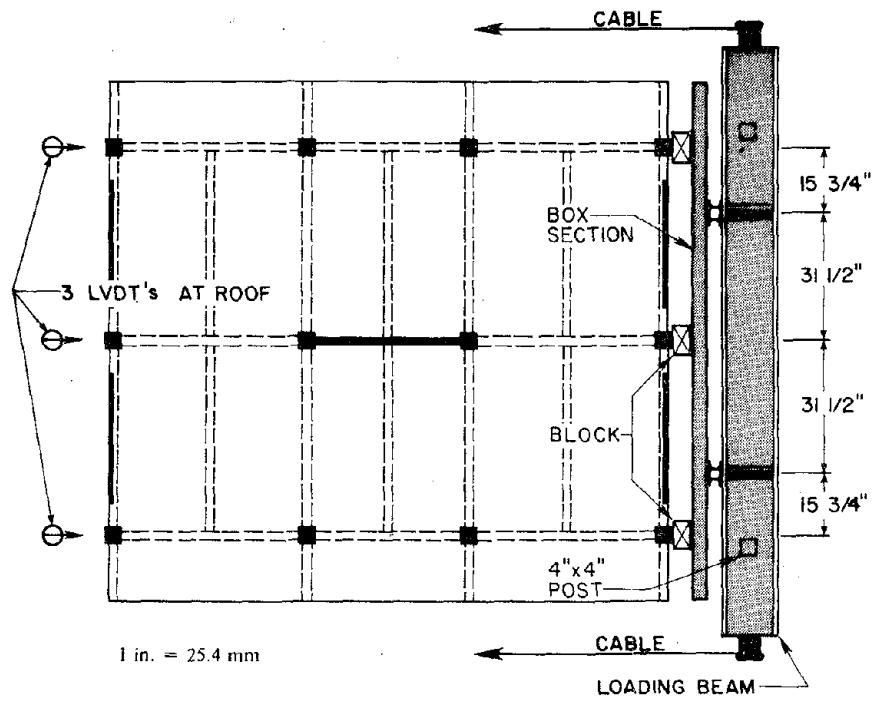
(a) LOADING BEAM, PLAN VIEW
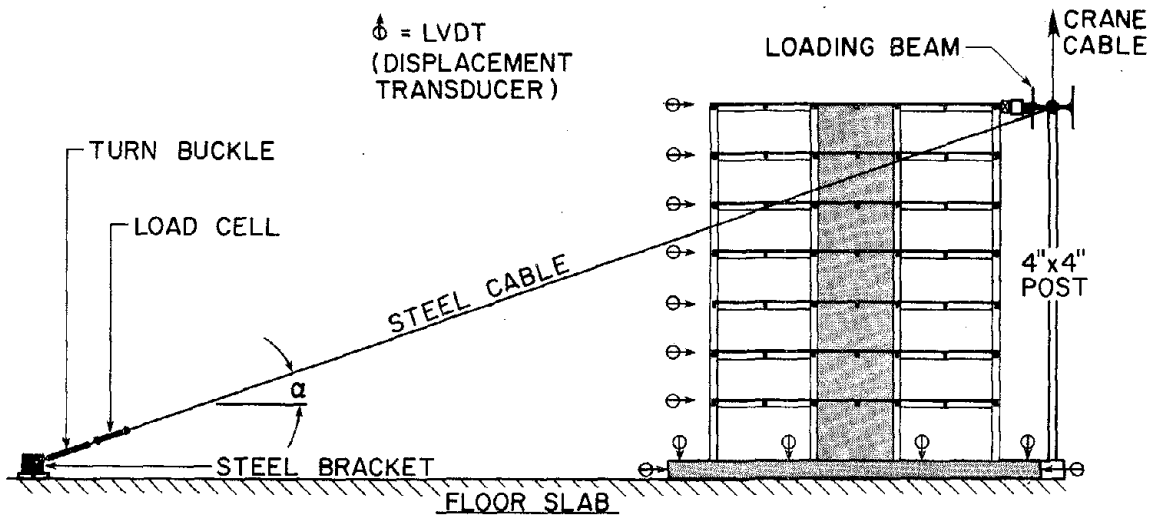
(b) LOADING SCHEME, ELEVATION (Also see photo 3.9 & 3.10)

FIG. 2-9   TEST SET-UP FOR DETERMINING THE LATERAL FLEXIBILITY
OF THE 1/5-SCALE MODEL.

88
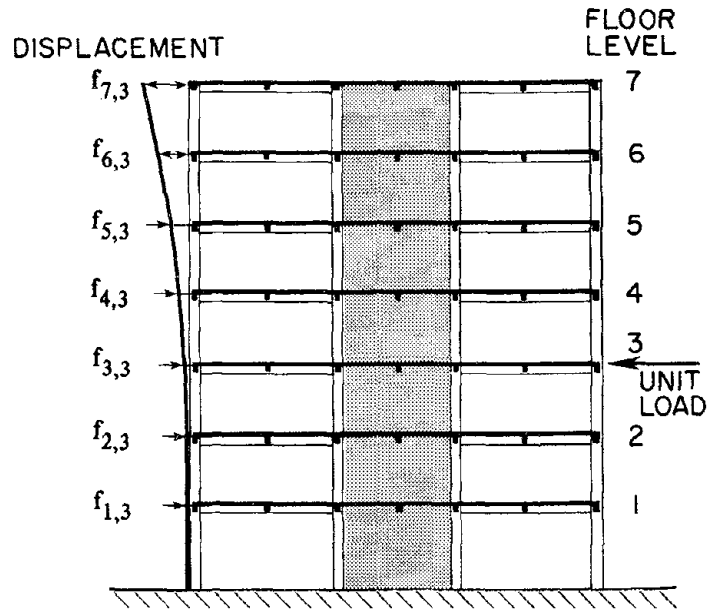
FIG. 2-10 PHYSICAL CORRESPONDENCE OF THE FLEXIBILITY
COEFFICIENTS, 3rd COLUMN OF THE FLEXIBILITY
MATRIX.
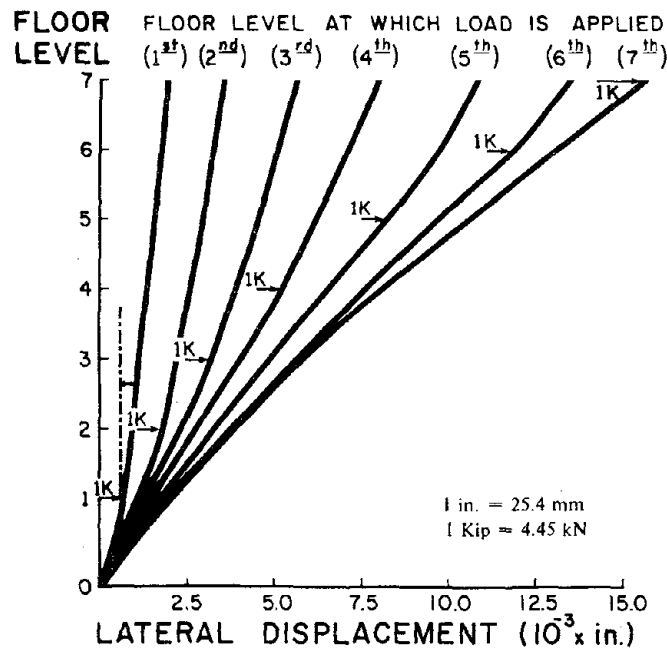
FIG. 2-11 EXPERIMENTAL DISPLACEMENT PROFILES OF 1/5-SCALE
MODEL PRIOR TO BALLAST LOADING.
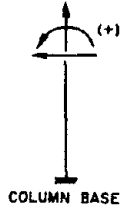
89

COLUMN BASE

All forces are normalized to 1000 lbs. of applied external force. All forces are incremental. Lateral load was applied at the right end and directed towards the left end.

25.63	35.36	32.49	30.61
30.68	667.24		33.13
39.31	34.14	39.71	31.70

SHEAR, lbs.
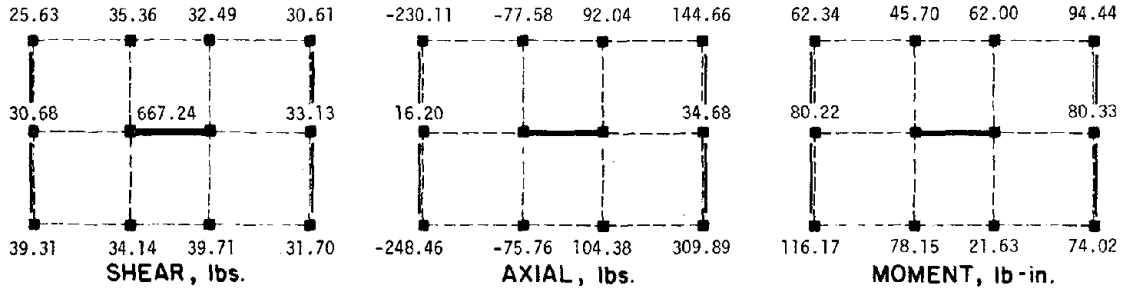
COLUMNS: 33.28%

SHEAR WALL: 66.72%

-230.11	-77.58	92.04	144.66
16.20			34.68
-248.46	-75.76	104.38	309.89

AXIAL, lbs.

LOAD AT 7th FLOOR

62.34	45.70	62.00	94.44
80.22			80.33
116.17	78.15	21.63	74.02

MOMENT, lb-in.

23.95	31.26	28.96	26.39
28.85	693.45		30.61
37.61	33.02	37.13	28.77

SHEAR, lbs.
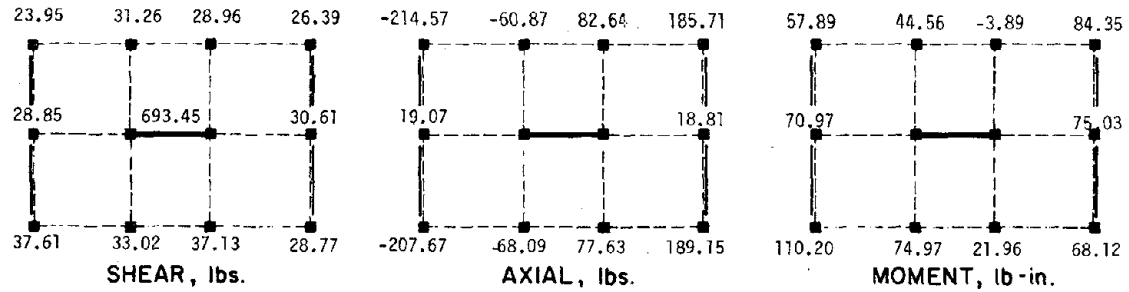
COLUMNS: 30.65%

SHEAR WALL: 69.35%

-214.57	-60.87	82.64	185.71
19.07			18.81
-207.67	-68.09	77.63	189.15

AXIAL, lbs.

LOAD AT 6th FLOOR

57.89	44.56	-3.89	84.35
70.97			75.03
110.20	74.97	21.96	68.12

MOMENT, lb-in.

23.35	29.14	28.29	26.35
27.06	711.05		29.40
34.11	29.77	34.15	27.33

SHEAR, lbs.

COLUMNS: 28.90%

SHEAR WALL: 71.10%

-160.72	-46.23	58.75	130.91
17.23			10.20
-181.03	-53.63	63.14	174.13

AXIAL, lbs.

LOAD AT 5th FLOOR

52.79	37.86	-3.17	78.30
67.49			69.19
96.98	65.73	18.67	57.85

MOMENT, lb-in.

1 lbf = 4.45 N
1 in. = 25.4 mm

FIG. 2-12 FORCE DISTRIBUTION AT TRANSDUCER LEVEL FROM FLEXIBILITY TESTS OF THE 1/5-SCALE MODEL WITHOUT AUXILIARY MASS.

90

LOAD AT 4th FLOOR

SHEAR, lbs.

```
21.49    26.12   25.34        23.71

23.82       738.71            26.72

30.47    27.31   31.18        25.13
```

AXIAL, lbs.

```
-124.20   -30.95   45.89      90.48

24.23                          0.00

-149.48   -32.14   49.37     121.50
```

MOMENT, lb-in.

```
50.76    28.96    -5.59       70.65

48.91                         60.10

82.76    57.54    15.85       57.93
```

COLUMNS: 26.13%

SHEAR WALL: 73.87%

LOAD AT 3rd FLOOR

SHEAR, lbs.

```
18.75    24.53   22.43        22.20

21.12       763.91            24.55

26.93    25.23   27.93        22.42
```

AXIAL, lbs.

```
-97.63   -20.34   32.83       51.06

23.72                         -8.63

-106.14  -21.91   35.58       86.94
```

MOMENT, lb-in.

```
40.00    20.57    -8.05       62.58

35.35                         49.52

68.48    48.18    13.53       50.17
```

COLUMNS: 23.61%

SHEAR WALL: 76.39%

LOAD AT 2nd FLOOR

SHEAR, lbs.

```
16.06    19.53   20.43        16.33

18.21       806.8             18.36

22.15    20.98   24.41        16.74
```

AXIAL, lbs.

```
-63.54   -9.49    20.25       30.86

24.72                        -15.65

-67.34   -7.17    20.15       46.62
```

MOMENT, lb-in.

```
32.66    19.93    -9.14       65.87

34.09                         58.93

53.38    38.22    6.99        58.99
```
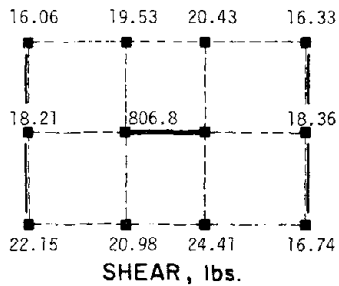
COLUMNS: 19.32%

SHEAR WALL: 80.68%

LOAD AT 1st FLOOR

SHEAR, lbs.

```
15.24    19.01   16.69        32.48

15.59       769.52            39.11

20.35    19.41   19.47        33.13
```

AXIAL, lbs.

```
-36.26   -3.96    18.11      -12.07

19.62                        -40.83

-44.41   -6.32    13.67       -4.05
```

MOMENT, lb-in.

```
-4.80    -1.40   -12.87      -51.79

-1.45                       -101.00

14.17    15.19    9.24       -63.88
```
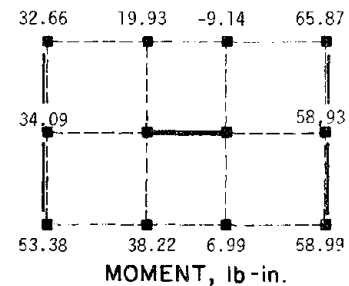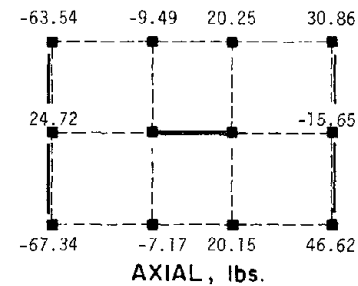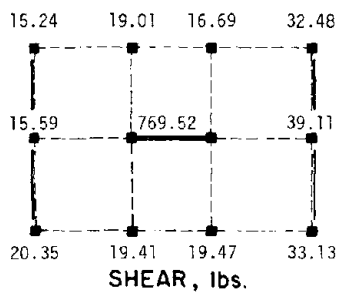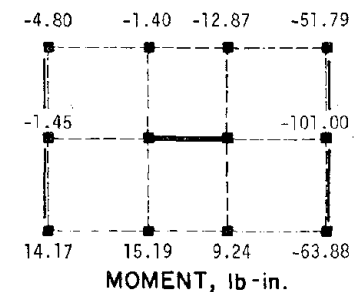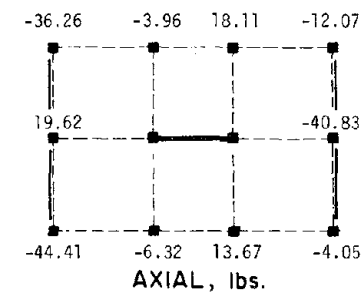
1 lbf = 4.45 N
1 in. = 25.4 mm

FIG. 2-12   CONTINUED...

91

1 in. = 25.4 mm
1 ft = 0.305 m

(a) THE DISTRIBUTION OF BALLAST WEIGHT ON FLOOR SLABS.
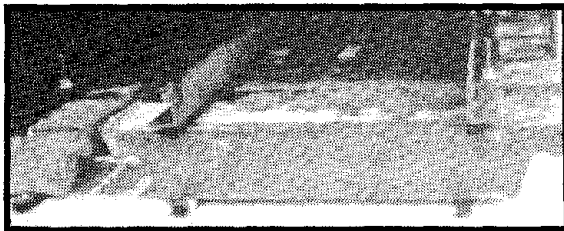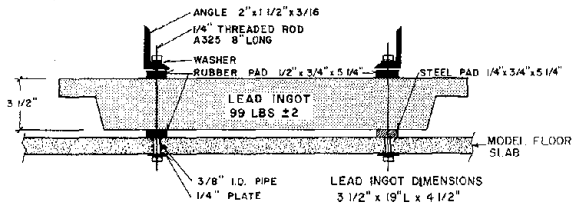
(b) TYPICAL LEAD INGOT USED AS BALLAST.
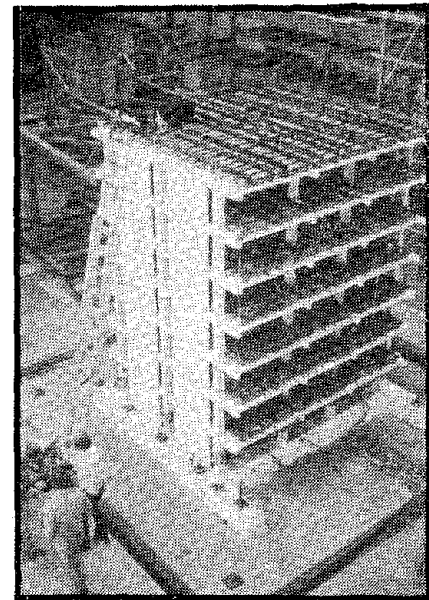
(c) 1/5-SCALE MODEL LOADED
     WITH BALLAST.

FIG. 3-1   LOADING OF BALLAST ON THE 1/5-SCALE MODEL.

92
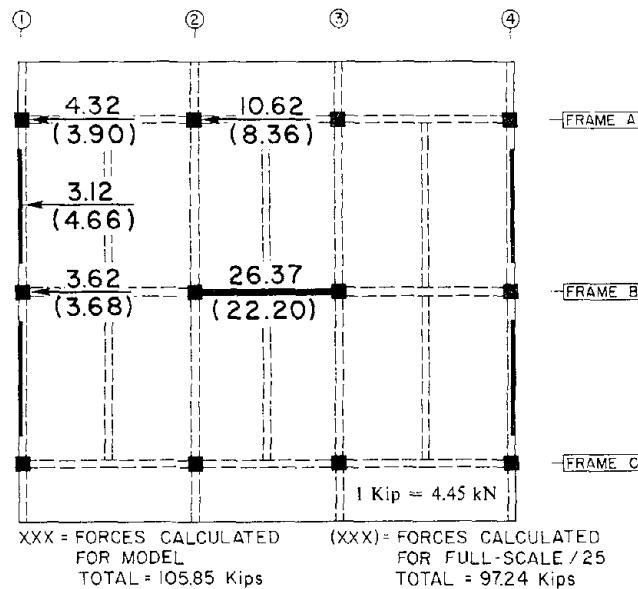
FIG. 3-2 COMPARISON OF AXIAL FORCES AT THE BASE OF
THE MODEL (Due to its' own weight & the added
ballast) WITH THOSE OBTAINED FROM THE FULL
SCALE MODEL. (Kips)
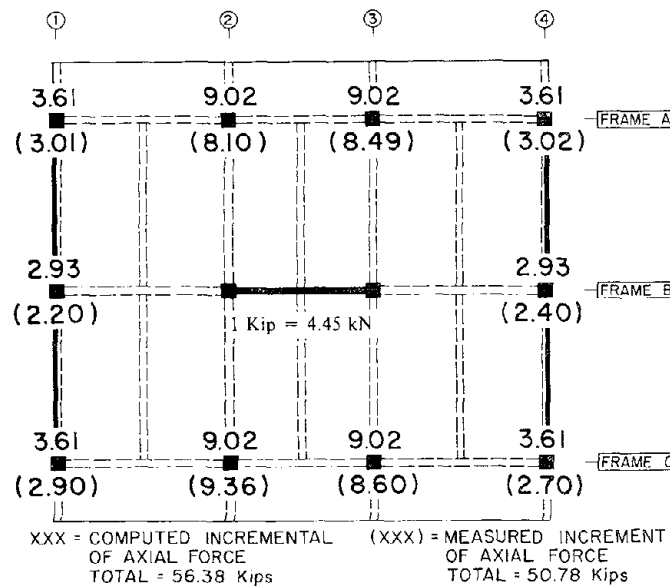
FIG. 3-3 COMPUTED AND MEASURED INCREMENTS
OF COLUMN AXIAL FORCES AFTER LOADING
THE BALLAST. (Kips)

93
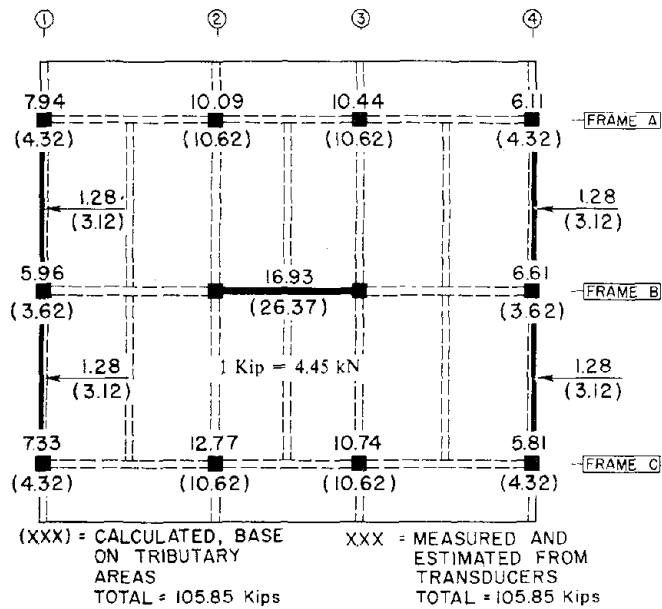
FIG. 3-4 EXPERIMENTALLY ESTIMATED AND CALCULATED
DISTRIBUTION OF THE AXIAL FORCES AT THE BASE
OF THE STRUCTURE. (Kips)
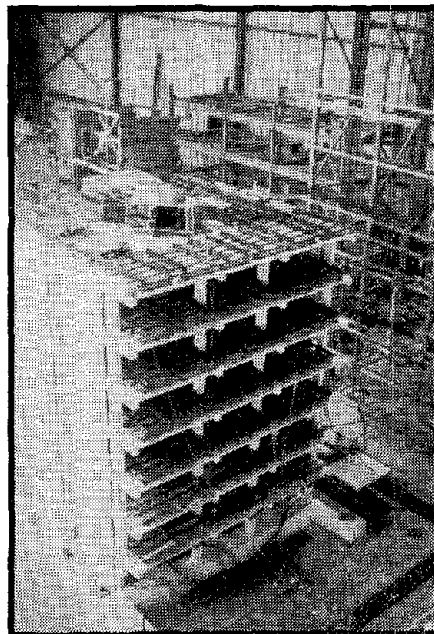
FIG. 3-5 FORCED VIBRATION TESTING OF THE MODEL
AFTER BEING LOADED WITH THE REQUIRED
BALLAST.

94
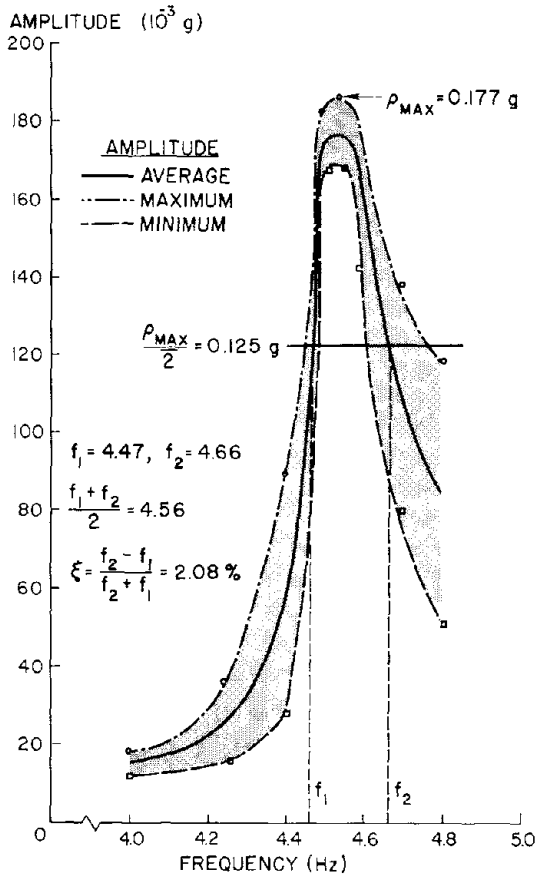
FIG. 3-6 TOP FLOOR ACCELERATION-FORCING FREQUENCY RELATIONS, FRAME A.
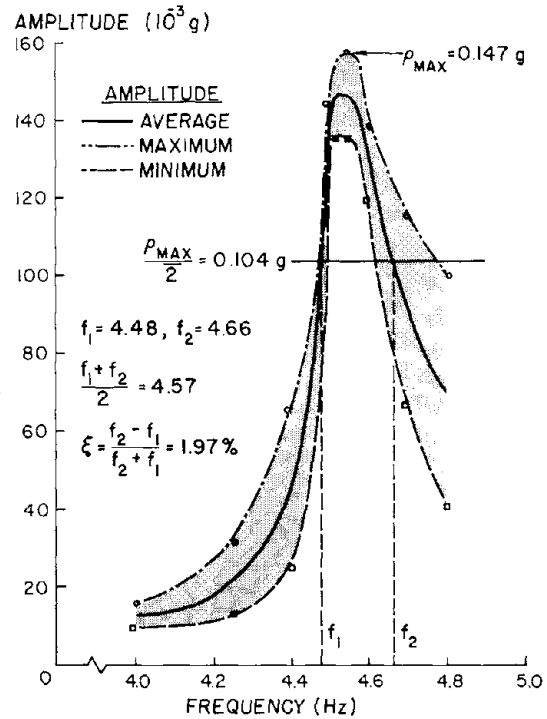
FIG. 3-7 TOP FLOOR ACCELERATION-FORCING FREQUENCY RELATIONS, FRAME B.
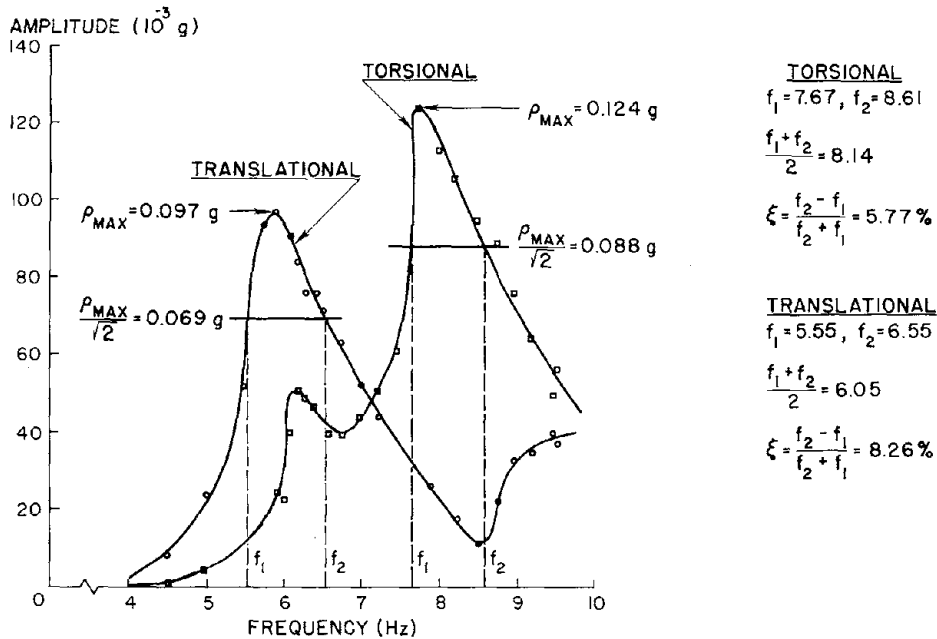
FIG. 3-8 TRANSLATIONAL AND ROTATIONAL RESPONSES OF TOP FLOOR FORCED WITH DIFFERENT FREQUENCIES.

95
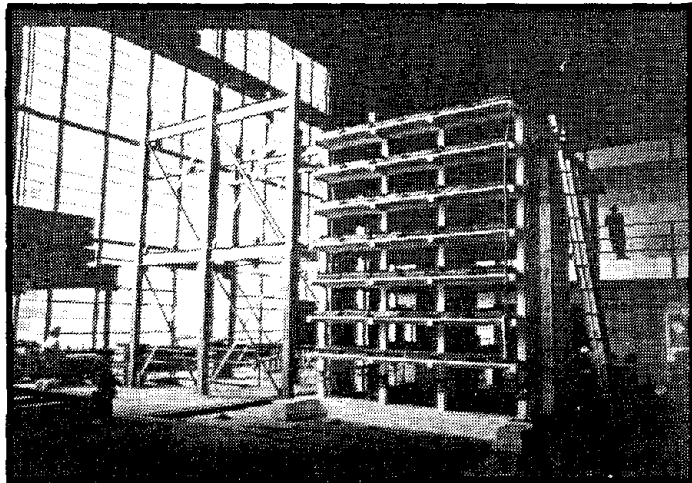
FIG. 3-9   STATIC TESTING OF MODEL.

96
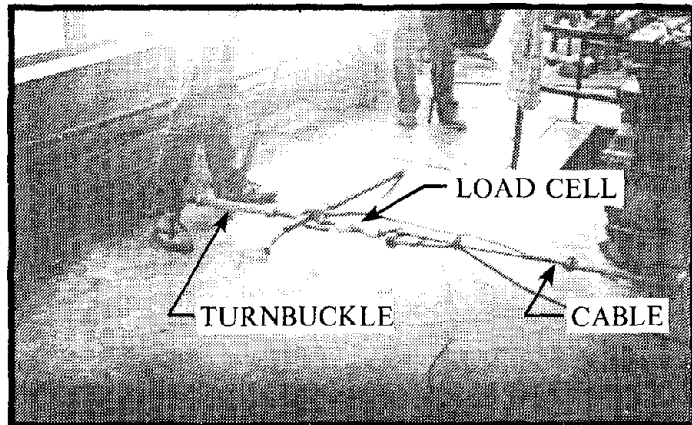
FIG. 3-10   TURNBUCKLE, LOAD CELL AND
CABLE USED IN STATIC TESTING.
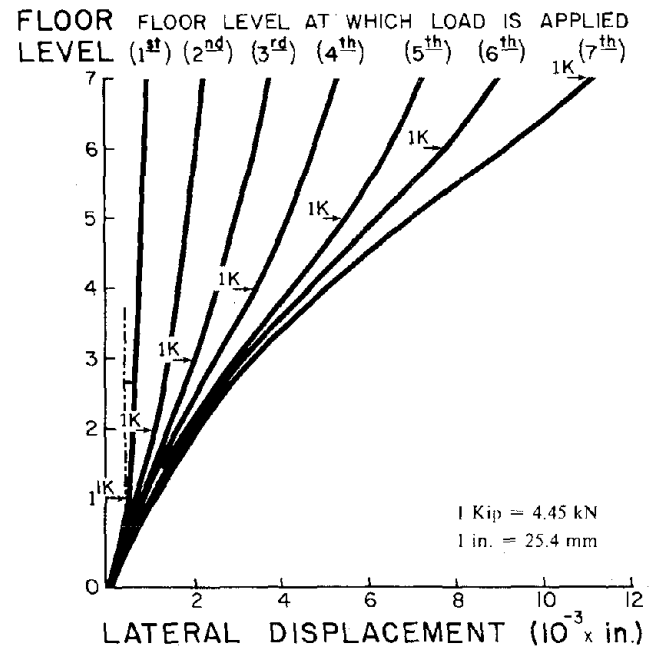
FIG. 3-11   EXPERIMENTAL DEFLECTION PROFILES
OF MODEL WITH FULL BALLAST LOAD.
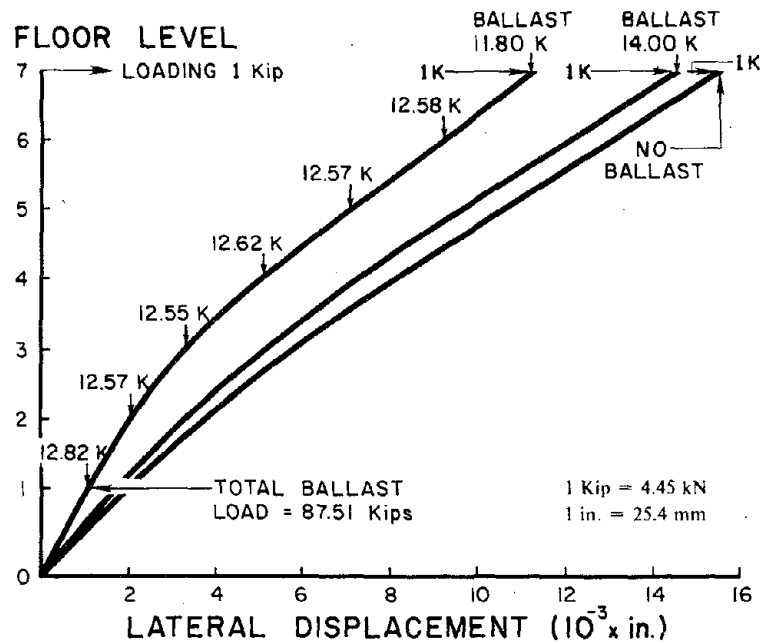
FIG. 3-12 EFFECTS OF ADDED GRAVITY LOADS ON THE
LATERAL DISPLACEMENT OF THE STRUCTURE
WHEN LATERALLY LOADED AT THE TOP FLOOR
(ROOF).
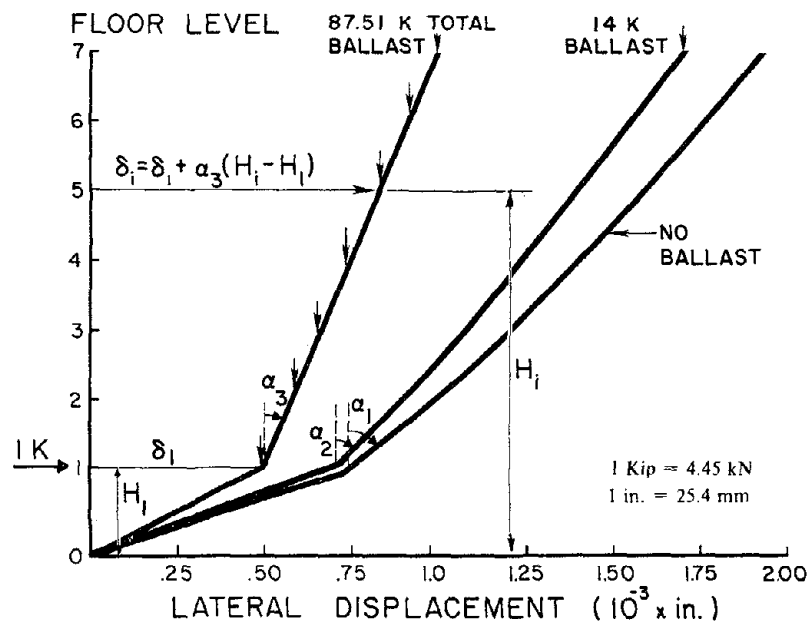
FIG. 3-13 EFFECTS OF ADDED GRAVITY LOADS ON THE
LATERAL DISPLACEMENT OF THE STRUCTURE
WHEN LATERALLY LOADED AT THE FIRST FLOOR.
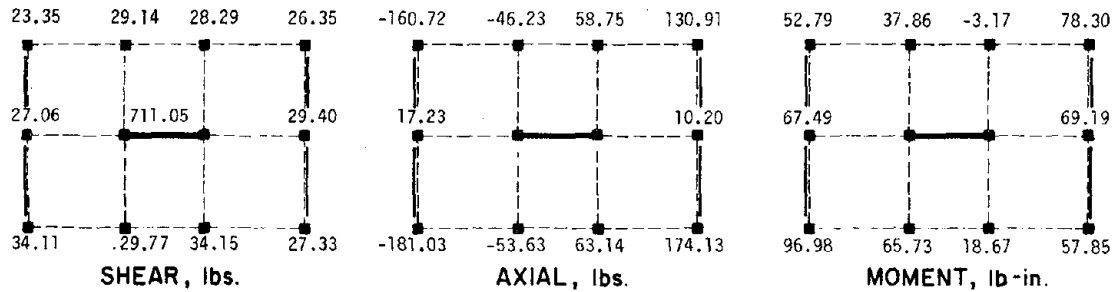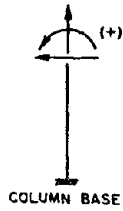
97

(+)

COLUMN BASE

All forces are normalized to 1000 lbs. of applied external force. All forces are incremental. Lateral load was applied at the right end and directed towards the left end.
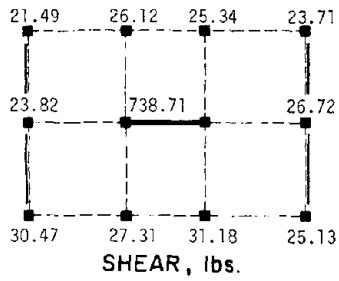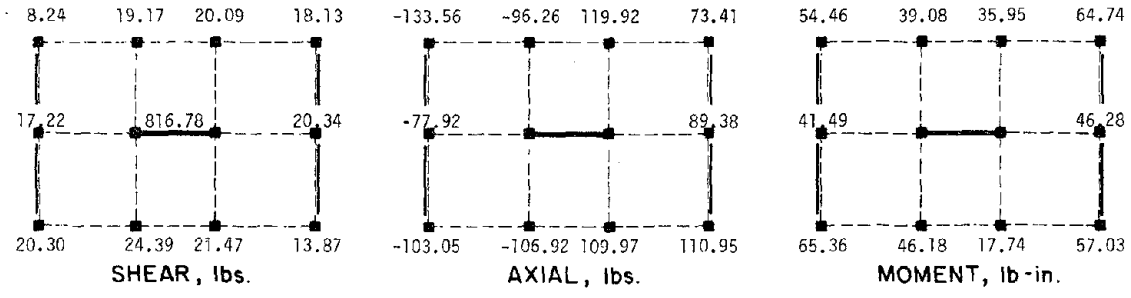
```
  8.24   19.17  20.09    18.13        -133.56  -96.26 119.92   73.41         54.46   39.08  35.95    64.74
17.22      816.78        20.34         -77.92            89.38              41.49               46.28
20.30   24.39  21.47    13.87        -103.05 -106.92 109.97  110.95         65.36   46.18  17.74    57.03
        SHEAR, lbs.                          AXIAL, lbs.                          MOMENT, lb-in.

    COLUMNS:    18.32%
  SHEAR WALL:   81.68%                       LOAD AT 7th FLOOR
```

```
  8.72   18.72  19.70    17.18        -105.66  -76.26 100.55   96.36         52.69   36.43  33.75    64.49
17.16      820.49        20.03         -60.24            65.88              40.57               43.67
19.66   23.56  20.65    14.13         -83.89  -91.51  85.36   65.33         62.04   43.47  16.22    55.94
        SHEAR, lbs.                          AXIAL, lbs.                          MOMENT, lb-in.

    COLUMNS:    17.95%

  SHEAR WALL:   82.05%                       LOAD AT 6th FLOOR
```

```
  8.63   17.87  19.47    16.77         -81.44  -61.35  80.65   80.65         49.31   32.84  28.69    57.81
16.26      827.00        19.71         -45.31            52.47              36.1                37.63
18.30   22.26  19.95    13.82         -68.74  -71.24  69.94   45.97         55.40   38.76  13.24    51.70
        SHEAR, lbs.                          AXIAL, lbs.                          MOMENT, lb-in.

    COLUMNS:    17.30%

  SHEAR WALL:   82.70%                       LOAD AT 5th FLOOR
```
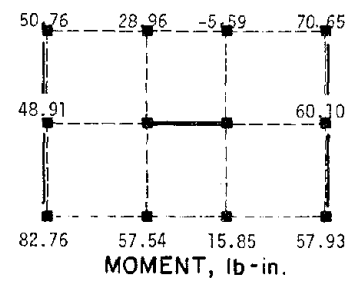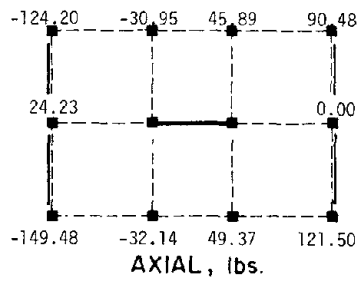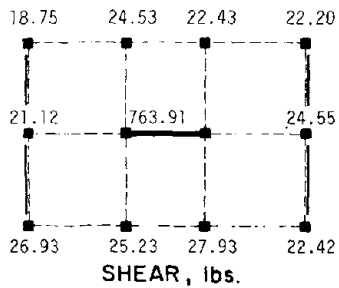
1 lbf = 4.45 N
1 in. = 25.4 mm

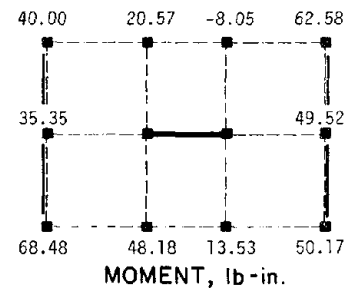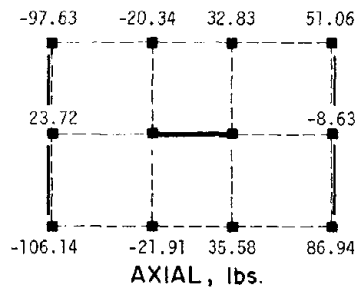FIG. 3-14   FORCE DISTRIBUTION AT TRANSDUCER LEVEL FROM FLEXIBILITY TESTS OF THE 1/5-SCALE MODEL WITH AUXILIARY MASS.

98

8.40   16.83   18.17   21.77   -63.96   -45.02   60.48   63.75   42.71   28.42   24.01   51.11

15.14   804.47   39.0   -33.56   29.79   30.09   34.08

16.98   20.92   18.62   19.70   -55.39   -53.94   46.11   37.84   48.41   31.61   11.06   -26.20

SHEAR, lbs.   **AXIAL, lbs.**   **MOMENT, lb-in.**

COLUMNS: 19.55%

SHEAR WALL: 80.45%   LOAD AT 4th FLOOR

8.30   16.16   17.52   15.22   -30.46   -29.10   46.85   1.23   41.76   24.90   21.03   32.60

14.16   854.47   16.42   -20.25   16.26   29.86   24.50

14.04   16.68   15.16   11.87   -54.44   -38.10   38.63   21.10   40.10   26.17   9.55   32.32

SHEAR, lbs.   **AXIAL, lbs.**   **MOMENT, lb-in.**
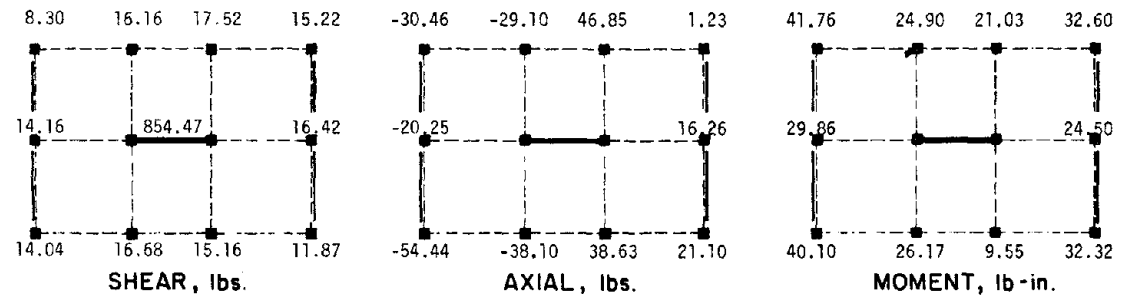
COLUMNS: 14.55%

SHEAR WALL: 85.45%   LOAD AT 3rd FLOOR

7.88   14.59   15.54   11.36   -14.60   -15.20   25.78   -6.44   36.16   21.78   15.27   50.21

12.28   880.12   11.29   -7.94   2.61   21.86   39.37

11.63   14.38   13.40   7.54   -41.03   -19.17   25.57   12.98   32.54   21.28   4.98   44.42

SHEAR, lbs.   **AXIAL, lbs.**   **MOMENT, lb-in.**
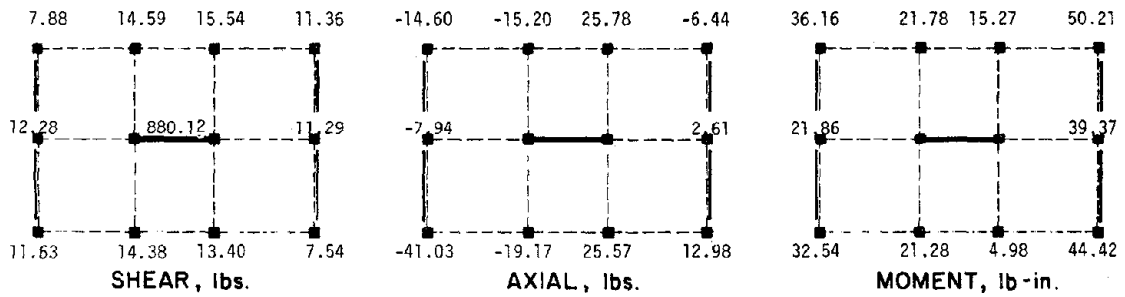
COLUMNS: 11.99%

SHEAR WALL: 88.01%   LOAD AT 2nd FLOOR

8.68   15.18   15.74   30.62   -6.07   -5.81   20.06   -12.98   11.42   -1.65   2.80   -72.15

12.20   835.20   14.03   2.42   -2.40   -3.98   4.58

12.48   14.90   12.60   28.36   -20.61   -7.55   13.57   -47.57   2.29   -5.57   0.00   -72.82

SHEAR, lbs.   **AXIAL, lbs.**   **MOMENT, lb-in.**
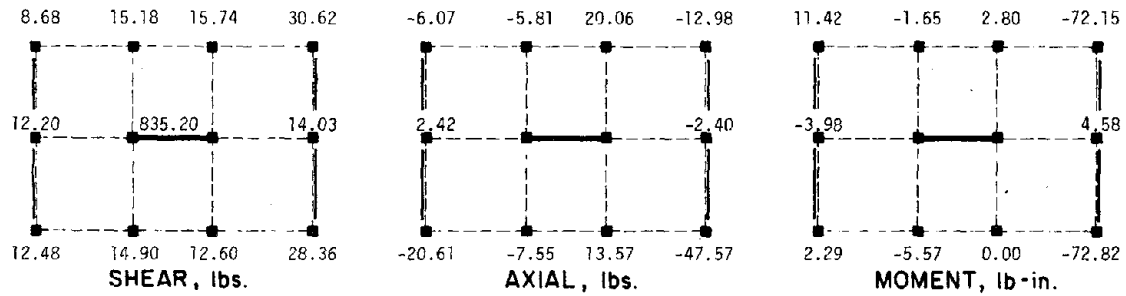
COLUMNS: 16.48%

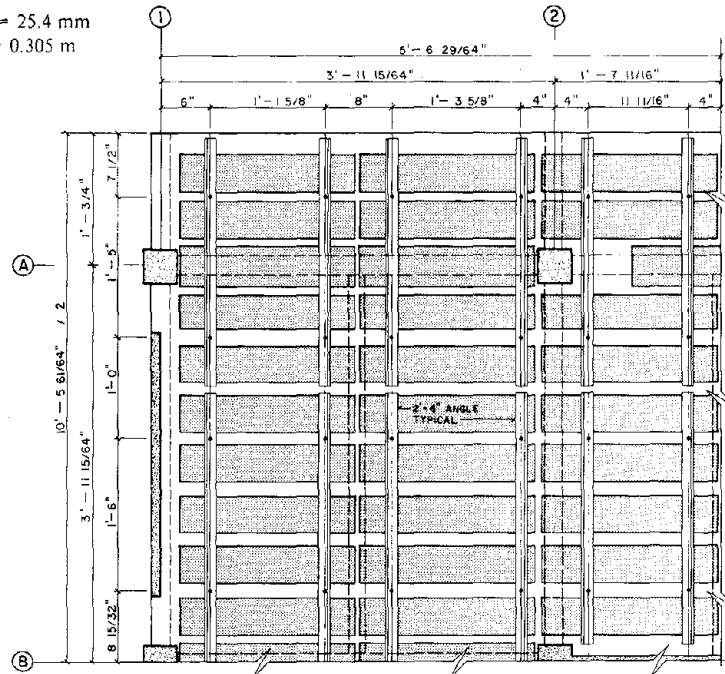SHEAR WALL: 83.52%   LOAD AT 1st FLOOR

1 lbf = 4.45 N

1 in. = 25.4 mm

FIG. 3-14   CONTINUED...

99
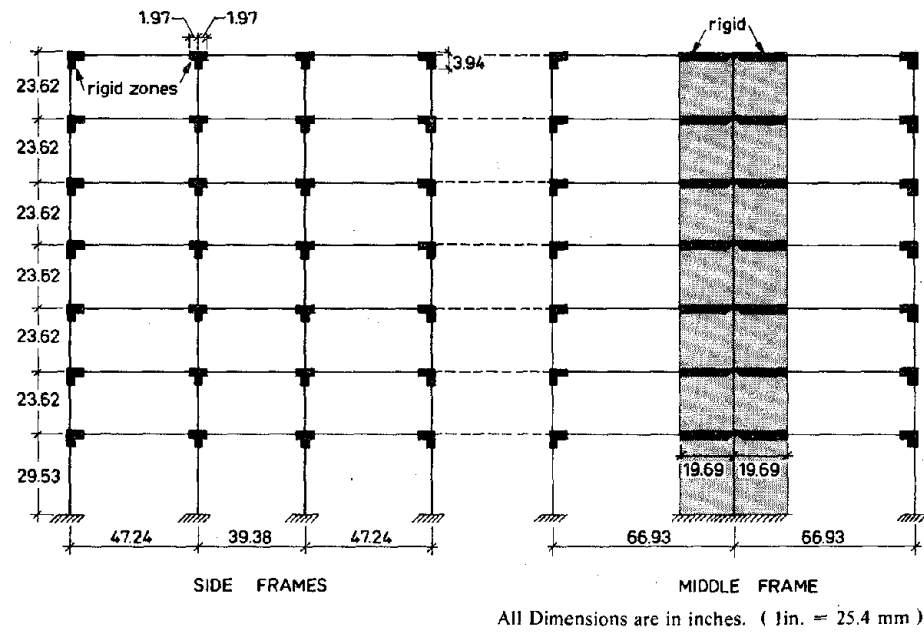
FIG. 4-1   IDEALIZATION OF FRAMES FOR ANALYSIS USING ETABS.

BAR SIZE	DIAMETER, mm	DIAMETER, in.
D2.0	2.0	.07874
D3.8	3.8	.1496
D4.4	4.4	.1732

$E_c = 3500$ ksi

$E_s = 2900$ ksi

$G = E_c / [2(1+\mu)]$ $\mu = 0.2$

(a) NOMENCLATURE AND MATERIAL CHARACTERISTICS

3 15/32" (88 mm)

$b \times D = 3\ 15/16" \times 3\ 15/16"$ (10 cm x 10 cm)	
PRINCIPAL REIN.	8 – D4.4 mm
HOOP D-2 SPACING O.C.	25/32" (20 mm)
CROSS TIE D-2 SPACING O.C.	VARIES
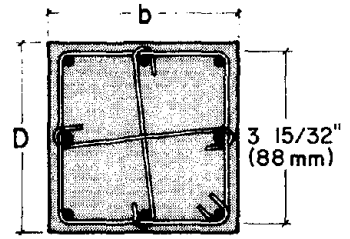
$I = 22.58$ in.^{4}

$A_v = \dfrac{(0.9)(3.94)(3.94)}{1.2}$ in.^{2}

$A = 16.87$ in.^{2}

NOTE: For columns adjacent to side walls the axial area has been increased by one-half & full transformed area of the side wall for corner and middle columns respectively.

Corner Column: $A = 35.76$ in.^{2}

Middle Column: $A = 54.36$ in.^{2}

(b) TYPICAL COLUMN CROSS SECTION

FIG. 4-2   CROSS-SECTIONAL PROPERTIES DEFINED IN THE ANALYTICAL MODEL.

MID SECTION   END SECTION
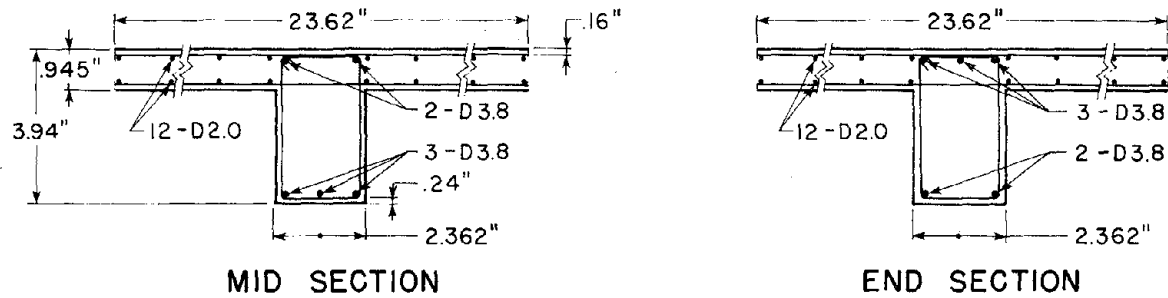
$$I_{MID} = 30.656 \text{ in.}^4$$
$$I_{END} = 29.837 \text{ in.}^4$$

$$I_{USED} = \frac{30.656 + 29.837}{2} = 30.250 \text{ in.}^4$$

$$A_V = \frac{(0.9)(2.362)(3.94)}{1.2} = 7.0 \text{ in.}^2 \qquad A = 30.88 \text{ in.}^2$$

(c) TYPICAL BEAM CROSS SECTION
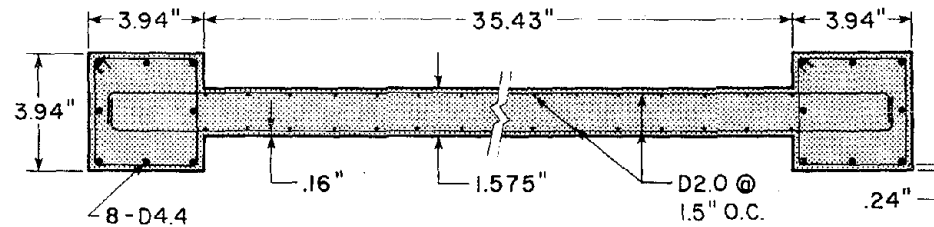
$$I = 19300 \text{ in.}^4$$

$$A_V = \frac{(0.8)(1.575)(43.31)}{1.2} = 45.47 \text{ in.}^2$$

$$A = 91.92 \text{ in.}^2$$

I = Uncracked Transformed Moment of Inertia

A_V = Shear Area

A = Uncracked Transformed Area

(d) SHEAR WALL CROSS SECTION

FIG. 4-2 CONTINUED...

MODE	f_i(HZ.)	MEASURED f (HZ.)	
		AMBIENT	FORCED
1	5.09	4.75	4.55
2	18.35		
3	36.61		

MODE	f_i(HZ.)	MEASURED f (HZ.)	
		AMBIENT	FORCED
1	12.45	9.75	8.25
2	44.72		
3	88.98		

MODEL LOADED WITH
REQUIRED BALLAST

BARE MODEL
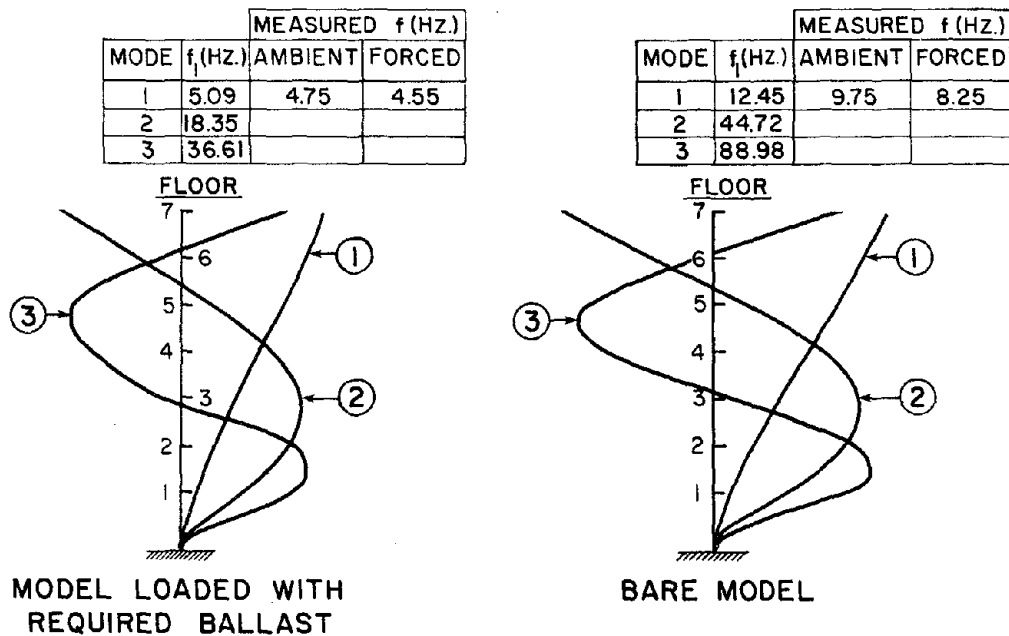
FIG. 4-3   ANALYTICAL MODE SHAPES AND FREQUENCIES
FOR MODEL BEFORE AND AFTER IT WAS LOADED
WITH THE REQUIRED BALLAST.
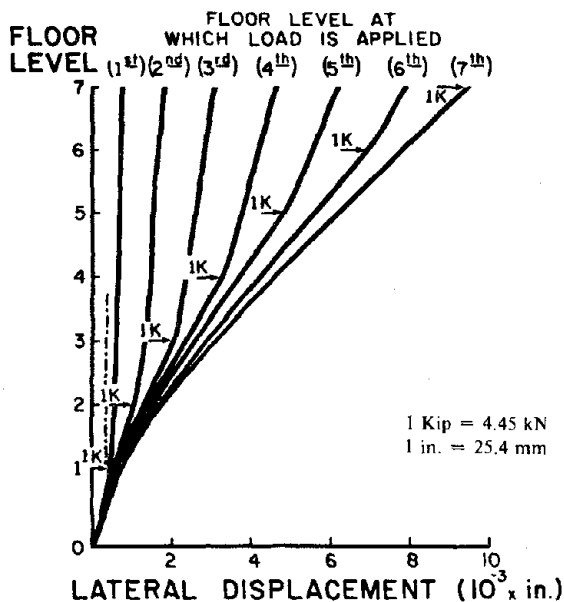
FIG. 4-4   ANALYTICALLY PREDICTED LATERAL DEFLECTION
PROFILES OF THE 1/5-SCALE MODEL.
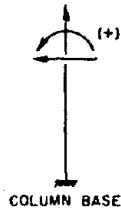
(+)

COLUMN BASE

All forces are normalized to 1000 lbs. of applied external force. All forces are incremental. Lateral load was applied at the right end and directed towards the left end.

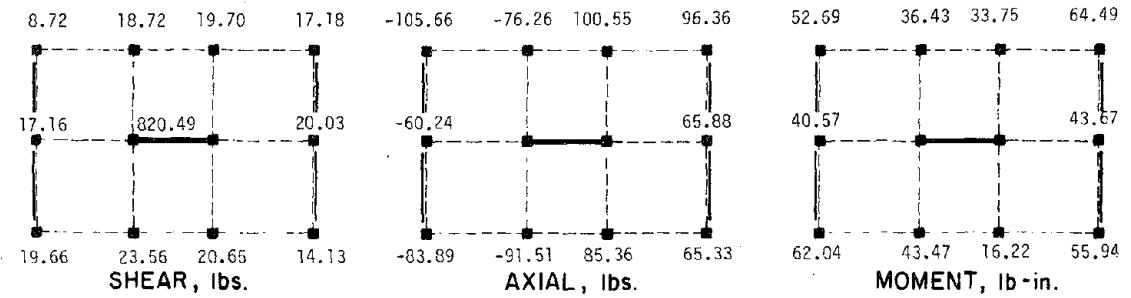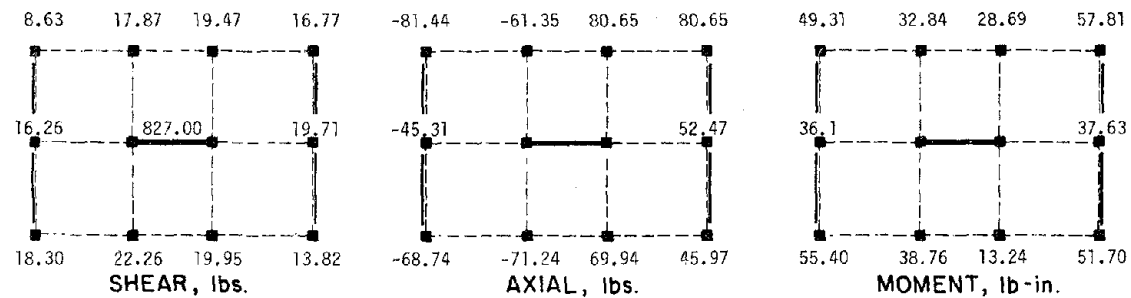| 14.94	22.35	22.35	14.94

17.38   816.08   17.38

-14.94	22.35	22.35	14.94

SHEAR, lbs.

-196.88	-52.52	52.52	196.88

-293.30   0.00   293.30

-196.88	-52.52	52.52	196.88

AXIAL, lbs.

282.14	350.80	350.80	282.14

304.80   72546.90   304.80

282.14	350.80	350.80	282.14

MOMENT, lb-in.
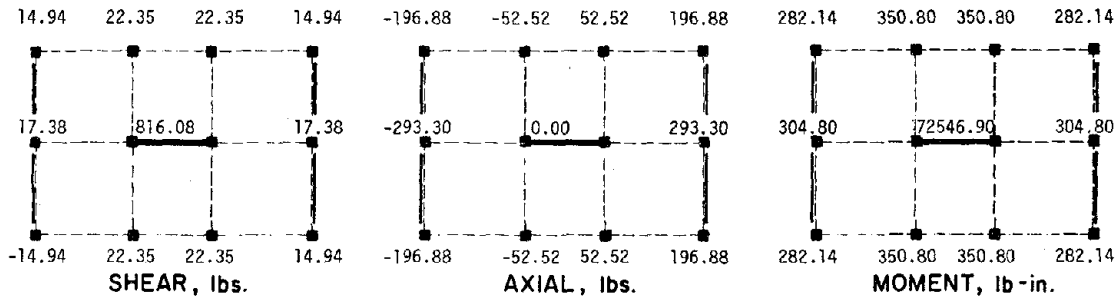
COLUMNS: 18.40%

SHEAR WALL: 81.60%

LOAD AT 7th FLOOR

14.62	21.69	21.69	14.62

16.78   821.23   16.78

14.62	21.69	21.69	14.62

SHEAR, lbs.

-159.65	-43.12	43.12	159.65

-232.94   0.00   232.94

-159.65	-43.12	43.12	159.65

AXIAL, lbs.

273.20	338.80	338.80	273.20

293.30   67277.30   293.30

273.20	338.80	338.80	273.20

MOMENT, lb-in.
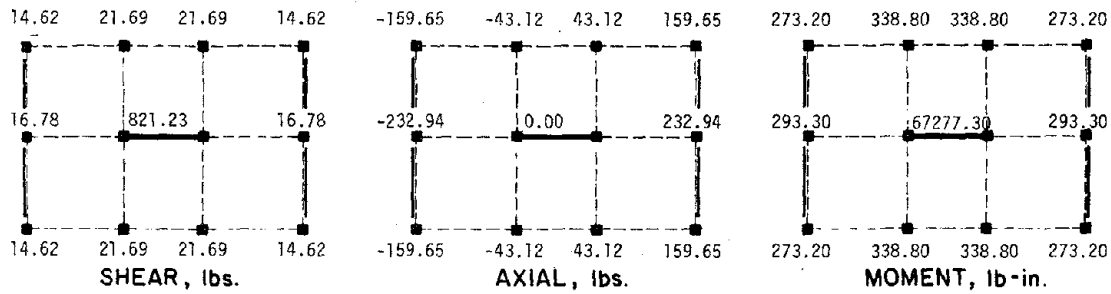
COLUMNS: 17.88%

SHEAR WALL: 82.12%

LOAD AT 6th FLOOR

14.25	20.94	20.94	14.25

16.09   827.06   16.09

14.25	20.94	20.94	14.25

SHEAR, lbs.

-124.14	-33.37	33.37	124.14

-178.48   0.00   178.48

-124.14	-33.37	33.37	124.14

AXIAL, lbs.

263.10	325.20	325.20	263.10

280.40   61342.85   280.40

263.10	325.20	325.20	263.10

MOMENT, lb-in.

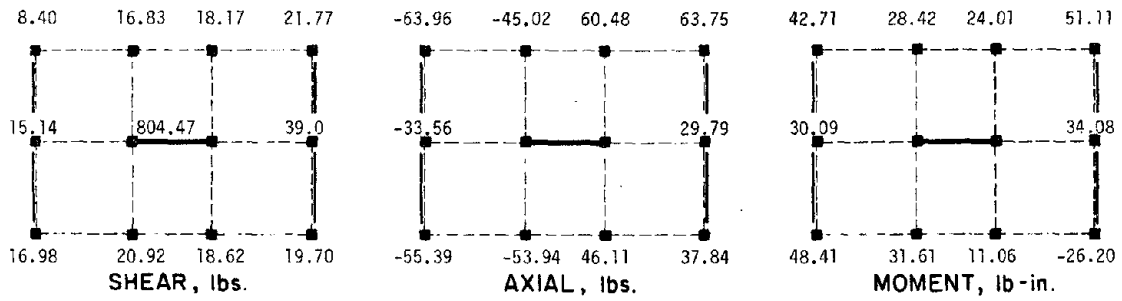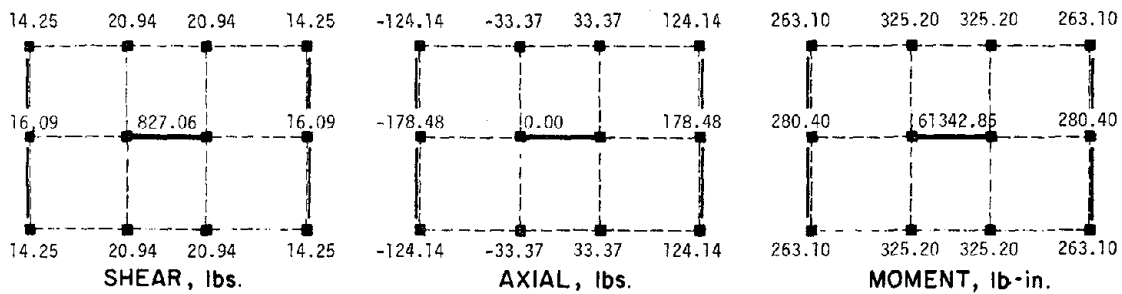COLUMNS: 17.29%

SHEAR WALL: 82.71%

LOAD AT 5th FLOOR

1 lbf = 4.45 N
1 in. = 25.4 mm

FIG. 4-5   FORCE DISTRIBUTION AT BASE FROM ANALYSIS.

104

13.78	20.08	20.08	13.78

```
15.27        |834.02|        15.27
```

```
13.78    20.08    20.08    13.78
```
SHEAR, lbs.
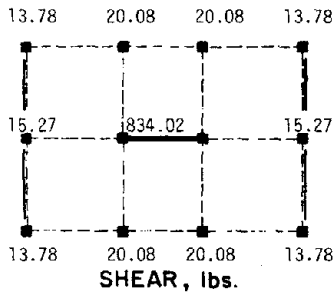
COLUMNS: 16.60%

SHEAR WALL: 83.40%

-90.30	-24.19	24.19	90.30

```
-175.24      |0.00|      175.24
```

```
-90.30   -24.19   24.19    90.30
```
AXIAL, lbs.

LOAD AT 4th FLOOR

251.20	305.50	305.50	251.20

```
280.30      |54466.10|      280.30
```

```
251.20   305.50   305.50   251.20
```
MOMENT, lb-in.

13.36	18.99	18.99	13.36

```
14.43        |841.74|        14.43
```

```
13.36    18.99    18.99    13.36
```
SHEAR, lbs.
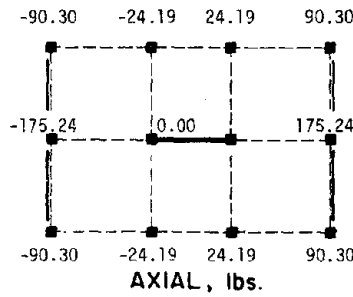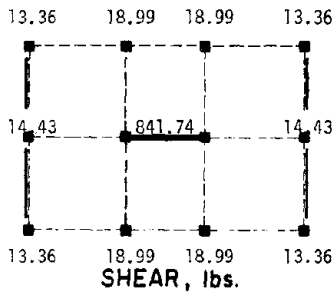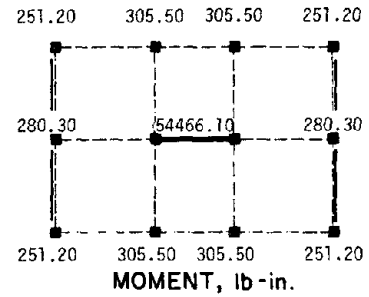
COLUMNS: 15.83%

SHEAR WALL: 84.17%

-59.33	-15.73	15.73	59.33

```
-81.77       |0.00|       81.77
```

```
-59.33   -15.73   15.73    59.33
```
AXIAL, lbs.

LOAD AT 3rd FLOOR

237.80	290.00	290.00	237.80

```
247.70      |46095.00|      247.70
```

```
237.80   290.00   290.00   237.80
```
MOMENT, lb-in.

12.06	17.47	17.47	12.06

```
12.45        |856.98|        12.45
```

```
12.06    17.47    17.47    12.06
```
SHEAR, lbs.
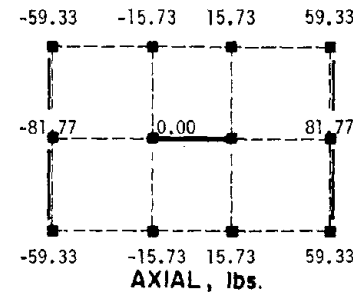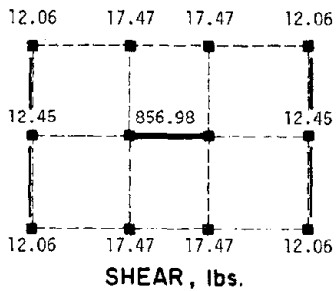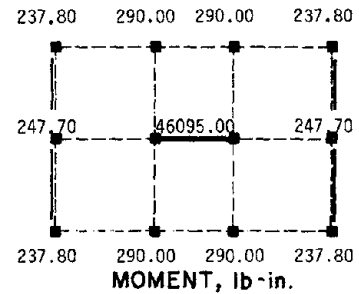
COLUMNS: 14.30%

SHEAR WALL: 85.70%

-32.56	-8.34	8.34	32.56

```
-43.32       |0.00|       43.38
```

```
-32.56   -8.34    8.34    32.56
```
AXIAL, lbs.

LOAD AT 2nd FLOOR

214.40	264.50	264.50	214.40

```
218.10      |35616.40|      218.10
```

```
214.40   264.50   264.50   214.40
```
MOMENT, lb-in.

14.89	18.17	18.17	14.89

```
14.83        |838.13|        14.83
```

```
14.89    18.17    18.17    14.89
```
SHEAR, lbs.
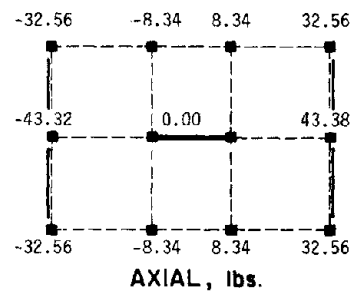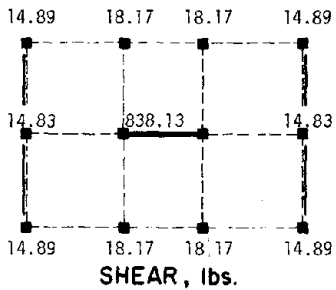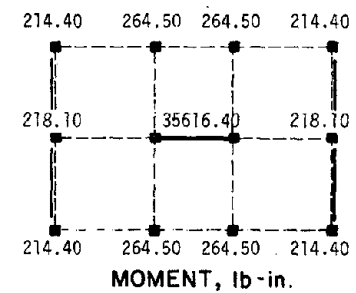
COLUMNS: 16.19%

SHEAR WALL: 83.81%

-11.79	-2.65	2.65	11.79

```
-14.66       |0.00|       14.66
```

```
-11.79   -2.65    2.65    11.79
```
AXIAL, lbs.

LOAD AT 1st FLOOR

223.00	253.50	253.50	223.00

```
222.50      |22041.30|      222.50
```

```
223.00   253.50   253.50   223.00
```
MOMENT, lb-in.
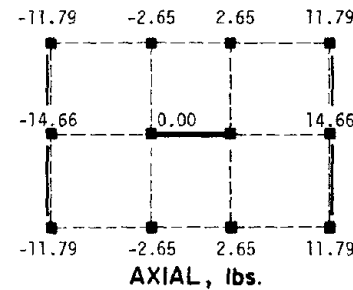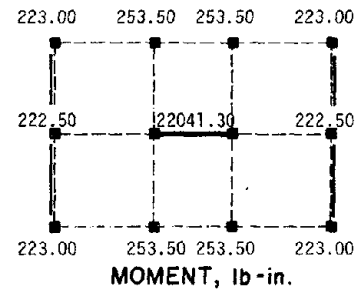
1 lbf = 4.45 N
1 in. = 25.4 mm

FIG. 4-5 CONTINUED...

105
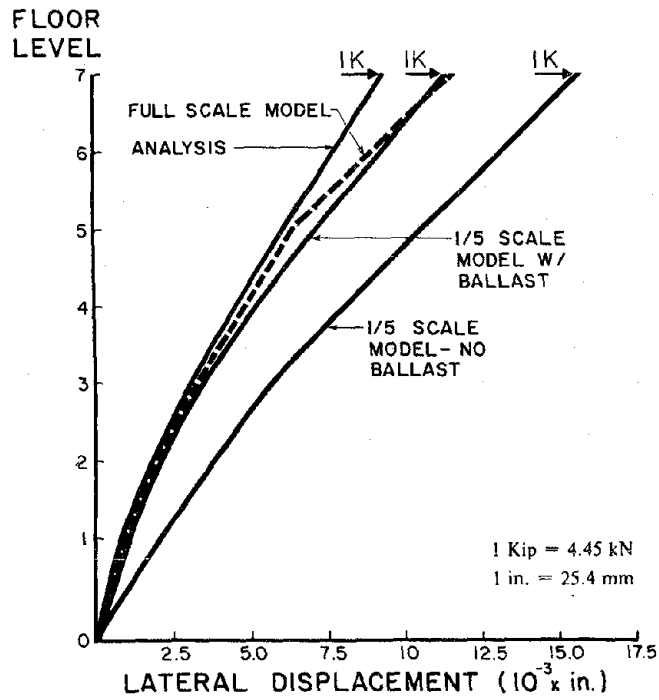
(a) LOADED AT 7TH FLOOR   (b) LOADED AT 1ST FLOOR
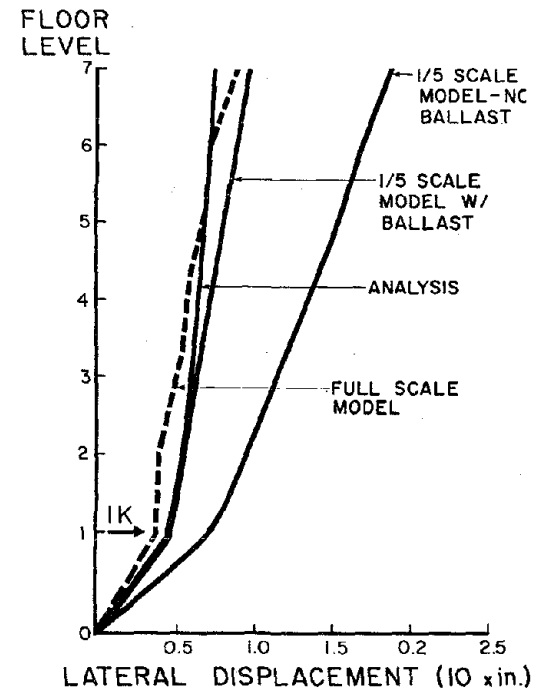
FIG. 5-1   DISPLACEMENT PROFILES OBTAINED FOR THE
1/5-SCALE MODEL AND FULL-SCALE STRUCTURE.

FLOOR LEVEL

NO SHEAR
DISTORTION

$G^* = \frac{1}{10} G$

$G^* = \frac{1}{4} G$

NOMINAL
G = 1458 KSI

EFFECT OF SHEAR DISTORTION
ON WALL FLEXIBILITY

$f = L^3/(3EI) + L/(GA_v)$

1ksi = 6.9 MN/m²
1 in. = 25.4 mm

LATERAL DISPLACEMENT ($10^3 \times$ in.)
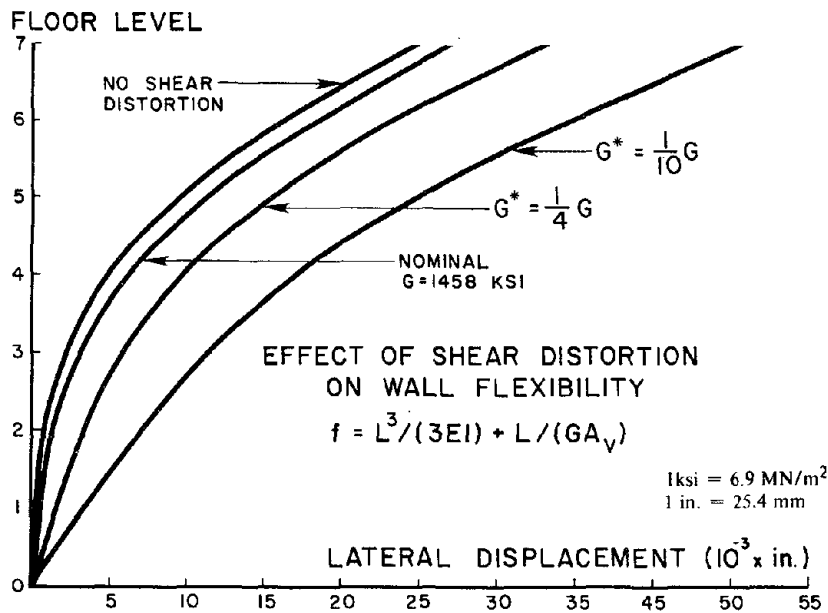
FIG. 5-2   EFFECTS OF SHEAR DISTORTION ON WALL FLEXIBILITY.

FLOOR LEVEL

1K 1K   1K   1K   1K

ANALYSIS, G = 1458
KSI FOR FRAMES
NO SHEAR DIS-
TORTION IN
SHEAR WALL

BARE MODEL,
EXPERIMENTAL

ANALYSIS, G = 145 KSI
FOR SHEAR WALL,
1458 KSI FOR OTHER
MEMBERS

MODEL LOADED WITH
BALLAST, EXPERIMENTAL

ANALYSIS, G = 1458 KSI
FOR ALL MEMBERS

1ksi = 6.9 MN/m²
1 in. = 25.4 mm
1 Kip = 4.45 kN

LATERAL DISPLACEMENT ($10^3 \times$ in.)
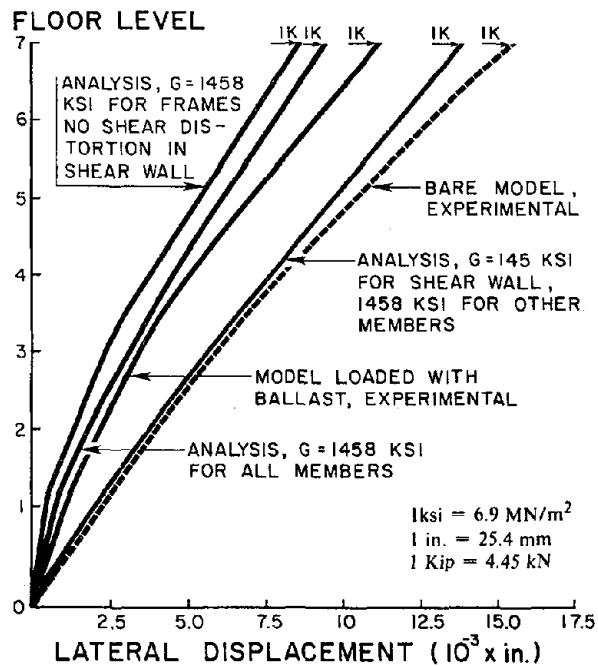
FIG. 5-3   EXPERIMENTAL AND ANALYTICAL LATERAL DISPLACEMENT
PROFILES OF THE STRUCTURE WHEN LOADED WITH
1 KIP LATERAL LOAD AT 7TH FLOOR LEVEL.

107
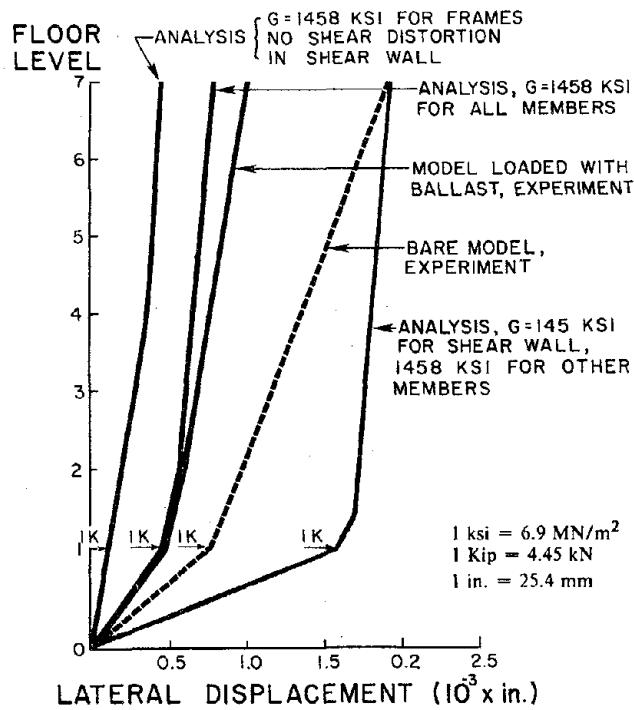
FIG. 5-4 EXPERIMENTAL AND ANALYTICAL LATERAL DISPLACEMENT
PROFILES OF THE STRUCTURE WHEN LOADED WITH
1 KIP LATERAL LOAD AT 1ST FLOOR LEVEL.
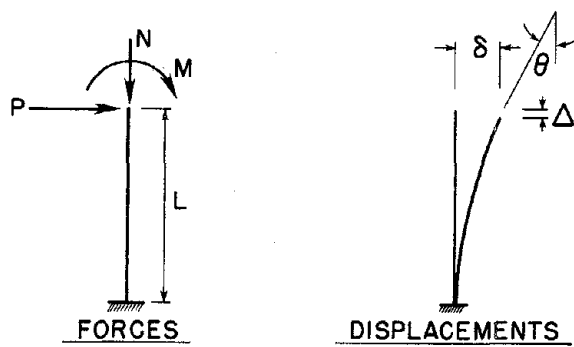
$$\begin{Bmatrix} \Delta \\ \delta \\ \theta \end{Bmatrix} = \begin{pmatrix} L/(EA) & 0 & 0 \\ 0 & L^3/(3EI) + L/(GA_v) & L^2/(2EI) \\ 0 & L^2/(2EI) & L/(EI) \end{pmatrix} \begin{Bmatrix} N \\ P \\ M \end{Bmatrix}$$

FIG. 5-5 DISPLACEMENT-FORCE RELATIONS FOR 1-D
CANTILEVER ELEMENT.

108

APPENDIX A

STIFFNESS MATRIX AND FREQUENCIES CALCULATED
FROM EXPERIMENTALLY GENERATED FLEXIBILITY MATRIX

A.1 General Remarks

Stiffness matrices and frequencies were calculated from experimentally generated flexibility matrices for the structure, using the computed values of translational masses and corresponding diagonal mass matrices. Problems in computation were identified and the reasons for non-symmetry of the experimentally generated flexibility matrix, as well as for the possible errors in the measurement of the displacement, were discussed in Sec. 2.3.3 of the report.

In this Appendix a feasible method is presented for conditioning the experimental flexibility matrix to become positive-definite in order to result in a realistic and positive-definite stiffness matrix. Accuracy of the stiffness matrix and frequencies are also discussed. This problem is considered relevant, particularly when it is desired to obtain the dynamic characteristics of a test structure by only a static flexibility test.

A.2 Results of Calculations

The flexibility matrices generated experimentally were not symmetric, as mentioned in Sec. 2.3.3. For the calculation of the stiffness matrices and frequencies, however, the flexibility matrices were rendered symmetric by using the average values of corresponding off-diagonal terms, i.e., $f_{ij} = (f_{ij} + f_{ji})/2$, for the following reasons:

(1) The corresponding stiffness matrix can be obtained as a symmetric matrix, simplifying the solution process of an eigenvalue problem, and facilitates the conceptual understanding of the results of the calculations. All eigenvalues will be real, and eigenvectors will be orthogonal

with respect to the mass matrix and with respect to the stiffness matrix, if the resulting stiffness matrix is symmetric.

(2) As mentioned in Sec. 2.3.3, to induce measurable displacements, the lateral loads that had to be applied to the different floors were sufficiently large to induce nonlinear response of the structure; this was considered to be a main reason leading to unsymmetry of the flexibility matrix. However, it was desired to apply the elastic theory in the analyses, which required that the flexibility matrix must be symmetric.

(3) In the computer code CAL 78 [A.1], used for the calculation, a symmetric stiffness matrix is required for the solution of an eigenvalue problem.

Using the computer code CAL 78 in which the Gauss elimination method is used for matrix inversion, the stiffness matrix was obtained by inverting the experimentally generated flexibility matrix. The resulting stiffness matrices for the structure, with and without ballast load, are presented in Tables A.1 and A.2, respectively. The stiffness matrix for the structure without ballast load, presented in Table A.1, has negative values in the main-diagonal terms (k_{22} and k_{33}) and is not positive-definite. This is contrary to the theory that a stiffness matrix (also flexibility matrix) should be positive definite if a structure is stable. Therefore, it has no meaning from the engineering standpoint. The stiffness matrix for the structure with ballast load, however, is positive definite.

In order to compare the result with an analytical result, an analytical flexibility matrix was generated, using the computer code SAP 81 [A.2] and was inverted to obtain a stiffness matrix. For the determination of the analytical flexibility matrix, the structure was idealized

A-2

as described in Sec. 4.1, and the cross-sectional properties of the elements shown in Fig. 4.2 were used. Compared with the analytical result presented in Table A.3, the coefficients of the main diagonal terms k_{11} to k_{77} of the stiffness matrix for the structure with ballast load, range from 0.86 to 1.09 times the corresponding co-efficients of the analytical stiffness matrix.

The frequencies of vibration were also calculated, using the computer code CAL 78 [A.1], in which the Jacobi diagonalization method is used to solve the following eigenvalue problem:

$$K\phi = M\phi\lambda$$

where K, M, ϕ and λ are a symmetric stiffness matrix, diagonal mass matrix, eigenvectors, and eigenvalues, respectively. The computed values of translational masses presented in Table 3.1 and the stiff-ness matrices obtained by inverting the experimental flexibility matrices were used. Results of calculations are presented in Table A.4 and Fig. A.1, with experimental results obtained from the dynamic tests and with the analytical results. An important observation is that the calculated frequencies (semi-analytical frequencies), of 1st and 2nd mode, agree well with the experimental frequencies for the structure with ballast load, and with the unloaded (bare) structure whose stiffness matrix contained negative diagonal elements.

It is also important to note that the semi-analytical frequency of the highest (7th) mode for the structure without ballast load was imaginary because the stiffness matrix was not positive-definite. There are some differences observed between analytical and semi-analytical frequencies as well as between analytical and experimental frequencies, especially in the 1st mode for the structure without ballast load. The reasons for these differences have been discussed in detail in

A-3

Sec. 5.1 and 5.2.

Results mentioned above indicate: (1) a stiffness matrix obtained by inverting an experimentally generated flexibility matrix may not be accurate, and occasionally conceptually meaningless; (2) frequencies of vibration still can be calculated with reasonable accuracy, especially for the lower modes, using such a stiffness matrix and a computed mass matrix, i.e., a semi-analytical process. It is also implicated that slight errors in the measured coefficients of a flexibility matrix may result in a meaningless stiffness matrix with negative diagonal elements and that some modifications would then be needed to obtain a meaningful positive-definite stiffness matrix from an experimental flexibility matrix.

In order to obtain such a real and positive-definite stiffness matrix for the structure without ballast load, the following modification to condition the experimental flexibility matrix to become positive-definite was carried out and evaluated.

From vibration theory,

$$K\phi_n = \omega_n^2 M\phi_n \tag{1}$$

where   K = stiffness matrix

   ϕ = normalized mode shape   ($\phi_n^T M\phi_n = 1$, $\phi_m^T M\phi_n = 0$ for any $m \neq n$)

   ω = circular frequency

   M = diagonal mass matrix

After premultiplying Eq. (1) by $(1/\omega_n^2) \phi_n^T Mf$ and $(1/\omega_n^2) \phi_m^T Mf$, respectively, the following expressions are obtained

$$1/\omega_n^2 = \phi_n^T Mf M\phi_n \tag{2a}$$

$$0 = \phi_m^T Mf M\phi_n \tag{2b}$$

where f is a flexibility matrix.

from Eqs. (2a) and (2b), the following equation can be obtained.

$$\Phi^T M f M \Phi = \begin{bmatrix} 1/\omega_1^2 & & 0 \\ & \ddots & \\ & 1/\omega_i^2 & \\ & & \ddots \\ 0 & & 1/\omega_n^2 \end{bmatrix} = \text{diag}\left[1/\omega_i^2\right] \qquad (3)$$

where, $\Phi = [\phi_1, \phi_2, \cdots, \phi_n]$

Using the equations, $\Phi^T M \Phi = I$, or $[\Phi^T M]^{-1} = \Phi$ and

$[M\Phi]^{-1} = \Phi^T$, a flexibility matrix can be written as follows:

$$f = \Phi \text{ diag}\left[1/\omega_i^2\right] \Phi^T \qquad (4)$$

or

$$f_{ij} = \sum_{k=1}^{n} (\phi_{ik} \cdot 1/\omega_k^2 \cdot \phi_{jk}) \qquad (5)$$

Using the Eqs. (4) and (5) and substituting the semi-analytical values
of ϕ and ω for the 1st to 6th modes, but the analytical values of
ϕ_7 and ω_7 instead of the semi-analytical ones because the semi-analytical
value of (ω_7) was imaginary, the experimental flexibility matrix for the
structure without ballast load was modified. The modified flexibility
matrix is presented in Table A.5 with the flexibility matrix before
modification. The stiffness matrix and frequencies (which were calcu-
lated from the modified flexibility matrix in the same manner as that
described earlier) are presented in Table A.6.

It is observed that the modified flexibility matrix is nearly equal
to the flexibility matrix before modification, such that the discrepancy
between the individual coefficients of the matrices before and after
modification, is not more than 0.7 percent. The stiffness matrix
calculated from the modified flexibility matrix differs considerably

A-5

from the one presented in Table A.1, and is a positive-definite matrix. Compared with the analytical stiffness matrix presented in Table A.3, the coefficients of the main-diagonal terms k_{11} to k_{77} range from 0.76 to 1.31 times the corresponding analytical values.

It is also important to note that the frequencies calculated after the modification of the flexibility matrix are almost identical to the frequencies before modification, except for the 7th mode frequency which was modified as previously described.

Using the analytical values of ω and ϕ for the 5th to 7th modes instead of the semi-analytical values for the structure without ballast load, the modification procedure described previously was carried out again in order to investigate the effects of more extensive modification on the stiffness matrix. In this case, the resulting stiffness matrix did not differ considerably from the previous one, presented in Table A.6, which was obtained from the flexibility matrix modified by using the analytical value of ω and ϕ for only the 7th mode. The difference in the coefficients of the main-diagonal terms k_{11} to k_{77} between the two stiffness matrices was not larger than 14 percent. The possible reason that the derived stiffness matrix in this case was quite similar to the previous one is that the discrepancy between the analytical and semi-analytical values of ω and ϕ for 5th and 6th modes was not very large when compared to the discrepancy observed for the 7th mode.

An explanation of the sensitivity of the stiffness matrix to higher frequencies of vibration may be as follows:

As expressed in the Eqs. (4) and (5), a flexibility matrix is a function of circular frequencies (ω_k). Since the value of ($1/\omega_k^2$) decreases from the order of 10^{-4} to the order of 10^{-7} as the order of mode (k) increases, as shown in Fig. A.1, the values of the coefficients

of the flexibility matrix are significantly affected by the values of $(1/\omega_k^2)$ for lower modes while the contribution of the values of $(1/\omega_k^2)$ for higher modes is very little.

In the same manner, a stiffness matrix is also expressed as a function of (ω_k), as shown below.

$$K = \Phi^T \ \text{diag} \ [\omega_i^2] \ \Phi \tag{6}$$

or

$$K_{ij} = \sum_{k=1}^{n} (\phi_{ki} \cdot \omega_k^2 \cdot \phi_{kj}) \tag{7}$$

It is obvious that the values of the terms in the stiffness matrix are significantly affected by the value of (ω_k^2) for higher modes while the values of (ω_k^2) for lower modes contribute very little. In other words, higher modes dominate the form of the stiffness matrix while lower modes are influential on the flexibility matrix.

A.3 Concluding Remarks

From the results described previously, the following conclusions may be drawn.

(1) A positive-definite stiffness matrix could not be obtained by inverting the experimentally generated flexibility matrix for the bare structure. The stiffness matrix contained negative values in the main-diagonal terms and, therefore, was meaningless. The stiffness matrix obtained for the structure with ballast load, however, was positive-definite. However, an uncertainty regarding the reliability of the stiffness matrix, attributed to very slight numerical inaccuracies in the measured coefficients of the flexibility matrix, was present for this case as well. Slight numerical inaccuracies in flexibility were observed to strongly affect the stiffness matrix through the

inversion process and such inaccuracies might still exist despite efforts made during the experiment to avoid them.

(2) The frequencies of vibration for the structure, with and without ballast load, were calculated with reasonable accuracy, except for higher modes, using the stiffness matrix obtained from the experimental flexibility matrix and the computed mass matrix, i.e., following a semi-analytical process. The semi-analytical frequencies of 1st and 2nd modes agreed well with the experimental results obtained from the dynamic tests. The slight numerical inaccuracies in the measured coefficients of the experimental flexibility matrix had no significant influence on the calculation of the frequencies of lower modes. These results indicate the significance of generating dynamic characteristics of a structure by carrying out a static flexibility test only.

(3) The stiffness matrix for the bare structure without ballast load, obtained from the flexibility matrix modified by using the method described in this Appendix, was a positive-definite matrix. This modification procedure was considered effective in conditioning the experimental flexibility matrix to become positive-definite in order to result in a realistic and positive-definite stiffness matrix.

(4) Since it was not possible to generate the structure's stiffness matrix experimentally, both in the U.S. and Japan, because of limitations in loading and measurement techniques, inversion of the experimental flexibility was the only possible way to generate this matrix. A strong sensitivity of the stiffness matrix to even slight errors in the measured flexibility coefficients was observed.

REFERENCES

A.1 Wilson, E. L., "CAL 78 User Information Manual," Report No. U.C./SESM 79-1, Structural Engineering and Structural Mechanics, Department of Civil Engineering, College of Engineering, University of California, Berkeley, Nov. 1978.

A.2 Wilson, E. L., "SAP-81 Structural Analysis Programs for CP/M Microcomputer Systems," March 1981.

TABLE A.1

STIFFNESS MATRIX CALCULATED FROM EXPERIMENTALLY GENERATED
FLEXIBILITY MATRIX FOR THE STRUCTURE WITHOUT BALLAST LOAD
(BARE STRUCTURE)

UNITS (KIP/IN)

CORRESPONDING:(j) FLOOR LEVEL: (i)	7	6	5	4	3	2	1
7	920						
6	563	-6058		SYMMETRIC:			
5	-3439	11607	-13380				
4	2048	-8032	7287	1469			
3	-115	2137	-2803	-3207	7890		
2	-176	1444	-2470	2441	-4957	6779	
1	383	2659	4439	-2708	1160	-3269	4635

1 kip/in. = 175 N/mm

Preceding page blank

TABLE A.2

STIFFNESS MATRIX CALCULATED FROM EXPERIMENTALLY GENERATED
FLEXIBILITY MATRIX FOR THE STRUCTURE WITH BALLAST LOAD

UNITS (KIP/IN)

CORRESPONDING:(j) FLOOR LEVEL: (i)	7	6	5	4	3	2	1
7	2212						
6	-3534	7981		SYMMETRIC:			
5	679	-4551	7802				
4	420	-164	-3746	6974			
3	433	24	-1138	-3546	8812		
2	363	-572	720	40	-4669	7799	
1	-1026	1581	-93	-42	43	-4140	6530

1 kip/in. = 175 N/mm

TABLE A.3

ANALYTICALLY GENERATED STIFFNESS MATRIX OF THE STRUCTURE

UNITS   (KIP/IN)

CORRESPONDING:(j) FLOOR LEVEL: (i)	7	6	5	4	3	2	1
7	2302						
6	-3477	7637		SYMMETRIC			
5	831	-4802	8045				
4	160	582	-4766	8066			
3	103	-271	626	-4764	8101		
2	56	42	-36	673	-4764	8084	
1	17	13	92	-10	654	-4505	7013

1 kip/in. = 175 N/mm

TABLE A.4

FREQUENCIES OF THE MODEL STRUCTURE

(A)BEFORE LOADING WITH BALLAST (THE BARE MODEL)

DETERMINATION TECHNIQUE	UNITS (Hz)						
	MODE						
	1st	2nd	3rd	4th	5th	6th	7th
* SEMI-ANALYSIS:	9.55	42.5	89.3	141.	164.	241.	N/A**
ANALYSIS:	12.2	46.0	94.6	144.	189.	229.	258.
DYNAMIC TESTS:	8.25/ 9.75	42.54					

(B)AFTER LOADING WITH BALLAST

DETERMINATION TECHNIQUE	UNITS (Hz)						
	MODE						
	1ST	2ND	3RD	4TH	5TH	6TH	7TH
SEMI-ANALYSIS:	4.79	18.1	35.4	71.0	73.4	95.1	99.8
ANALYSIS:	4.97	18.9	38.9	59.3	78.2	94.5	106.
DYNAMIC TESTS:	4.55/ 4.78	17.86					

* SEMI-ANALYSIS:BASED ON ANALYTICAL MASS AND MEASURED FLEXIBILITY CHARACTERISTICS

** 7th FREQUENCY IS IMAGINARY

TABLE A.5

FLEXIBILITY MATRIX GENERATED EXPERIMENTALLY FOR THE STRUCTURE WITHOUT BALLAST LOAD

(a) BEFORE MODIFICATION: UNITS (10^{-3} IN/KIP)

CORRESPONDING:(j) FLOOR LEVEL: (i)	7	6	5	4	3	2	1
7	15.59						
6	13.31	11.87		SYMMETRIC:			
5	10.64	9.72	8.08				
4	8.00	7.36	6.33	5.20			
3	5.68	5.35	4.64	3.91	3.21		
2	3.67	3.50	3.05	2.61	2.21	1.77	
1	1.95	1.82	1.64	1.39	1.20	.99	.74

(b) AFTER MODIFICATION:

CORRESPONDING:(j) FLOOR LEVEL: (i)	7	6	5	4	3	2	1
7	15.60						
6	13.30	11.90		SYMMETRIC			
5	10.66	9.67	8.13				
4	7.98	7.38	6.30	5.21			
3	5.67	5.35	4.64	3.91	3.21		
2	3.67	3.50	3.06	2.60	2.21	1.77	
1	1.96	1.83	1.63	1.40	1.20	.99	.74

1 in./kip = 5.59 mm/kN

TABLE A.6

STIFFNESS MATRIX AND FREQUENCIES CALCULATED FROM THE MODIFIED FLEXIBILITY MATRIX FOR THE STRUCTURE WITHOUT BALLAST LOAD

(a) STIFFNESS MATRIX: UNITS   (KIP/IN)

CORRESPONDING:(j) FLOOR LEVEL: (i)	7	6	5	4	3	2	1
7	1740						
6	-2797	8143		SYMMETRIC			
5	799	-6689	10502				
4	64	736	-4306	7158			
3	305	243	267	-4470	8192		
2	415	-1047	725	935	-4690	7353	
1	634	1671	-1161	-31	651	-4163	6070

(b)FREQUENCIES: UNITS   (Hz)

| | MODE | | | | | | |
	1ST	2ND	3RD	4TH	5TH	6TH	7TH
BEFORE MODIFICATION:	9.55	42.5	89.3	141.	164.	241.	N/A*
AFTER MODIFICATION:	9.55	42.5	89.3	143.	165.	243.	264.

* 7TH FREQUENCY IS IMAGINARY

kip/in. = 175 N/mm
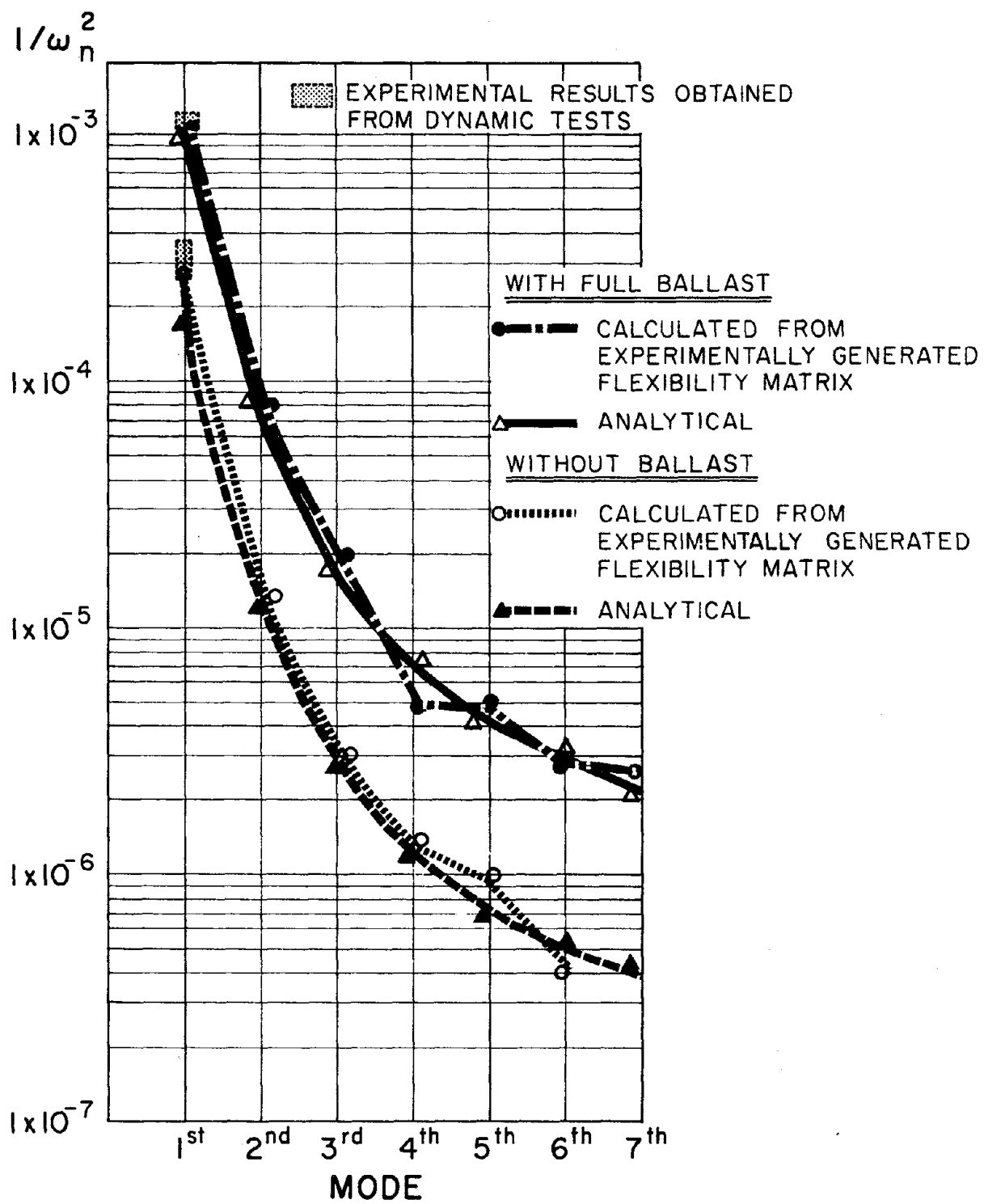
FIG. A-1   COMPARISON OF CALCULATED CIRCULAR FREQUENCIES OBTAINED
FROM EXPERIMENTALLY GENERATED FLEXIBILITY MATRIX AND
ANALYTICALLY PREDICTED STIFFNESS MATRIX

APPENDIX B

U.S. CUSTOMARY-SI CONVERSION FACTORS

1 in.   =   25.40 mm

1 in.   =   0.0254 m

1 ft   =   0.305 m

1 sq in. =   6.45 cm^2

1 cu in. =   16.40 cm^3

1 cu yd   =   0.765 m^3

1 lb   =   0.453 kg

1 ton   =   907.2 kg

1 lbf   =   4.45 N

1 psi   =   6.9 kN/m^2

EARTHQUAKE ENGINEERING RESEARCH CENTER REPORTS

NOTE: Numbers in parentheses are Accession Numbers assigned by the National Technical Information Service; these are
followed by a price code. Copies of the reports may be ordered from the National Technical Information Service, 5285
Port Royal Road, Springfield, Virginia, 22161. Accession Numbers should be quoted on orders for reports (PB --- ---)
and remittance must accompany each order. Reports without this information were not available at time of printing.
The complete list of EERC reports (from EERC 67-1) is available upon request from the Earthquake Engineering Research
Center, University of California, Berkeley, 47th Street and Hoffman Boulevard, Richmond, California 94804.

UCB/EERC-77/01   "PLUSH - A Computer Program for Probabilistic Finite Element Analysis of Seismic Soil-Structure Inter-
                 action," by M.P. Romo Organista, J. Lysmer and H.B. Seed - 1977 (PB81 177 651)A05

UCB/EERC-77/02   "Soil-Structure Interaction Effects at the Humboldt Bay Power Plant in the Ferndale Earthquake of June
                 7, 1975," by J.E. Valera, H.B. Seed, C.F. Tsai and J. Lysmer - 1977 (PB 265 795)A04

UCB/EERC-77/03   "Influence of Sample Disturbance on Sand Response to Cyclic Loading," by K. Mori, H.B. Seed and C.K.
                 Chan - 1977 (PB 267 352)A04

UCB/EERC-77/04   "Seismological Studies of Strong Motion Records," by J. Shoja-Taheri - 1977 (PB 269 655)A10

UCB/EERC-77/05   Unassigned

UCB/EERC-77/06   "Developing Methodologies for Evaluating the Earthquake Safety of Existing Buildings," by No. 1 -
                 B. Bresler; No. 2 - B. Bresler, T. Okada and D. Zisling; No. 3 - T. Okada and B. Bresler; No. 4 - V.V.
                 Bertero and B. Bresler - 1977 (PB 267 354)A08

UCB/EERC-77/07   "A Literature Survey - Transverse Strength of Masonry Walls," by Y. Omote, R.L. Mayes, S.W. Chen and
                 R.W. Clough - 1977 (PB 277 933)A07

UCB/EERC-77/08   "DRAIN-TABS: A Computer Program for Inelastic Earthquake Response of Three Dimensional Buildings," by
                 R. Guendelman-Israel and G.H. Powell - 1977 (PB 270 693)A07

UCB/EERC-77/09   "SUBWALL: A Special Purpose Finite Element Computer Program for Practical Elastic Analysis and Design
                 of Structural Walls with Substructure Option," by D.Q. Le, H. Peterson and E.P. Popov - 1977
                 (PB 270 567)A05

UCB/EERC-77/10   "Experimental Evaluation of Seismic Design Methods for Broad Cylindrical Tanks," by D.P. Clough
                 (PB 272 280)A13

UCB/EERC-77/11   "Earthquake Engineering Research at Berkeley - 1976," - 1977 (PB 273 507)A09

UCB/EERC-77/12   "Automated Design of Earthquake Resistant Multistory Steel Building Frames," by N.D. Walker, Jr. - 1977
                 (PB 276 526)A09

UCB/EERC-77/13   "Concrete Confined by Rectangular Hoops Subjected to Axial Loads," by J. Vallenas, V.V. Bertero and
                 E.P. Popov - 1977 (PB 275 165)A06

UCB/EERC-77/14   "Seismic Strain Induced in the Ground During Earthquakes," by Y. Sugimura - 1977 (PB 284 201)A04

UCB/EERC-77/15   Unassigned

UCB/EERC-77/16   "Computer Aided Optimum Design of Ductile Reinforced Concrete Moment Resisting Frames," by S.W.
                 Zagajeski and V.V. Bertero - 1977 (PB 280 137)A07

UCB/EERC-77/17   "Earthquake Simulation Testing of a Stepping Frame with Energy-Absorbing Devices," by J.M. Kelly and
                 D.F. Tsztoo - 1977 (PB 273 506)A04

UCB/EERC-77/18   "Inelastic Behavior of Eccentrically Braced Steel Frames under Cyclic Loadings," by C.W. Roeder and
                 E.P. Popov - 1977 (PB 275 526)A15

UCB/EERC-77/19   "A Simplified Procedure for Estimating Earthquake-Induced Deformations in Dams and Embankments," by F.I.
                 Makdisi and H.B. Seed - 1977 (PB 276 820)A04

UCB/EERC-77/20   "The Performance of Earth Dams during Earthquakes," by H.B. Seed, F.I. Makdisi and P. de Alba - 1977
                 (PB 276 821)A04

UCB/EERC-77/21   "Dynamic Plastic Analysis Using Stress Resultant Finite Element Formulation," by P. Lukkunapvasit and
                 J.M. Kelly - 1977 (PB 275 453)A04

UCB/EERC-77/22   "Preliminary Experimental Study of Seismic Uplift of a Steel Frame," by R.W. Clough and A.A. Huckelbridge
                 1977 (PB 278 769)A08

UCB/EERC-77/23   "Earthquake Simulator Tests of a Nine-Story Steel Frame with Columns Allowed to Uplift," by A.A.
                 Huckelbridge - 1977 (PB 277 944)A09

UCB/EERC-77/24   "Nonlinear Soil-Structure Interaction of Skew Highway Bridges," by M.-C. Chen and J. Penzien - 1977
                 (PB 276 176)A07

UCB/EERC-77/25   "Seismic Analysis of an Offshore Structure Supported on Pile Foundations," by D.D.-N. Liou and J. Penzien
                 1977 (PB 283 180)A06

UCB/EERC-77/26   "Dynamic Stiffness Matrices for Homogeneous Viscoelastic Half-Planes," by G. Dasgupta and A.K. Chopra -
                 1977 (PB 279 654)A06

EERC-1

UCB/EERC-77/27   "A Practical Soft Story Earthquake Isolation System," by J.M. Kelly, J.M. Eidinger and C.J. Derham - 1977 (PB 276 814)A07

UCB/EERC-77/28   "Seismic Safety of Existing Buildings and Incentives for Hazard Mitigation in San Francisco: An Exploratory Study," by A.J. Meltsner - 1977 (PB 281 970)A05

UCB/EERC-77/29   "Dynamic Analysis of Electrohydraulic Shaking Tables," by D. Rea, S. Abedi-Hayati and Y. Takahashi 1977 (PB 282 569)A04

UCB/EERC-77/30   "An Approach for Improving Seismic - Resistant Behavior of Reinforced Concrete Interior Joints," by B. Galunic, V.V. Bertero and E.P. Popov - 1977 (PB 290 870)A06

UCB/EERC-78/01   "The Development of Energy-Absorbing Devices for Aseismic Base Isolation Systems," by J.M. Kelly and D.F. Tsztoo - 1978 (PB 284 978)A04

UCB/EERC-78/02   "Effect of Tensile Prestrain on the Cyclic Response of Structural Steel Connections, by J.G. Bouwkamp and A. Mukhopadhyay - 1978

UCB/EERC-78/03   "Experimental Results of an Earthquake Isolation System using Natural Rubber Bearings," by J.M. Eidinger and J.M. Kelly - 1978 (PB 281 686)A04

UCB/EERC-78/04   "Seismic Behavior of Tall Liquid Storage Tanks," by A. Niwa - 1978 (PB 284 017)A14

UCB/EERC-78/05   "Hysteretic Behavior of Reinforced Concrete Columns Subjected to High Axial and Cyclic Shear Forces," by S.W. Zagajeski, V.V. Bertero and J.G. Bouwkamp - 1978 (PB 283 858)A13

UCB/EERC-78/06   "Three Dimensional Inelastic Frame Elements for the ANSR-I Program," by A. Riahi, D.G. Row and G.H. Powell - 1978 (PB 295 755)A04

UCB/EERC-78/07   "Studies of Structural Response to Earthquake Ground Motion," by O.A. Lopez and A.K. Chopra - 1978 (PB 282 790)A05

UCB/EERC-78/08   "A Laboratory Study of the Fluid-Structure Interaction of Submerged Tanks and Caissons in Earthquakes," by R.C. Byrd - 1978 (PB 284 957)A08

UCB/EERC-78/09   Unassigned

UCB/EERC-78/10   "Seismic Performance of Nonstructural and Secondary Structural Elements," by I. Sakamoto - 1978 (PB81 154 593)A05

UCB/EERC-78/11   "Mathematical Modelling of Hysteresis Loops for Reinforced Concrete Columns," by S. Nakata, T. Sproul and J. Penzien - 1978 (PB 298 274)A05

UCB/EERC-78/12   "Damageability in Existing Buildings," by T. Blejwas and B. Bresler - 1978 (PB 80 166 978)A05

UCB/EERC-78/13   "Dynamic Behavior of a Pedestal Base Multistory Building," by R.M. Stephen, E.L. Wilson, J.G. Bouwkamp and M. Button - 1978 (PB 286 650)A08

UCB/EERC-78/14   "Seismic Response of Bridges - Case Studies," by R.A. Imbsen, V. Nutt and J. Penzien - 1978 (PB 286 503)A10

UCB/EERC-78/15   "A Substructure Technique for Nonlinear Static and Dynamic Analysis," by D.G. Row and G.H. Powell - 1978 (PB 288 077)A10

UCB/EERC-78/16   "Seismic Risk Studies for San Francisco and for the Greater San Francisco Bay Area," by C.S. Oliveira - 1978 (PB 81 120 115)A07

UCB/EERC-78/17   "Strength of Timber Roof Connections Subjected to Cyclic Loads," by P. Gülkan, R.L. Mayes and R.W. Clough - 1978 (HUD-000 1491)A07

UCB/EERC-78/18   "Response of K-Braced Steel Frame Models to Lateral Loads," by J.G. Bouwkamp, R.M. Stephen and E.P. Popov - 1978

UCB/EERC-78/19   "Rational Design Methods for Light Equipment in Structures Subjected to Ground Motion," by J.L. Sackman and J.M. Kelly - 1978 (PB 292 357)A04

UCB/EERC-78/20   "Testing of a Wind Restraint for Aseismic Base Isolation," by J.M. Kelly and D.E. Chitty - 1978 (PB 292 833)A03

UCB/EERC-78/21   "APOLLO - A Computer Program for the Analysis of Pore Pressure Generation and Dissipation in Horizontal Sand Layers During Cyclic or Earthquake Loading," by P.P. Martin and H.B. Seed - 1978 (PB 292 835)A04

UCB/EERC-78/22   "Optimal Design of an Earthquake Isolation System," by M.A. Bhatti, K.S. Pister and E. Polak - 1978 (PB 294 735)A06

UCB/EERC-78/23   "MASH - A Computer Program for the Non-Linear Analysis of Vertically Propagating Shear Waves in Horizontally Layered Deposits," by P.P. Martin and H.B. Seed - 1978 (PB 293 101)A05

UCB/EERC-78/24   "Investigation of the Elastic Characteristics of a Three Story Steel Frame Using System Identification," by I. Kaya and H.D. McNiven - 1978 (PB 296 225)A06

UCB/EERC-78/25   "Investigation of the Nonlinear Characteristics of a Three-Story Steel Frame Using System Identification," by I. Kaya and H.D. McNiven - 1978 (PB 301 363)A05

UCB/EERC-78/26   "Studies of Strong Ground Motion in Taiwan," by Y.M. Hsiung, B.A. Bolt and J. Penzien - 1978
(PB 298 436)A06

UCB/EERC-78/27   "Cyclic Loading Tests of Masonry Single Piers: Volume 1 - Height to Width Ratio of 2," by P.A. Hidalgo,
R.L. Mayes, H.D. McNiven and R.W. Clough - 1978 (PB 296 211)A07

UCB/EERC-78/28   "Cyclic Loading Tests of Masonry Single Piers: Volume 2 - Height to Width Ratio of 1," by S.-W.J. Chen,
P.A. Hidalgo, R.L. Mayes, R.W. Clough and H.D. McNiven - 1978 (PB 296 212)A09

UCB/EERC-78/29   "Analytical Procedures in Soil Dynamics," by J. Lysmer - 1978 (PB 298 445)A06

UCB/EERC-79/01   "Hysteretic Behavior of Lightweight Reinforced Concrete Beam-Column Subassemblages," by B. Forzani,
E.P. Popov and V.V. Bertero - April 1979(PB 298 267)A06

UCB/EERC-79/02   "The Development of a Mathematical Model to Predict the Flexural Response of Reinforced Concrete Beams
to Cyclic Loads, Using System Identification," by J. Stanton & H. McNiven - Jan. 1979(PB 295 875)A10

UCB/EERC-79/03   "Linear and Nonlinear Earthquake Response of Simple Torsionally Coupled Systems," by C.L. Kan and
A.K. Chopra - Feb. 1979(PB 298 262)A06

UCB/EERC-79/04   "A Mathematical Model of Masonry for Predicting its Linear Seismic Response Characteristics," by
Y. Mengi and H.D. McNiven - Feb. 1979(PB 298 266)A06

UCB/EERC-79/05   "Mechanical Behavior of Lightweight Concrete Confined by Different Types of Lateral Reinforcement,"
by M.A. Manrique, V.V. Bertero and E.P. Popov - May 1979(PB 301 114)A06

UCB/EERC-79/06   "Static Tilt Tests of a Tall Cylindrical Liquid Storage Tank," by R.W. Clough and A. Niwa - Feb. 1979
(PB 301 167)A06

UCB/EERC-79/07   "The Design of Steel Energy Absorbing Restrainers and Their Incorporation into Nuclear Power Plants
for Enhanced Safety: Volume 1 - Summary Report," by P.N. Spencer, V.F. Zackay, and E.R. Parker -
Feb. 1979(UCB/EERC-79/07)A09

UCB/EERC-79/08   "The Design of Steel Energy Absorbing Restrainers and Their Incorporation into Nuclear Power Plants
for Enhanced Safety: Volume 2 - The Development of Analyses for Reactor System Piping,""Simple Systems"
by M.C. Lee, J. Penzien, A.K. Chopra and K, Suzuki "Complex Systems" by G.H. Powell, E.L. Wilson,
R.W. Clough and D.G. Row - Feb. 1979(UCB/EERC-79/08)A10

UCB/EERC-79/09   "The Design of Steel Energy Absorbing Restrainers and Their Incorporation into Nuclear Power Plants
for Enhanced Safety: Volume 3 - Evaluation of Commercial Steels," by W.S. Owen, R.M.N. Pelloux,
R.O. Ritchie, M. Faral, T. Ohhashi, J. Toplosky, S.J. Hartman, V.F. Zackay and E.R. Parker -
Feb. 1979(UCB/EERC-79/09)A04

UCB/EERC-79/10   "The Design of Steel Energy Absorbing Restrainers and Their Incorporation into Nuclear Power Plants
for Enhanced Safety: Volume 4 - A Review of Energy-Absorbing Devices," by J.M. Kelly and
M.S. Skinner - Feb. 1979(UCB/EERC-79/10)A04

UCB/EERC-79/11   "Conservatism In Summation Rules for Closely Spaced Modes," by J.M. Kelly and J.L. Sackman - May
1979(PB 301 328)A03

UCB/EERC-79/12   "Cyclic Loading Tests of Masonry Single Piers; Volume 3 - Height to Width Ratio of 0.5," by
P.A. Hidalgo, R.L. Mayes, H.D. McNiven and R.W. Clough - May 1979(PB 301 321)A08

UCB/EERC-79/13   "Cyclic Behavior of Dense Course-Grained Materials in Relation to the Seismic Stability of Dams," by
N.G. Banerjee, H.B. Seed and C.K. Chan - June 1979(PB 301 373)A13

UCB/EERC-79/14   "Seismic Behavior of Reinforced Concrete Interior Beam-Column Subassemblages," by S. Viwathanatepa,
E.P. Popov and V.V. Bertero - June 1979(PB 301 326)A10

UCB/EERC-79/15   "Optimal Design of Localized Nonlinear Systems with Dual Performance Criteria Under Earthquake
Excitations," by M.A. Bhatti - July 1979(PB 80 167 109)A06

UCB/EERC-79/16   "OPTDYN - A General Purpose Optimization Program for Problems with or without Dynamic Constraints,"
by M.A. Bhatti, E. Polak and K.S. Pister - July 1979(PB 80 167 091)A05

UCB/EERC-79/17   "ANSR-II, Analysis of Nonlinear Structural Response, Users Manual," by D.P. Mondkar and G.H. Powell
July 1979(PB 80 113 301)A05

UCB/EERC-79/18   "Soil Structure Interaction in Different Seismic Environments," A. Gomez-Masso, J. Lysmer, J.-C. Chen
and H.B. Seed - August 1979(PB 80 101 520)A04

UCB/EERC-79/19   "ARMA Models for Earthquake Ground Motions," by M.K. Chang, J.W. Kwiatkowski, R.F. Nau, R.M. Oliver
and K.S. Pister - July 1979(PB 301 166)A05

UCB/EERC-79/20   "Hysteretic Behavior of Reinforced Concrete Structural Walls," by J.M. Vallenas, V.V. Bertero and
E.P. Popov - August 1979(PB 80 165 905)A12

UCB/EERC-79/21   "Studies on High-Frequency Vibrations of Buildings - 1: The Column Effect," by J. Lubliner - August 1979
(PB 80 158 553)A03

UCB/EERC-79/22   "Effects of Generalized Loadings on Bond Reinforcing Bars Embedded in Confined Concrete Blocks," by
S. Viwathanatepa, E.P. Popov and V.V. Bertero - August 1979(PB 81 124 018)A14

UCB/EERC-79/23   "Shaking Table Study of Single-Story Masonry Houses, Volume 1: Test Structures 1 and 2," by P. Gülkan,
R.L. Mayes and R.W. Clough - Sept. 1979 (HUD-000 1763)A12

UCB/EERC-79/24   "Shaking Table Study of Single-Story Masonry Houses, Volume 2: Test Structures 3 and 4," by P. Gülkan,
R.L. Mayes and R.W. Clough - Sept. 1979 (HUD-000 1836)A12

UCB/EERC-79/25   "Shaking Table Study of Single-Story Masonry Houses, Volume 3: Summary, Conclusions and Recommendations,"
by R.W. Clough, R.L. Mayes and P. Gülkan - Sept. 1979 (HUD-000 1837)A06

UCB/EERC-79/26 "Recommendations for a U.S.-Japan Cooperative Research Program Utilizing Large-Scale Testing Facilities," by U.S.-Japan Planning Group - Sept. 1979(PB 301 407)A06

UCB/EERC-79/27 "Earthquake-Induced Liquefaction Near Lake Amatitlan, Guatemala," by H.B. Seed, I. Arango, C.K. Chan, A. Gomez-Masso and R. Grant de Ascoli - Sept. 1979(NUREG-CR1341)A03

UCB/EERC-79/28 "Infill Panels: Their Influence on Seismic Response of Buildings," by J.W. Axley and V.V. Bertero Sept. 1979(PB 80 163 371)A10

UCB/EERC-79/29 "3D Truss Bar Element (Type 1) for the ANSR-II Program," by D.P. Mondkar and G.H. Powell - Nov. 1979 (PB 80 169 709)A02

UCB/EERC-79/30 "2D Beam-Column Element (Type 5 - Parallel Element Theory) for the ANSR-II Program," by D.G. Row, G.H. Powell and D.P. Mondkar - Dec. 1979(PB 80 167 224)A03

UCB/EERC-79/31 "3D Beam-Column Element (Type 2 - Parallel Element Theory) for the ANSR-II Program," by A. Riahi, G.H. Powell and D.P. Mondkar - Dec. 1979(PB 80 167 216)A03

UCB/EERC-79/32 "On Response of Structures to Stationary Excitation," by A. Der Kiureghian - Dec. 1979(PB 80166 929)A03

UCB/EERC-79/33 "Undisturbed Sampling and Cyclic Load Testing of Sands," by S. Singh, H.B. Seed and C.K. Chan Dec. 1979(ADA 087 298)A07

UCB/EERC-79/34 "Interaction Effects of Simultaneous Torsional and Compressional Cyclic Loading of Sand," by P.M. Griffin and W.N. Houston - Dec. 1979(ADA 092 352)A15

UCB/EERC-80/01 "Earthquake Response of Concrete Gravity Dams Including Hydrodynamic and Foundation Interaction Effects," by A.K. Chopra, P. Chakrabarti and S. Gupta - Jan. 1980(AD-A087297)A10

UCB/EERC-80/02 "Rocking Response of Rigid Blocks to Earthquakes," by C.S. Yim, A.K. Chopra and J. Penzien - Jan. 1980 (PB80 166 002)A04

UCB/EERC-80/03 "Optimum Inelastic Design of Seismic-Resistant Reinforced Concrete Frame Structures," by S.W. Zagajeski and V.V. Bertero - Jan. 1980(PB80 164 635)A06

UCB/EERC-80/04 "Effects of Amount and Arrangement of Wall-Panel Reinforcement on Hysteretic Behavior of Reinforced Concrete Walls," by R. Iliya and V.V. Bertero - Feb. 1980(PB81 122 525)A09

UCB/EERC-80/05 "Shaking Table Research on Concrete Dam Models," by A. Niwa and R.W. Clough - Sept. 1980(PB81 122 368)A06

UCB/EERC-80/06 "The Design of Steel Energy-Absorbing Restrainers and their Incorporation into Nuclear Power Plants for Enhanced Safety (Vol 1A): Piping with Energy Absorbing Restrainers: Parameter Study on Small Systems," by G.H. Powell, C. Oughourlian and J. Simons - June 1980

UCB/EERC-80/07 "Inelastic Torsional Response of Structures Subjected to Earthquake Ground Motions," by Y. Yamazaki April 1980(PB81 122 327)A08

UCB/EERC-80/08 "Study of X-Braced Steel Frame Structures Under Earthquake Simulation," by Y. Ghanaat - April 1980 (PB81 122 335)A11

UCB/EERC-80/09 "Hybrid Modelling of Soil-Structure Interaction," by S. Gupta, T.W. Lin, J. Penzien and C.S. Yeh May 1980(PB81 122 319)A07

UCB/EERC-80/10 "General Applicability of a Nonlinear Model of a One Story Steel Frame," by B.I. Sveinsson and H.D. McNiven - May 1980(PB81 124 877)A06

UCB/EERC-80/11 "A Green-Function Method for Wave Interaction with a Submerged Body," by W. Kioka - April 1980 (PB81 122 269)A07

UCB/EERC-80/12 "Hydrodynamic Pressure and Added Mass for Axisymmetric Bodies," by F. Nilrat - May 1980(PB81 122 343)A08

UCB/EERC-80/13 "Treatment of Non-Linear Drag Forces Acting on Offshore Platforms," by B.V. Dao and J. Penzien May 1980(PB81 153 413)A07

UCB/EERC-80/14 "2D Plane/Axisymmetric Solid Element (Type 3 - Elastic or Elastic-Perfectly Plastic) for the ANSR-II Program," by D.P. Mondkar and G.H. Powell - July 1980(PB81 122 350)A03

UCB/EERC-80/15 "A Response Spectrum Method for Random Vibrations," by A. Der Kiureghian - June 1980(PB81 122 301)A03

UCB/EERC-80/16 "Cyclic Inelastic Buckling of Tubular Steel Braces," by V.A. Zayas, E.P. Popov and S.A. Mahin June 1980(PB81 124 885)A10

UCB/EERC-80/17 "Dynamic Response of Simple Arch Dams Including Hydrodynamic Interaction," by C.S. Porter and A.K. Chopra - July 1980(PB81 124 000)A13

UCB/EERC-80/18 "Experimental Testing of a Friction Damped Aseismic Base Isolation System with Fail-Safe Characteristics," by J.M. Kelly, K.E. Beucke and M.S. Skinner - July 1980(PB81 148 595)A04

UCB/EERC-80/19 "The Design of Steel Energy-Absorbing Restrainers and their Incorporation into Nuclear Power Plants for Enhanced Safety (Vol 1B): Stochastic Seismic Analyses of Nuclear Power Plant Structures and Piping Systems Subjected to Multiple Support Excitations," by M.C. Lee and J. Penzien - June 1980

UCB/EERC-80/20 "The Design of Steel Energy-Absorbing Restrainers and their Incorporation into Nuclear Power Plants for Enhanced Safety (Vol 1C): Numerical Method for Dynamic Substructure Analysis," by J.M. Dickens and E.L. Wilson - June 1980

UCB/EERC-80/21 "The Design of Steel Energy-Absorbing Restrainers and their Incorporation into Nuclear Power Plants for Enhanced Safety (Vol 2): Development and Testing of Restraints for Nuclear Piping Systems," by J.M. Kelly and M.S. Skinner - June 1980

UCB/EERC-80/22 "3D Solid Element (Type 4-Elastic or Elastic-Perfectly-Plastic) for the ANSR-II Program," by D.P. Mondkar and G.H. Powell - July 1980(PB81 123 242)A03

UCB/EERC-80/23 "Gap-Friction Element (Type 5) for the ANSR-II Program," by D.P. Mondkar and G.H. Powell - July 1980 (PB81 122 285)A03

UCB/EERC-80/24   "U-Bar Restraint Element (Type 11) for the ANSR-II Program," by C. Oughourlian and G.H. Powell
July 1980(PB81 122 293)A03

UCB/EERC-80/25   "Testing of a Natural Rubber Base Isolation System by an Explosively Simulated Earthquake," by
J.M. Kelly - August 1980(PB81 201 360)A04

UCB/EERC-80/26   "Input Identification from Structural Vibrational Response," by Y. Hu - August 1980(PB81 152 308)A05

UCB/EERC-80/27   "Cyclic Inelastic Behavior of Steel Offshore Structures," by V.A. Zayas, S.A. Mahin and E.P. Popov
August 1980(PB81 196 180)A15

UCB/EERC-80/28   "Shaking Table Testing of a Reinforced Concrete Frame with Biaxial Response," by M.G. Oliva
October 1980(PB81 154 304)A10

UCB/EERC-80/29   "Dynamic Properties of a Twelve-Story Prefabricated Panel Building," by J.G. Bouwkamp, J.P. Kollegger
and R.M. Stephen - October 1980(PB82 117 128)A06

UCB/EERC-80/30   "Dynamic Properties of an Eight-Story Prefabricated Panel Building," by J.G. Bouwkamp, J.P. Kollegger
and R.M. Stephen - October 1980(PB81 200 313)A05

UCB/EERC-80/31   "Predictive Dynamic Response of Panel Type Structures Under Earthquakes," by J.P. Kollegger and
J.G. Bouwkamp - October 1980(PB81 152 316)A04

UCB/EERC-80/32   "The Design of Steel Energy-Absorbing Restrainers and their Incorporation into Nuclear Power Plants
for Enhanced Safety (Vol 3): Testing of Commercial Steels in Low-Cycle Torsional Fatigue," by
P. Spencer, E.R. Parker, E. Jongewaard and M. Drory

UCB/EERC-80/33   "The Design of Steel Energy-Absorbing Restrainers and their Incorporation into Nuclear Power Plants
for Enhanced Safety (Vol 4): Shaking Table Tests of Piping Systems with Energy-Absorbing Restrainers,"
by S.F. Stiemer and W.G. Godden - Sept. 1980

UCB/EERC-80/34   "The Design of Steel Energy-Absorbing Restrainers and their Incorporation into Nuclear Power Plants
for Enhanced Safety (Vol 5): Summary Report," by P. Spencer

UCB/EERC-80/35   "Experimental Testing of an Energy-Absorbing Base Isolation System," by J.M. Kelly, M.S. Skinner and
K.E. Beucke - October 1980(PB81 154 072)A04

UCB/EERC-80/36   "Simulating and Analyzing Artificial Non-Stationary Earthquake Ground Motions," by R.F. Nau, R.M. Oliver
and K.S. Pister - October 1980(PB81 153 397)A04

UCB/EERC-80/37   "Earthquake Engineering at Berkeley - 1980," - Sept. 1980(PB81 205 874)A09

UCB/EERC-80/38   "Inelastic Seismic Analysis of Large Panel Buildings," by V. Schricker and G.H. Powell - Sept. 1980
(PB81 154 338)A13

UCB/EERC-80/39   "Dynamic Response of Embankment, Concrete-Gravity and Arch Dams Including Hydrodynamic Interaction,"
by J.F. Hall and A.K. Chopra - October 1980(PB81 152 324)A11

UCB/EERC-80/40   "Inelastic Buckling of Steel Struts Under Cyclic Load Reversal," by R.G. Black, W.A. Wenger and
E.P. Popov - October 1980(PB81 154 312)A08

UCB/EERC-80/41   "Influence of Site Characteristics on Building Damage During the October 3, 1974 Lima Earthquake," by
P. Repetto, I. Arango and H.B. Seed - Sept. 1980(PB81 161 739)A05

UCB/EERC-80/42   "Evaluation of a Shaking Table Test Program on Response Behavior of a Two Story Reinforced Concrete
Frame," by J.M. Blondet, R.W. Clough and S.A. Mahin

UCB/EERC-80/43   "Modelling of Soil-Structure Interaction by Finite and Infinite Elements," by F. Medina -
December 1980(PB81 229 270)A04

UCB/EERC-81/01   "Control of Seismic Response of Piping Systems and Other Structures by Base Isolation," edited by J.M.
Kelly - January 1981 (PB81 200 735)A05

UCB/EERC-81/02   "OPTNSR - An Interactive Software System for Optimal Design of Statically and Dynamically Loaded
Structures with Nonlinear Response," by M.A. Bhatti, V. Ciampi and K.S. Pister - January 1981
(PB81 218 851)A09

UCB/EERC-81/03   "Analysis of Local Variations in Free Field Seismic Ground Motions," by J.-C. Chen, J. Lysmer and H.B.
Seed - January 1981 (AD-A099508)A13

UCB/EERC-81/04   "Inelastic Structural Modeling of Braced Offshore Platforms for Seismic Loading," by V.A. Zayas,
P.-S.B. Shing, S.A. Mahin and E.P. Popov - January 1981(PB82 138 777)A07

UCB/EERC-81/05   "Dynamic Response of Light Equipment in Structures," by A. Der Kiureghian, J.L. Sackman and B. Nour-
Omid - April 1981 (PB81 218 497)A04

UCB/EERC-81/06   "Preliminary Experimental Investigation of a Broad Base Liquid Storage Tank," by J.G. Bouwkamp, J.P.
Kollegger and R.M. Stephen - May 1981(PB82 140 385)A03

UCB/EERC-81/07   "The Seismic Resistant Design of Reinforced Concrete Coupled Structural Walls," by A.E. Aktan and V.V.
Bertero - June 1981(PB82 113 358)A11

UCB/EERC-81/08   "The Undrained Shearing Resistance of Cohesive Soils at Large Deformations," by M.R. Pyles and H.B.
Seed - August 1981

UCB/EERC-81/09   "Experimental Behavior of a Spatial Piping System with Steel Energy Absorbers Subjected to a Simulated
Differential Seismic Input," by S.F. Stiemer, W.G. Godden and J.M. Kelly - July 1981

UCB/EERC-81/10   "Evaluation of Seismic Design Provisions for Masonry in the United States," by B.I. Sveinsson, R.L. Mayes and H.D. McNiven - August 1981 (PB82 166 075)A08

UCB/EERC-81/11   "Two-Dimensional Hybrid Modelling of Soil-Structure Interaction," by T.-J. Tzong, S. Gupta and J. Penzien - August 1981(PB82 142 118)A04

UCB/EERC-81/12   "Studies on Effects of Infills in Seismic Resistant R/C Construction," by S. Brokken and V.V. Bertero - September 1981 (PB82 166 190)A09

UCB/EERC-81/13   "Linear Models to Predict the Nonlinear Seismic Behavior of a One-Story Steel Frame," by H. Valdimarsson, A.H. Shah and H.D. McNiven - September 1981(PB82 138 793)A07

UCB/EERC-81/14   "TLUSH: A Computer Program for the Three-Dimensional Dynamic Analysis of Earth Dams," by T. Kagawa, L.H. Mejia, H.B. Seed and J. Lysmer - September 1981(PB82 139 940)A06

UCB/EERC-81/15   "Three Dimensional Dynamic Response Analysis of Earth Dams," by L.H. Mejia and H.B. Seed - September 1981 (PB82 137 274)A12

UCB/EERC-81/16   "Experimental Study of Lead and Elastomeric Dampers for Base Isolation Systems," by J.M. Kelly and S.B. Hodder - October 1981 (PB82 166 182)A05

UCB/EERC-81/17   "The Influence of Base Isolation on the Seismic Response of Light Secondary Equipment," by J.M. Kelly - April 1981 (PB82 255 266)A04

UCB/EERC-81/18   "Studies on Evaluation of Shaking Table Response Analysis Procedures," by J. Marcial Blondet - November 1981 (PB82 197 278)A10

UCB/EERC-81/19   "DELIGHT.STRUCT: A Computer-Aided Design Environment for Structural Engineering," by R.J. Balling, K.S. Pister and E. Polak - December 1981 (PB82 218 496)A07

UCB/EERC-81/20   "Optimal Design of Seismic-Resistant Planar Steel Frames," by R.J. Balling, V. Ciampi, K.S. Pister and E. Polak - December 1981 (PB82 220 179)A07

UCB/EERC-82/01   "Dynamic Behavior of Ground for Seismic Analysis of Lifeline Systems," by T. Sato and A. Der Kiureghian - January 1982 (PB82 218 926)A05

UCB/EERC-82/02   "Shaking Table Tests of a Tubular Steel Frame Model," by Y. Ghanaat and R. W. Clough - January 1982 (PB82 220 161)A07

UCB/EERC-82/03   "Behavior of a Piping System under Seismic Excitation: Experimental Investigations of a Spatial Piping System supported by Mechanical Shock Arrestors and Steel Energy Absorbing Devices under Seismic Excitation," by S. Schneider, H.-M. Lee and W. G. Godden - May 1982 (PB83 172 544)A09

UCB/EERC-82/04   "New Approaches for the Dynamic Analysis of Large Structural Systems," by E. L. Wilson - June 1982 (PB83 148 080)A05

UCB/EERC-82/05   "Model Study of Effects of Damage on the Vibration Properties of Steel Offshore Platforms," by F. Shahrivar and J. G. Bouwkamp - June 1982 (PB83 148 742)A10

UCB/EERC-82/06   "States of the Art and Practice in the Optimum Seismic Design and Analytical Response Prediction of R/C Frame-Wall Structures," by A. E. Aktan and V. V. Bertero - July 1982 (PB83 147 736)A05

UCB/EERC-82/07   "Further Study of the Earthquake Response of a Broad Cylindrical Liquid-Storage Tank Model," by G. C. Manos and R. W. Clough - July 1982 (PB83 147 744)A11

UCB/EERC-82/08   "An Evaluation of the Design and Analytical Seismic Response of a Seven Story Reinforced Concrete Frame - Wall Structure," by F. A. Charney and V. V. Bertero - July 1982(PB83 157 628)A09

UCB/EERC-82/09   "Fluid-Structure Interactions: Added Mass Computations for Incompressible Fluid," by J. S.-H. Kuo - August 1982 (PB83 156 281)A07

UCB/EERC-82/10   "Joint-Opening Nonlinear Mechanism: Interface Smeared Crack Model," by J. S.-H. Kuo - August 1982 (PB83 149 195)A05

UCB/EERC-82/11   "Dynamic Response Analysis of Techi Dam," by R. W. Clough, R. M. Stephen and J. S.-H. Kuo - August 1982 (PB83 147 496)A06

UCB/EERC-82/12   "Prediction of the Seismic Responses of R/C Frame-Coupled Wall Structures," by A. E. Aktan, V. V. Bertero and M. Piazza - August 1982 (PB83 149 203)A09

UCB/EERC-82/13   "Preliminary Report on the SMART 1 Strong Motion Array in Taiwan," by B. A. Bolt, C. H. Loh, J. Penzien, Y. B. Tsai and Y. T. Yeh - August 1982 (PB83 159 400)A10

UCB/EERC-82/14   "Shaking-Table Studies of an Eccentrically X-Braced Steel Structure," by M. S. Yang - September 1982

UCB/EERC-82/15   "The Performance of Stairways in Earthquakes," by C. Roha, J. W. Axley and V. V. Bertero - September 1982 (PB83 157 693)A07

UCB/EERC-82/16   "The Behavior of Submerged Multiple Bodies in Earthquakes," by W.-G. Liao - Sept. 1982 (PB83 158 709)A07

UCB/EERC-82/17   "Effects of Concrete Types and Loading Conditions on Local Bond-Slip Relationships," by A. D. Cowell, E. P. Popov and V. V. Bertero - September 1982 (PB83 153 577)A04

UCB/EERC-82/18   "Mechanical Behavior of Shear Wall Vertical Boundary Members: An Experimental Investigation," by M. T. Wagner and V. V. Bertero - October 1982 (PB83 159 764)A05

UCB/EERC-82/19   "Experimental Studies of Multi-support Seismic Loading on Piping Systems," by J. M. Kelly and A. D. Cowell - November 1982

UCB/EERC-82/20   "Generalized Plastic Hinge Concepts for 3D Beam-Column Elements," by P. F.-S. Chen and G. H. Powell - November 1982

UCB/EERC-82/21   "ANSR-III: General Purpose Computer Program for Nonlinear Structural Analysis," by C. V. Oughourlian and G. H. Powell - November 1982

UCB/EERC-82/22   "Solution Strategies for Statically Loaded Nonlinear Structures," by J. W. Simons and G. H. Powell - November 1982

UCB/EERC-82/23   "Analytical Model of Deformed Bar Anchorages under Generalized Excitations," by V. Ciampi, R. Eligehausen, V. V. Bertero and E. P. Popov - November 1982 (PB83 169 532)A06

UCB/EERC-82/24   "A Mathematical Model for the Response of Masonry Walls to Dynamic Excitations," by H. Sucuoğlu, Y. Mengi and H. D. McNiven - November 1982 (PB83 169 011)A07

UCB/EERC-82/25   "Earthquake Response Considerations of Broad Liquid Storage Tanks," by F. J. Cambra - November 1982

UCB/EERC-82/26   "Computational Models for Cyclic Plasticity, Rate Dependence and Creep," by B. Mosaddad and G. H. Powell - November 1982

UCB/EERC-82/27   "Inelastic Analysis of Piping and Tubular Structures," by M. Mahasuverachai and G. H. Powell - November 1982

UCB/EERC-83/01   "The Economic Feasibility of Seismic Rehabilitation of Buildings by Base Isolation," by J. M. Kelly - January 1983

UCB/EERC-83/02   "Seismic Moment Connections for Moment-Resisting Steel Frames," by E. P. Popov - January 1983

UCB/EERC-83/03   "Design of Links and Beam-to-Column Connections for Eccentrically Braced Steel Frames," by E. P. Popov and J. O. Malley - January 1983

UCB/EERC-83/04   "Numerical Techniques for the Evaluation of Soil-Structure Interaction Effects in the Time Domain," by E. Bayo and E. L. Wilson - February 1983

UCB/EERC-83/05   "A Transducer for Measuring the Internal Forces in the Columns of a Frame-Wall Reinforced Concrete Structure," by R. Sause and V. V. Bertero - May 1983

UCB/EERC-83/06   "Dynamic Interactions between Floating Ice and Offshore Structures," by P. Croteau - May 1983

UCB/EERC-83/07   "Dynamic Analysis of Multiply Tunnelled and Arbitrarily Supported Secondary Systems," by T. Igusa and A. Der Kiureghian - June 1983

UCB/EERC-83/08   "A Laboratory Study of Submerged Multi-body Systems in Earthquakes," by G. R. Ansari - June 1983

UCB/EERC-83/09   "Effects of Transient Foundation Uplift on Earthquake Response of Structures," by C.-S. Yim and A. K. Chopra - June 1983

UCB/EERC-83/10   "Optimal Design of Friction-Braced Frames under Seismic Loading," by M. A. Austin and K. S. Pister - June 1983

UCB/EERC-83/11   "Shaking Table Study of Single-Story Masonry Houses: Earthquake Performance under Three Component Simulated Seismic Input and Recommendations," by G. C. Manos, R. W. Clough and R. L. Mayes - June 1983

UCB/EERC-83/12   "Experimental Error Propagation in Pseudodynamic Testing," by P. B. Shing and S. A. Mahin - June 1983

UCB/EERC-83/13   "Experimental and Analytical Predictions of the Mechanical Characteristics of a 1/5-scale Model of a 7-story R/C Frame-Wall Building Structure," by A. E. Aktan, V. V. Bertero, A. A. Chowdhury and T. Nagashima - August 1983